ISAS - INTERNATIONAL SCHOOL FOR ADVANCED STUDIES

New results for interacting Fermi systems: the 2D Hubbard model at low density and the two coupled chain problem

Thesis submitted for the degree of

"Doctor Philosophiæ"

CANDIDATE

Michele Fabrizio

SUPERVISORS

Prof. Erio Tosatti

Prof. Alberto Parola

November 1992

TRIESTE

SISSA - SCUOLA INTERNAZIONALE SUPERIORE STUDI AVANZATI
TRIESTE
Strada Costiera 11

SISSA ISAS
SCUOLA INTERNAZIONALE SUPERIORE DI STUDI AVANZATI
INTERNATIONAL SCHOOL FOR ADVANCED STUDIES

New results for interacting Fermi systems: the 2D Hubbard model at low density and the two coupled chain problem

Thesis submitted for the degree of

"Doctor Philosophiæ"

CANDIDATE

Michele Fabrizio

SUPERVISORS

Prof. Erio Tosatti

Prof. Alberto Parola

November 1992

Aknowledgements

This thesis collects the work of four years in Trieste, quite a long period, even though the size of the thesis does not testify it enough.

I want to thank Erio Tosatti. He has continuously stimulated and encouraged me during all this time. His ideas have inspired most of the work present in the thesis.

I am sincerely grateful to Alberto Parola, who has shared with me all the moments of enthusiasm and discouragement during this work. Without his invaluable help and collaboration, this thesis could not have been ever done.

In the course of this work, I have benefited helpful discussions with other peoples, whom I wish to thank.

I thank Karl Penc. He let us know about the possibility to apply the renormalization group to the problem of coupled chains.

I thank Johannes Voit. He made me notice that spin–charge separation may occur without modifying at all the ground–state properties of a one dimensional Fermi gas. Anyone can realize how this feature excited me, because this concept appears quite often, maybe too often, in this thesis.

I also want to express my gratitude to prof. P. Nozières for the interest showed for our results on the two–chains. He introduced us to the problematic of the stability of spin–charge separation in coupled chains, which we feel a very stimulating problem.

At last I thank my university teachers Claudio Castellani and Carlo Di Castro, who have always been disposable to discuss with me my work.

Un grazie particolare a tutti gli amici che, con me, hanno condiviso questi anni alla SISSA. In loro compagnia questo periodo è trascorso abbastanza piacevolmente, nonostante tutte le difficoltà incontrate.

Table of Contents

Introduction

A central problem in the theory of strongly correlated fermion systems, concerns the nature of their low–lying excitations. It is generally accepted that, except for special cases with symmetry breaking, three dimensional (3D) interacting Fermi systems, are well described in terms of weakly correlated quasi–particles with quantum numbers in one–to–one correspondence with those identifying the excitations of a non–interacting Fermi gas. This is the basic assumption underlying the Landau theory of Fermi liquids (FL), which was originally proposed as a phenomenological description of strongly interacting fermions by Landau in early 1956[1], an then established microscopically by Nozières and Luttinger in 1962[2].

Quite a different scenario occurs in 1D interacting Fermi systems. Apart from specific models developing gaps in the excitation spectrum, most fermion systems in one dimension with repulsive interactions, do have low–lying gapless excitations, like ordinary Fermi liquids, but totally different from the quasi–particles predicted by Landau theory. The low–energy behavior of most of these 1D interacting fermion systems with gapless linear excitations, can be understood in terms of few model dependent constants, which parametrize all the long–wavelength properties. Such a feature was first recognized in

a simple exactly solvable 1D model, the "Luttinger model", introduced by Luttinger in 1963[3], and exactly solved by Mattis and Lieb two years later[4]. Afterwards, Haldane[5] realized that such a behavior was common to most 1D models with gapless excitations, which he collected in the class of *Luttinger liquids*, as opposed to the class of *Fermi liquids*, whose low–energy behavior is similar to that of the ideal Fermi gas.

A Luttinger liquid is characterized by asymptotically power–law decaying correlation functions, with coupling dependent exponents. In particular, for the single–particle Green function, an anomalous (coupling dependent) exponent, modifies the discontinuity of the momentum distribution at the Fermi surface, which becomes a power law singularity. The vanishing of this jump, is often considered as the key signature of non–Fermi liquid behavior in 1D, even though this is a ground state property rather than a characteristic of the low–energy excitations.

This is however not the only way in which non FL is realized in 1D electronic models. In fact, an equally effective mechanism leading to the breakdown of FL, without generating anomalous exponents, is the well known *spin–charge decoupling*[6]. When it occurs, no quasi–particle exists as a stable excitation, simply because spin and charge fluctuations are dynamically independent. For instance, if a spin and charge density fluctuation is induced by adding an extra particle to a 1D electron system, initially they both are centered on the position where the electron is created. However, the dynamical evolution splits the two excitations which, after a sufficiently long time, become spatially well separated. Therefore, due to many–body effects, the original electron "decays" into two distinct elementary excitations: the "holon" and the "spinon"[6].

So far, we have contrasted 3D with 1D Fermi systems. The discovery of cuprate su-

perconductors, has recently stimulated a big debate on the nature of low–lying excitations of 2D interacting electron systems. Firstly Anderson[7], proposed that, both the anomalous normal state properties and the mechanism leading to superconductivity, could be explained by assuming a breakdown of FL theory in 2D, as a consequence of spin–charge decoupling with possibly anomalous exponents modifying the asymptotic power–law decaying of correlation functions. Afterwards, other realizations of 2D non–FL, besides the simple 2D generalization of 1D Luttinger liquid, have been proposed, e.g. the *marginal Fermi liquid*[8] or the *anyon gas*[9]. Most of them, however, are expected to occur only under certain conditions, such as proximity to a magnetic or a charge–transfer instability, or such as the presence of an infinite on–site repulsion in an almost half–filled 2D square lattice, which can give rise to exotic phenomena by projecting out part of the Hilbert space.

On the other hand, a recent proposal of Anderson[10], based on quite general dimensionality arguments, suggests that in 2D, Fermi liquid theory is never valid, rather independently from the specific features of a model, similarly to the 1D case.

It has therefore become of great interest, to establish whether the mechanisms leading to the breakdown of Fermi liquid theory in 1D, can be generalized to higher dimensions, in particular to 2D. This problem is the background theme of this thesis. Two different aspects of this question are separately investigated.

Non perturbative results for few electrons in the Hubbard model

The first aspect, regards the ground state properties of a 2D interacting Fermi gas. As was said previously, it has been proposed by Anderson, that this system should show

anomalous asymptotic long–wavelength behavior, similarly to 1D.

We have succeeded in calculating exactly some of these properties by obtaining the ground state wavefunction for any finite number of electrons n in the low density limit $(n/N \to 0)$ of the N–site Hubbard model in dimension greater than one. In this limit, however, we do not find any anomalous ground state behavior. This calculation, which is presented in Chapter 1, through Sections 1.1–1.4, and in Appendix A, is performed using a method we have developed[11], which allows to obtain the exact and consistent expansion of any ground state property, in powers of $(n/N)^{1/3}$ in 3D, and of $1/\log(n/N)$ in 2D, at any order in this small parameter. The method is based on an interesting connection which we have found at low (actually zero) density, between the interaction correction to the total energy $\Delta\mathcal{E}_U$, defined as:

$$\Delta\mathcal{E}_U = E_{U\neq 0} - E_{U=0} \tag{1}$$

with U the on–site Hubbard repulsion, and the free–particle level spacing $\Delta\mathcal{E}_{\rm exc}$

$$\Delta\mathcal{E}_{\rm exc} = (E_{U=0})_{\rm excited-state} - (E_{U=0})_{\rm ground-state}\,. \tag{2}$$

We in fact show that, if

$$\lim_{N\to\infty} \frac{\Delta\mathcal{E}_U}{\Delta\mathcal{E}_{\rm exc}} = 0, \tag{3}$$

then it is possible to solve self–consistently the Schrœdinger equation for n electrons in the $N \to \infty$ limit, and obtain the total energy and the ground–state wavefunction. Notice that the assumption (3) is compatible only with zero density $(n/N) \to 0$ for $N \to \infty$[1]. The self–consistency is verified only in dimension $d \geq 2$, which means that in $d < 2$ the interaction correction (1) is of the same order than the free–particle level spacing (2). The consequence

[1] If the density were finite in the thermodynamic limit, the interaction correction to the total energy (1), would instead be finite and proportional to the number of electrons, whereas (2) would still vanish

of this difference is that, while in $d \geq 2$, the ground–state is not fundamentally modified by the interaction, e.g. it still has a step singularity in the momentum distribution, in $d < 2$ anomalous ground state properties are predicted, in agreement with the exact results known for 1D Fermi systems. These results extrapolate quite naturally to finite density, because the number of sites N appears always in the combination n/N with the number of particles n. In fact, this extrapolation exactly reproduces all the known results obtained by ordinary perturbation theory in the dilute limit, both in 3D[12] and 2D[13, 14, 15, 16] (see Section 1.4).

All these calculations agree upon a point: *no signature of anomalous exponents, characterizing the power–law decay of ground state correlation functions, is present in 2D*, at least at very low density. In particular the jump of the momentum distribution at the Fermi surface, is finite.

This conclusion, however, does not exclude an alternative scenario, where *spin–charge decoupling occurs in 2D, without anomalous exponents* (see Section 1.5). In fact, while anomalous correlation exponents affect also the ground state properties, spin–charge decoupling characterizes only the excitations, and can, in principle, occur even if the ground state is not modified by interaction (see Section 2.4).

In particular, we show (Section 1.5.2) that the mechanism which, according to Anderson, would lead to the breakdown of FL theory in 2D, i.e. the presence of an infinite repulsion in reciprocal space which prevents two opposite spin electrons to share the same momentum, produces quite naturally *spin–charge decoupling*, but does not generate anomalous exponents as well. The exact results we have obtained in the dilute limit, are perfectly compatible with this scenario, as they give information only about ground–

state properties. The analysis of the perturbation expansion of the single–particle Green function[13, 14, 15], is, in principle, capable of detecting spin–charge separation. However, this requires a more detailed study of the perturbation series, than that needed to search just for anomalous exponents. This analysis is, till now, not available.

Therefore, we conclude that while *the interaction does not modify in 2D the asymptotic behavior of the ground–state properties*, it is still an open question whether *spin–charge decoupling* as opposed to *ordinary Fermi liquid behavior* occurs.

The results of Sections 1.1–1.4, as well as those obtained in Refs. [13], [14], and [15], are strictly valid only at very low density. This point is never emphasized enough in the literature. In fact, it is not difficult to show (see Section 1.5.3) that in 2D there is a strong tendency of the highest occupied energy states (i.e. those near to the Fermi surface) to spin–polarize. The lowest order expansion in the density, predicts this instability towards ferrimagnetic states to occur at extremely low density ($\rho \sim 10^{-5}$). Higher order terms in the virial expansion, are therefore essential to make definitive statements on the Fermi liquid properties in 2D at reasonable densities.

Stability of 1D Luttinger liquid behavior in models of coupled chains

Another interesting aspect of the problem regarding the ground state and excitation properties of 2D interacting Fermi systems, concerns the way in which the crossover from a quasi–one–dimensional to an isotropic 2D or 3D behavior, occurs in arrays of coupled chains, upon increasing the interchain coupling. This is quite important, due to the well–known anomalous properties of 1D Fermi systems. In fact, the absence of coherent quasi–particle motion induced in 1D both by the *spin–charge decoupling* and by *the*

anomalous exponents, is expected to strongly reduce the effects of a single–particle tunnelling coupling such 1D systems, but it is believed to be less effective for pair–hopping processes. This circumstance raises some important questions. First of all, it is not clear if a transverse correlation can be generated at all, or if intra–chain *confinement* occurs with the chains behaving asymptotically as they were completely un–coupled. Furthermore, even if the former situation occurs, it is quite important to determine whether the transverse correlation is supported by single–particle or by pair–tunnelling processes. The latter event would be quite important, as it represents a possible mechanism for superconductivity. When applied to hypothetical 2D Luttinger planes coupled together, in fact, dominant pair tunnelling suggests a potential explanation of the high temperature superconductivity[17].

A very simple model, where the stability of the Luttinger liquid behavior and the competition between single–particle and pair–hopping can be studied, is given by two chains of interacting fermions, coupled by a transverse hopping $t_\perp$, which is the subject of Chapter 2.

The relevance of the anomalous exponents to this problem, can be studied by means of the renormalization group (RG), which has been already successfully applied to the single chain[18] and to quasi–1D systems[19, 20]. In Sections 2.2, we show how to apply this technique to the two chain model, with a supplementary ingredient: we allow for the renormalization of the transverse hopping. This is important in order to examine the possible occurrence of intra–chain *confinement*, which has been invoked by Anderson[21] to justify the stability of Luttinger behavior.

The method is first of all applied (Section 2.1) to two chains of spinless fermions, which

is actually the prototype model to estimate the importance of the anomalous exponents, independently from spin–charge separation. This is also an interesting model because it can be easily mapped onto a single chain of fermions with spin 1/2, in presence of a magnetic field, for which exact results are known. In this representation, the role of the spin index is played by the chain index, and that of the magnetic field by the transverse hopping. The spin sector corresponds to the antisymmetric combination of the densities of the two chains, while the charge one refers to the symmetric combination. While the latter is obviously not affected by $t_\perp$, so that it remains a "Luttinger liquid", the former is not. In particular, the transverse hopping introduces the analogous of a spin–anisotropy in the model, which, as it is shown in Section 2.1, does strongly modify the low–lying excitations in the antisymmetric (pseudo–spin) sector, eventually generating a gap. Depending on the strength of the intra–chain repulsion, four different low $t_\perp$ regimes are found. In particular, for intermediate values of the intra–chain interaction, we find a strong coupling regime with a gap in the antisymmetric sector. This gap, in terms of the pseudo–spin representation, is in the same direction of the transverse hopping, that is of the pseudo–magnetic field. Consequently, the pseudo–magnetization, which is simply the average value of the transverse hopping operator, is zero, and this phase is therefore confined. However, even though single–particle transverse hopping is asymptotically irrelevant, the two chains get strongly coupled, and in fact they show dominant in–phase charge density wave fluctuations. Although this phase is found as the outcome of RG calculations, we tend to believe that strict confinement is an artifact of weak coupling RG. Rather, we expect, on the basis of a combined RG plus bosonization technique calculation (see Section 2.1.3), that the system has gapless low–lying excitations

both in the symmetric and in the antisymmetric sector, with a finite average value of the transverse hopping operator.

The method is further generalized in Section 2.2, to the case of spinful fermions. Instead of having just a "flavour" index labelling the two chains, here a real spin is present. However, as it is shown in Section 2.2, the mechanism leading to the instability of the Luttinger liquid behavior, remains the same, namely, just the "flavour" anisotropy introduced by the transverse hopping. In fact, also in this case, four different small $t_\perp$ regimes are found, depending on the intra–chain repulsion, which are quite analogous to those encountered in the spinless model. Like in the previous case, the symmetric charge sector is totally unaffected by $t_\perp$ (see Section 2.3.1), and therefore it still describes a Luttinger liquid, while the antisymmetric charge sector is driven by $t_\perp$ towards strong coupling. Furthermore, this sector gets coupled to the spin modes, and it drives also these latter towards strong coupling regimes, where they all acquire gaps in the excitation spectrum. Dominant pair fluctuations exist in these phases, which confirms a strong enhancement of pair hopping processes[17, 19]. Analogously to the spinless case, at strong intra–chain repulsion, a confined phase is found (see Section 2.3), where the average value of the transverse hopping operator is asymptotically zero, even though strong inter–chain interactions are generated, leading to divergent pair susceptibilities.

The conclusion of these RG calculations, is that transverse hopping is always a relevant perturbation, which completely changes the form of the excitation spectrum, by generating gaps. This confirms the conclusions of previous studies, e.g. of Refs. [6], [?], [19], [22]. These gaps may lead, even for repulsive intra–chain interaction, to dominant pairing fluctuations (see Section 2.3).

The RG approach is well suited to analyse the effects of the anomalous exponents, but it does not help when the problem in hand is the role of spin charge separation. Actually, in spite of the fact that the RG correctly reproduces spin–charge separation at the level of the scaling equations (see Section 2.1), the detailed consequences of this decoupling are not directly accessible. On the other hand, it is very important to establish if spin–charge decoupling survives when two or more chains are coupled together. A very simple model where this problem can be studied, is given by two chains coupled by a transverse hopping, where the intra–chain repulsion is such that, in absence of $t_\perp$, only spin–charge decoupling occurs, without anomalous exponents. This is the case, in the so called g–ology modelling in 1D, when only g_4 interaction is non–zero. In Section 2.4, we show that two such 1D chains can be exactly solved by means of bosonization technique. The results are quite interesting. First of all, they prove that spin–charge separation alone does not produce confinement[21]. Secondly, they show that the inter–chain hopping generates further singularities in the electron Green function, besides those due to spin–charge decoupling, which, nevertheless partly survives. These singularities modify the properties of the system only at large distances, $x \gg \xi = (u_\rho - u_\sigma)/4t_\perp$, where $u_\rho(u_\sigma)$ is the sound velocity of the gapless excitations in the charge(spin) sector, while at smaller distances the independent chain behavior is recovered.

Chapter 1

Non perturbative results for few electrons in the Hubbard model

In this Chapter, we present a simple new method[11] which provides the ground state properties of the L^d–site Hubbard model, at arbitrary on–site repulsion U and for any finite number of electrons n, in the low–density limit ($n/L^d \to 0$).

In Section 1.1, we first review the solution of the two–body problem. This case is quite interesting because, even though it is an elementary exercise, it already shows the basic procedure leading to the solution of the n–body problem, and gives some physical insight about the behavior of the more general case. In fact, the way we calculate the ground–state energy and wave–function for any finite number of electrons in the limit of large system size, is just a generalization of the solution of the two–body problem.

In Section 1.2, we then solve the three–body problem, by applying the same asymptotic technique developed for two electrons. The method is checked against exact numerical diagonalization, and the total energy is shown, by finite–size scaling, to agree well with that of the asymptotic solution.

In Section 1.3, we generalize the method to any number of electrons. In particular, we

calculate the total energy and momentum distribution for a system of n electrons, whose unperturbed Fermi sea is not degenerate. The results are simple, analytical, and formally exact. However, they are again asymptotic in the sense that only the lowest–order terms of an ordered expansion in powers of $1/\log L$ (for 2D) and $1/L$ (for 3D), L being the linear size of the d–dimensional square lattice, is obtained. Nevertheless, the method allows in principle to obtain all the terms of the expansion.

In Section 1.4, we show how our results can be extrapolated to low but finite density $\rho = n/L^d$. This extrapolation coincides with well known perturbative results, which have been obtained in dilute systems of electrons, interacting via a short range repulsion[12, 30, 13, 14, 16, 15]. Provided the extension to finite density works, we find that the momentum distribution has a finite Fermi jump $Z = 1 - 4\log 2/\log^2(n/L^d)$.

Finally, in Section 1.5, the consequences of our results in connection with the important problem of the validity of Landau Fermi liquid theory in 2D, are discussed. In particular, we examine a recent argument proposed by Anderson[10], which suggests that the Landau quasi–particles are not stable excitations in 2D, due to the existence of a singularity in the two–body scattering when the opposite spin electrons have the same momentum. We show that our results are compatible with the presence of such a singular interaction, even though we are not able to prove Anderson's conclusion that this singularity causes non Fermi liquid behavior. We also review some recent calculations of different authors[34, 33, 14, 16, 15], on this issue.

The contents of Appendix A, which presents the exact asymptotic solution for four electrons and larger open shells, is also related to the arguments treated in this Chapter. In fact, the case of degenerate unperturbed Fermi sea, was not explicitly solved in Section

1.3. We find the solution to this problem too, and we show how the interaction partially removes the original degeneracy.

1.1 Two electrons in the Hubbard model: asymptotic versus exact solution

Let us consider two electrons in a d-dimensional hypercubic lattice of linear dimension L and containing L^d sites. The Hubbard Hamiltonian in momentum space is

$$\hat{H} = \sum_{\mathbf{k}\sigma} \epsilon_{\mathbf{k}} c^\dagger_{\mathbf{k}\sigma} c_{\mathbf{k}\sigma} + \frac{U}{L^d} \sum_{\mathbf{p}\mathbf{p}'\mathbf{q}} c^\dagger_{\mathbf{p}+\mathbf{q}\uparrow} c^\dagger_{\mathbf{p}'-\mathbf{q}\downarrow} c_{\mathbf{p}'\downarrow} c_{\mathbf{p}\uparrow}, \tag{1.1}$$

where

$$\epsilon_{\mathbf{k}} = -2t \sum_{i=1}^{d} \cos \mathrm{k}_i a,$$

and a is the lattice spacing. Since this hamiltonian conserves the total momentum $\mathbf{P}$, we limit ourselves in a subspace in which $\mathbf{P}$ is fixed. A generic wave function is

$$|\Psi\rangle = \sum_{\mathbf{q}} L(\mathbf{q}) c^\dagger_{\mathbf{q}\uparrow} c^\dagger_{\mathbf{P}-\mathbf{q}\downarrow} |0\rangle. \tag{1.2}$$

This function is the eigenvector of eigenvalue E if the coefficients $L(\mathbf{q})$ satisfy the Schrœdinger equation

$$(E - \epsilon_{\mathbf{q}} - \epsilon_{\mathbf{P}-\mathbf{q}}) L(\mathbf{q}) = \frac{U}{L^d} \sum_{\mathbf{p}} L(\mathbf{p}).$$

We call J the right hand side of this equation, so that

$$L(\mathbf{q}) = \frac{J}{(E - \epsilon_{\mathbf{q}} - \epsilon_{\mathbf{P}-\mathbf{q}})}. \tag{1.3}$$

By substituting this expression in that for J it is easy to obtain a self consistent equation of the usual type for the energy, i.e.[23, 24]

$$1 = \frac{U}{L^d} \sum_{\mathbf{q}} \frac{1}{(E - \epsilon_{\mathbf{q}} - \epsilon_{\mathbf{P}-\mathbf{q}})}. \tag{1.4}$$

The solution to this equation can be found analytically in 1D and asymptotically (large L) or numerically in $d \geq 2$. A possible approach to this problem was presented earlier in

Ref.[24]. Our strategy in the following will be to reconsider the asymptotic solution in a form which emphasizes (a) applicability to all space dimensions, (b) the crucial importance of the scattering amplitude, and (c) transferability to more than two electrons.

Let us write the difference ΔE between a generic eigenvalue E of Eq. (1.4) and the $U = 0$ ground state energy $2\epsilon_{\mathbf{0}}$ as

$$\Delta E = E - 2\epsilon_{\mathbf{0}} = \frac{\alpha(L)}{L^2}. \tag{1.5}$$

We may distinguish two classes of eigenvalues. In the first class we include all the eigenvalues whose $\alpha(L)$ goes to zero when $L \to \infty$, while the second class contains all the other eigenvalues. If the first class is not empty, than it obviously includes the ground state, since $\alpha(L) > 0$ for the repulsive Hubbard model. We note that, by construction, the interaction corrections to the eigenvalues ΔE in the first class go to zero faster than the $U = 0$ excitation energies (which go like $1/L^2$). Let us assume that the first class is indeed not empty, and let us solve Eq. (1.4) for a generic eigenvalue belonging to it. This assumption will be justified *a posteriori*. We also assume $\mathbf{P} = \mathbf{0}$, as we want to find the ground state. In order to solve the self consistent equation let us extract from the sum the term with $\mathbf{q} = \mathbf{0}$, which is the most divergent for $L \to \infty$. In this way Eq. (1.4) becomes

$$1 = \frac{U}{\alpha(L) L^{d-2}} + \frac{U}{L^d} \sum_{\mathbf{q} \neq 0} \frac{1}{(\Delta E + 2\epsilon_{\mathbf{0}} - 2\epsilon_{\mathbf{q}})}. \tag{1.6}$$

In the second term of the right hand side, we can neglect the interaction correction ΔE (we will show later that this is asymptotically correct for $d \geq 2$) with respect to $\epsilon_{\mathbf{q}} - \epsilon_{\mathbf{0}}$ when taking the limit $L \to \infty$, thus obtaining

$$\frac{U}{L^d} \sum_{\mathbf{q} \neq 0} \frac{1}{(\Delta E + 2\epsilon_{\mathbf{0}} - 2\epsilon_{\mathbf{q}})} \simeq -U a^d \int_{\frac{2\pi}{La}}^{k_0} \frac{d^d q}{(2\pi)^d} \frac{1}{(2\epsilon_{\mathbf{q}} - 2\epsilon_{\mathbf{0}})} \simeq -U a^{d-2} \frac{1}{2 t f_0}, \tag{1.7}$$

where $k_0 \sim \pi/a$ is an upper cutoff and f_0 is the usual low–energy scattering amplitude, that is

$$f_0 = \begin{cases} 4\pi a & \text{in 3D} \\ -\dfrac{2\pi}{\log ka} \sim \dfrac{2\pi}{\log L} & \text{in 2D} \\ \dfrac{(2\pi)^2}{La} & \text{in 1D.} \end{cases} \tag{1.8}$$

Equation (1.4) at last reduces to

$$1 = \frac{U}{\alpha(L)L^{d-2}} - \frac{Ua^{d-2}}{2tf_0}, \tag{1.9}$$

whose solution is unique (i.e. the first class for $\mathbf{P} = \mathbf{0}$ contains just the ground state) and yields simply

$$\alpha(L) = \frac{1}{L^{d-2}} \frac{U}{1 + \dfrac{Ua^{d-2}}{2tf_0}} = \begin{cases} L^{-1} \dfrac{U}{1 + U/(8\pi t)} & \text{in 3D} \\ \dfrac{4\pi t}{\log L} & \text{in 2D} \\ 8\pi^2 t & \text{in 1D.} \end{cases} \tag{1.10}$$

This general expression of $\alpha(L)$ shows that, when $f_0 \to 0$ in the large size limit, i.e. in $d \leq 2$, the asymptotic limit $L \to \infty$ drives the system towards strong coupling (i.e. $U \to \infty$) and $\alpha(L)$ tends to a limiting value independent of U, as long as U is not zero[24].

These results are consistent with the initial assumption $\lim_{L\to\infty} \alpha(L) = 0$ only in $d \geq 2$. In 1D (more generally in $d < 2$) $\alpha(L)$ is instead finite for $L \to \infty$. Therefore in this case, the result (1.7) does not apply and the first class of eigenvalues is empty. The exact solution of Eq. (1.4) in 1D is[24] (for large size and for the ground state) $\Delta E \simeq 2t(\pi/L)^2$ and indeed does not belong to the first class, as the previous simple calculation predicts. We can now address the error made in neglecting ΔE in Eq. (1.7). For $d = 2$, for example, inserting $\Delta E = 4\pi t/(L^2 \log L)$ yields a further correction of order $1/(L^2 \log^3 L)$ to ΔE.

Therefore, neglect of ΔE in (1.7) is asymptotically exact to order $1/(L^2 \log^2 L)$ (in general f_0^2/L^2).

Besides the ground state energy given by (1.5)–(1.10), we also obtain an explicit form for the ground state wave function. By using Eq. (1.5), it follows that, for any dimension d, the "envelope function" L is

$$L(\mathbf{q}) = \begin{cases} \dfrac{JL^2}{\alpha(L)} & \text{if } \mathbf{q} = \mathbf{0} \\ \dfrac{J}{2\epsilon_{\mathbf{0}} + \alpha(L)L^{-2} - 2\epsilon_{\mathbf{q}}} & \text{otherwise.} \end{cases} \tag{1.11}$$

Finally, the momentum distribution $n(\mathbf{p})$ is given by

$$n(\mathbf{p}) = \frac{L^2(\mathbf{p})}{L^2(\mathbf{0}) + \sum_{\mathbf{q}\neq 0} L^2(\mathbf{q})}. \tag{1.12}$$

In the limit $L \to \infty$ the second term in the denominator behaves as L^4, so that if $\alpha(L) \to 0$ (which is the case in $d \geq 2$), the behavior of the denominator is dominated by $L^2(\mathbf{0}) \simeq L^4/\alpha(L)$. This implies that, inside the $U = 0$ Fermi surface (i.e., for two electrons, just for the wave–vector $\mathbf{0}$), the momentum distribution is

$$n(\mathbf{0}) \simeq 1 - u\alpha^2(L) \tag{1.13}$$

while, just outside the Fermi surface, it is

$$n(2\pi/La, 0, 0, \cdots) = v\alpha^2(L), \tag{1.14}$$

giving a Fermi jump

$$Z = 1 - (u+v)\alpha^2(L), \tag{1.15}$$

where u and v are positive coefficients. Inserting (1.10) we get

$$1 - Z \sim \begin{cases} L^{-2} & \text{in 3D} \\ \log^{-2} N & \text{in 2D.} \end{cases} \tag{1.16}$$

This result shows that the $U \neq 0$ momentum distribution for $L \to \infty$ reaches the $U = 0$ value in $d \geq 2$. In 1D this is not the case. Exact solution of the Schrœdinger equation yields $\alpha(L) = 2t\pi^2$, which inserted into (1.11) and (1.18) gives the known result[24]

$$n\left(p = \frac{2\pi l}{La}\right) = \frac{8}{\pi^2}\frac{1}{(4l^2-1)^2}, \tag{1.17}$$

which is characterized by a jump across the Fermi surface strictly smaller than 1. The main results of this section can be summarized as follows.

(i) The two–electron problem is particularly simplified by working in the asymptotic limit $L \to \infty$, and by focusing on the asymptotic behaviour of the ground state energy shift ΔE. The asymptotic shift is a simple function of the scattering amplitude, and so are all other ground state properties.

(ii) There is a similarity between $d = 1$ and $d = 2$, in that (for $L \to \infty$) all properties of two electrons are modified by the presence of the interaction U by *U-independent terms. In other words, both cases are in the strong-coupling limit*[24].

(iii) By contrast, there is a similarity between $d = 3$ and $d = 2$ in that the energy correction $\Delta E = L^{-2}\alpha(L)$ vanishes for large L faster than the non-interacting energy level spacing. A remarkable consequence of this fact is that *the Fermi jump $Z \to 1$ in the asymptotic limit, for $d \geq 2$, but not for $d < 2$.*

1.2 Three electrons

Having solved the two-electron problem, the next question which arises is to what extent the behavior just described is stable or instead radically modified by the presence of a third electron. Mattis considered this problem long ago, in his study of the pair stability for attractive Hubbard U[23].

Let us consider three electrons in the subspace of total momentum $\mathrm{P} = (\frac{2\pi}{La}, 0, 0, ...)$ (in d dimension). A generic wave function is

$$|\Psi\rangle = \sum_{\mathbf{qk}} L(\mathbf{q}, \mathrm{P} - \mathbf{q} - \mathbf{k}, \mathbf{k}) c^{\dagger}_{\mathbf{q}\uparrow} c^{\dagger}_{\mathrm{P}-\mathbf{k}-\mathbf{q}\downarrow} c^{\dagger}_{\mathbf{k}\uparrow} |0\rangle. \tag{1.18}$$

The coefficients L must be antisymmetric in the first and third variable. The Schrœdinger equation for the L's is

$$\begin{aligned}(E - \epsilon_{\mathbf{q}} - \epsilon_{\mathrm{P}-\mathbf{q}-\mathbf{k}} - \epsilon_{\mathbf{k}}) L(\mathbf{q}, \mathrm{P} - \mathbf{q} - \mathbf{k}, \mathbf{k}) &= \frac{U}{L^d} \sum_{\mathbf{p}} [L(\mathbf{p}, \mathrm{P} - \mathbf{p} - \mathbf{k}, \mathbf{k}) + \\ &\quad - L(\mathbf{p}, \mathrm{P} - \mathbf{p} - \mathbf{q}, \mathbf{q})],\end{aligned} \tag{1.19}$$

whose solution is

$$L(\mathbf{q}, \mathrm{P} - \mathbf{q} - \mathbf{k}, \mathbf{k}) = \frac{J(\mathbf{k}) - J(\mathbf{q})}{(E - \epsilon_{\mathbf{q}} - \epsilon_{\mathrm{P}-\mathbf{q}-\mathbf{k}} - \epsilon_{\mathbf{k}})}, \tag{1.20}$$

where

$$J(\mathbf{k}) = \frac{U}{L^d} \sum_{\mathbf{q}} L(\mathbf{q}, \mathrm{P} - \mathbf{q} - \mathbf{k}, \mathbf{k}). \tag{1.21}$$

Substituting the expression of L in that of J we obtain a homogeneous set of equations[23] (instead of a simple self consistent equation as for two electrons)

$$\begin{aligned}J(\mathbf{k}) &= J(\mathbf{k}) \frac{U}{L^d} \sum_{q} \frac{1}{(E - \epsilon_{\mathbf{q}} - \epsilon_{\mathrm{P}-\mathbf{q}-\mathbf{k}} - \epsilon_{\mathbf{k}})} + \\ &\quad - \frac{U}{L^d} \sum_{q} \frac{J(\mathbf{q})}{(E - \epsilon_{\mathbf{q}} - \epsilon_{\mathrm{P}-\mathbf{q}-\mathbf{k}} - \epsilon_{\mathbf{k}})},\end{aligned} \tag{1.22}$$

which can be formally written in matrix form

$$\vec{J} = U\hat{T}(E) \cdot \vec{J} \tag{1.23}$$

Together with (1.22), this equation defines the operator $\hat{T}(E)$. The rows and columns of this matrix are labelled by the k vector of the third particle only. The third particle is a "spectator", while the other two are getting virtually excited. The final ground state is, if $\alpha(L) \to 0$, a linear superposition of the unperturbed Fermi Sea (FS) plus all these doubly excited states (which would not be the case if $\alpha(L) \neq 0$ for $L \to \infty$). The crucial point which will make the asymptotic solution very easy, is, as it will turn out, that *the spectator particle belongs to the unperturbed Fermi Sea with probability one, as* $L \to \infty$. This makes the (otherwise infinite) matrix $\hat{T}(E)$ finite and very small, as we now show.

The self-consistent set of equations (1.23) will only find solution when E corresponds to an eigenvalue of Schrœdinger equation (1.19). We now show how the asymptotic procedure of the previous Section can be applied to the ground state problem. Let us define as usual $\alpha(L) = (E - E_0)L^2$, where $E_0 = 2\epsilon_{\mathbf{0}} + \epsilon_{\mathbf{P}} \simeq t(-6d + (2\pi)^2/L^2)$ is the $U = 0$ ground state energy of three electrons. If we assume that the ground state satisfies the asymptotic condition $\lim_{L\to\infty} \alpha(L) = 0$, then it is possible to show, using Eq. (1.22), that the matrix $\hat{T}(E)$ has a part $\hat{T}^{(s)}$ which dominates for $L \to \infty$. Let us consider first the off-diagonal elements of the full $\hat{T}(E)$, which are of the form

$$\frac{1}{L^d(E - \epsilon_{\mathbf{q}} - \epsilon_{\mathbf{P-q-k}} - \epsilon_{\mathbf{k}})} \sim \begin{cases} L^{(2-d)}/\alpha(L) & \text{if } (\mathbf{k},\mathbf{q}) = (\mathbf{0},\mathbf{0}) \text{ or } (\mathbf{0},\mathbf{P}) \text{ or } (\mathbf{P},\mathbf{0}) \\ L^{(2-d)} & \text{otherwise.} \end{cases} \tag{1.24}$$

Hence, if $\alpha(L) \to 0$, the upper case, when all momenta belong to the unperturbed Fermi Sea (FS) (which consists only of the two wavevectors $\mathbf{0}$ and $\mathbf{P}$), dominates the second. If we extract from the diagonal elements the dominant terms in the sense of Eq. (1.24), the

remaining terms may be used to define a function $\chi(\mathbf{k})$

$$\chi(\mathbf{k}) = -L^{-d} \sum_{\mathbf{q}\notin \mathrm{FS}} \frac{1}{(E - \epsilon_{\mathbf{q}} - \epsilon_{\mathbf{P}-\mathbf{q}-\mathbf{k}} - \epsilon_{\mathbf{k}})} \simeq \frac{a^{d-2}}{2tf_0},$$

the last equality holding only for small k. For small wavevectors this function is of the same order in L as the leading terms of Eq. (1.24). Asymptotically we obtain the dominant part of $\hat{T}(E)$, which is

$$\hat{T}^{(s)} = \begin{pmatrix} \frac{1}{\alpha(L)L^{d-2}} - \chi(\mathbf{0}) & -\frac{1}{\alpha(L)L^{d-2}} & 0 & 0 & 0 & \cdots \\ -\frac{1}{\alpha(L)L^{d-2}} & \frac{1}{\alpha(L)L^{d-2}} - \chi(\mathbf{P}) & 0 & 0 & 0 & \cdots \\ 0 & 0 & -\chi(\mathbf{k}_3) & 0 & 0 & \cdots \\ 0 & 0 & 0 & -\chi(\mathbf{k}_4) & 0 & \cdots \\ \vdots & \vdots & \vdots & \vdots & \vdots & \vdots\vdots\vdots \end{pmatrix}, \quad (1.25)$$

where some ordering of the k's is implicit in order to change a matrix of dimension $(L \times L \times L \times L)$ in one $(L^2 \times L^2)$. In Eq. (1.25), the first 2×2 block represents the two states where $\mathbf{k} = \mathbf{0}, \mathbf{P}$, that is precisely those where the spectator particle belongs to the unperturbed Fermi Sea. As one can see, all couplings to other spectator states is exactly zero in the asymptotic limit. Eq. (1.22) now becomes $\vec{J} = U\hat{T}^{(s)} \cdot \vec{J}$ in $d > 2$ and $\hat{T}^{(s)} \cdot \vec{J} = 0$ in $d \leq 2$. The solution of these equations (in $d = 3$ we take $U \to \infty$ for simplicity) is

$$\begin{aligned} \frac{J(\mathbf{0})}{J(\mathbf{P})} &= -\frac{1 + U\chi(\mathbf{P})}{1 + U\chi(\mathbf{0})}, \\ J(\mathbf{k}) &= 0 \quad \text{if } \mathbf{k} \neq \mathbf{0}, \mathbf{P}, \end{aligned} \quad (1.26)$$

$$\alpha(L) = L^{2-d}\left(\frac{U}{1 + U\chi(\mathbf{0})} + \frac{U}{1 + U\chi(\mathbf{P})}\right) \simeq \frac{4tf_0}{(aL)^{d-2}}. \quad (1.27)$$

In $d \geq 2$ Eq. (1.27) is compatible with the initial assumption $\lim_{L\to\infty} \alpha(L) = 0$. On the contrary, in $d < 2$, the result does not satisfy that assumption, exactly as we found for two electrons.

The $d = 2$ three electron ground state energy is thus predicted to be, according to Eq. (1.27)

$$E \simeq -12t + \frac{t(2\pi)^2}{L^2} + \frac{16\pi t}{L^2 \log L^2} + \cdots. \tag{1.28}$$

The persistence of the logarithmic term already found for two electrons (however a factor two larger), suggests that the essential physics of that case is stable against addition of a third electron. From Eq. (1.18) it is easy to derive the expression of the momentum distribution in terms of the function $J(\mathbf{k})$, i.e.

$$n_{\mathbf{k}\uparrow} = 4 \sum_{\mathbf{q}} \left(\frac{J(\mathbf{q}) - J(\mathbf{k})}{E - \epsilon_{\mathbf{k}} - \epsilon_{\mathbf{q}} - \epsilon_{\mathbf{P}-\mathbf{q}-\mathbf{k}}} \right)^2, \tag{1.29}$$

$$n_{\mathbf{k}\downarrow} = 2 \sum_{\mathbf{q}} \left(\frac{J(\mathbf{q}) - J(\mathbf{P} - \mathbf{q} - \mathbf{k})}{E - \epsilon_{\mathbf{k}} - \epsilon_{\mathbf{q}} - \epsilon_{\mathbf{P}-\mathbf{q}-\mathbf{k}}} \right)^2. \tag{1.30}$$

We calculate the momentum distribution simply substituting Eqs. (1.26), (1.27), and (1.28) into Eqs. (1.29), and (1.30). Again the result does not differ substantially from the the two electron problem. In fact it is easy to convince ourselves (although we do not show it in detail here) that the momentum distribution again differs by terms of order $\alpha^2(L)$ from the unperturbed $n(\mathbf{q}) = 1$ only when $\mathbf{q} = \mathbf{0}, \mathbf{P}$, while $n(\mathbf{q}) \to 0$ otherwise.

We have also solved numerically the three electron Schrœdinger equation (1.22), in order to provide an independent check of the asymptotic solution given above. The numerical solution is obtained by exact diagonalization of (1.22) for squares lattices of size 8×8, 9×9, $\cdots$, 23×23, 24×24. In Fig. 1.1, we have plotted the asymptotic ground state energy of Eq. (1.28) versus linear size L, together with the numerical solution of (1.22) for $U = 10t$ (black squares), $U = 100t$ (open squares) and $U = 1000t$ (starred points). The agreement at larger sizes appears to be quite good. In order to get quantitative accuracy, we have also performed a finite-size scaling of the numerical results. We note that,

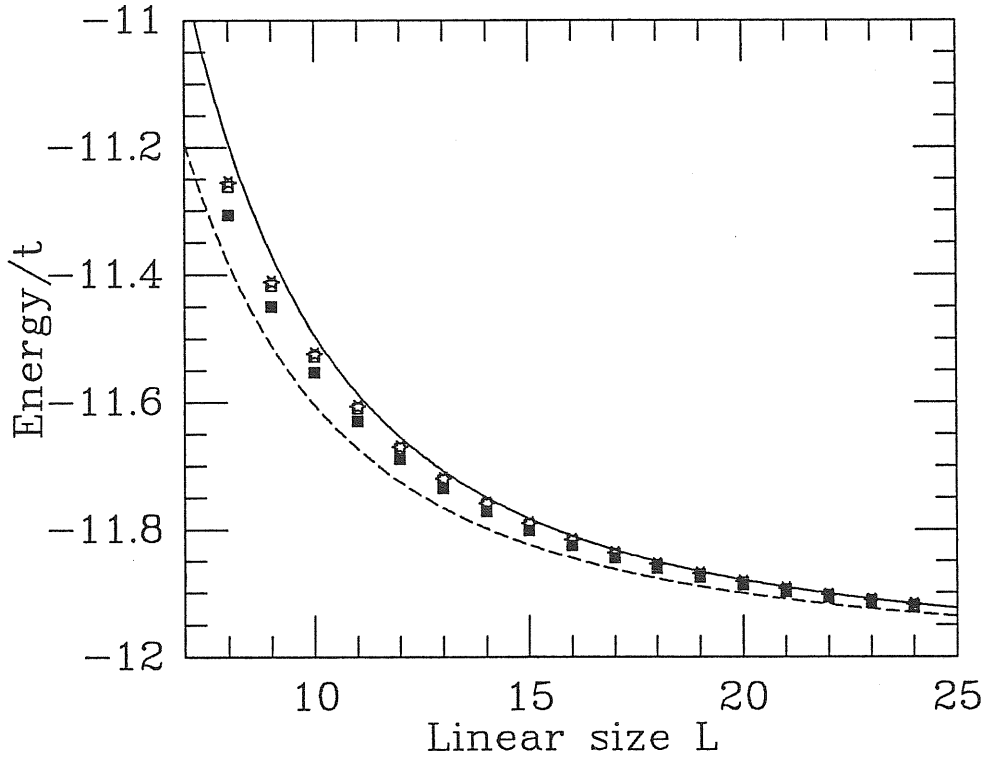

Figure 1.1: Ground state energy of three electrons on a 2D $L \times L$ square lattice versus L. The points are the exact numerical results for $U = 10t$ (black squares), $U = 100t$ (open squares), and $U = 1000t$ (starred points). The solid curve is the asymptotic solution Eq. (refunoundici), while the dashed curve is the $U = 0$ ground–state energy

according to our asymptotic solution, the quantity

$$\alpha(L) \log L = (E - E_0) L^2 \log L \tag{1.31}$$

is predicted to be equal to $8\pi t + O(1/\log L)$. In Fig. 1.2, we have plotted the right hand side of Eq. (1.31) versus $1/\log L$ for the exact numerical results. The solid lines are a fitting of Eq. (1.31) with a three parameter function

$$(E - E_0) L^2 \log L = A + B/\log L + C/\log^2 L \tag{1.32}$$

suggested by the asymptotic expansion. Even if the exact results are not in the asymptotic regime ($1/\log L \to 0$), the fitted parameter A, as shown by the zero intercept of Fig. 1.2,

is not far from the predicted asymptotic value 8π (the isolated black point). In conclusion, we believe the remaining error to be due to slow convergence of the expansion (1.32), and 8π to be asymptotically exact.

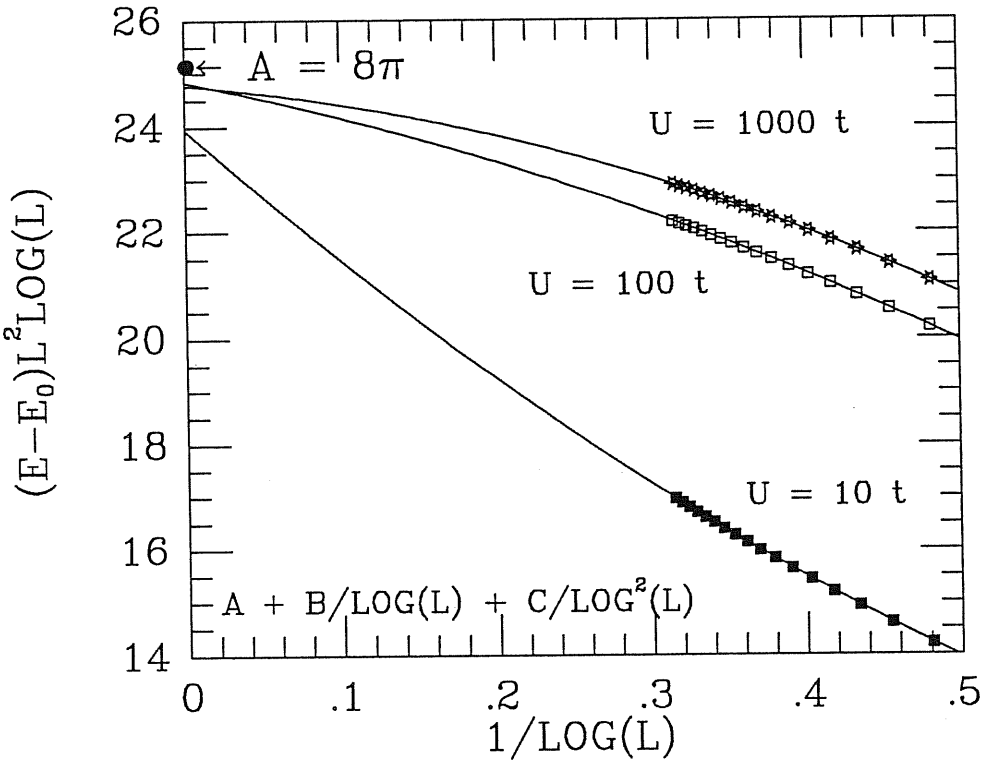

Figure 1.2: Finite–size scaling of the asymptotic solution Eq. (1.28). We have plotted the quantity $(E-E_0)L^2 \log L$ vs $1/\log L$. The points are the numerical results. The curves are fittings by using a three–parameter function $(E-E_0)L^2 \log L = A + B/\log L + C/\log^2 L$. The isolated point at $1/\log L = 0$ is the asymptotic result $A_\infty = 8\pi$, to be compared with the zero intercepts of the three curves.

1.3 Generalization to any finite number of electrons

We have shown that also the three electron problem can be solved using as an asymptotic assumption that $\alpha(L) = (E_{U\neq 0} - E_{U=0})L^2 \to 0$, at least in $d \geq 2$. The result is compatible with the initial hypothesis if the size of the system is very large, and it agrees quite well with the exact solution. In this section we generalize the method to any number of electrons n and solve approximately the problem when the $U = 0$ Fermi surface is not degenerate (closed k–shells).

Let us suppose to have n electrons in a subspace of $\mathbf{P}$ total momentum (for simplicity n is taken even). A generic wave function can be written as

$$|\Psi_n\rangle = \sum_{\mathbf{k}_1\mathbf{k}_2...} L(\mathbf{k}_1, \mathbf{k}_2, ..., \mathbf{k}_n) c^\dagger_{\mathbf{k}_1\uparrow} c^\dagger_{\mathbf{k}_2\downarrow} .... c^\dagger_{\mathbf{k}_n\downarrow} |0\rangle. \tag{1.33}$$

The coefficients L are odd functions with respect to the interchange of two odd (even) momenta. Notice that L depends only on $n-1$ momenta because of the conservation of the total momentum. The eigenvalue equation is

$$\begin{aligned}(E - \epsilon_{\mathbf{k}_1} - ... - \epsilon_{\mathbf{k}_n}) L(\mathbf{k}_1, ..., \mathbf{k}_n) &= \frac{U}{L^d} \sum_{\mathbf{q}} \Big[L(\mathbf{k}_1 + \mathbf{q}, \mathbf{k}_2 - \mathbf{q}, \mathbf{k}_3, ..., \mathbf{k}_n) + \\ &+ L(\mathbf{k}_1 + \mathbf{q}, \mathbf{k}_2, \mathbf{k}_3, \mathbf{k}_4 - \mathbf{q}, ..., \mathbf{k}_n) + \cdots \Big], \end{aligned} \tag{1.34}$$

where the dots correspond to all the possible pairings of momenta of one spin up and one spin down electron. Analogously to the three electron problem we define a function of $n-2$ momenta

$$J(\mathbf{k}_3, ..., \mathbf{k}_n) = \frac{U}{L^d} \sum_{\mathbf{q}} L(\mathbf{q}, \mathbf{P} - \mathbf{q} - \sum_{i=3}^{n} \mathbf{k}_i, \mathbf{k}_3, ..., \mathbf{k}_n), \tag{1.35}$$

which allows rewriting the coefficients L as

$$L(\mathbf{k}_1, \mathbf{k}_2, \mathbf{k}_3, ..., \mathbf{k}_n) = \frac{J(\mathbf{k}_3, \mathbf{k}_4, ..., \mathbf{k}_n) - J(\mathbf{k}_3, \mathbf{k}_2 ..., \mathbf{k}_n) + \cdots}{(E - \epsilon_{\mathbf{k}_1} - ... - \epsilon_{\mathbf{k}_n})}. \tag{1.36}$$

The self consistent set of equations that the J's have to satisfy, turns out again to be of the general form

$$\vec{J} = U\hat{T}(E)\cdot\vec{J}. \tag{1.37}$$

The main advantage in working with the J rather than the L, is that the asymptotic expansion for large system size $L \to \infty$ is far more straightforward. To solve the set of equations we assume again that

$$E = E_0 + \frac{\alpha(L)}{L^2} \qquad \text{where} \quad \lim_{L\to\infty} \alpha(L) = 0. \tag{1.38}$$

This condition is fully compatible with zero density (n/L^d) for $L \to \infty$ (if the the density were finite in the thermodynamic limit, the interaction correction to the total energy would instead be finite and proportional to the number of electrons). As in the case of three electrons, the matrix $\hat{T}(E)$ has a singular part $\hat{T}(E)^{(s)}$ which includes terms like

$$\frac{1}{(E - \epsilon_{\mathbf{k}_1} - \ldots - \epsilon_{\mathbf{k}_n})} \sim \frac{L^2}{\alpha(L)}$$

and

$$\frac{1}{L^d}\sum_{\mathbf{q},\mathbf{q}'\notin \mathrm{FS}} \delta(\mathbf{q}' + \mathbf{q} + \sum_{i=3}^{n}\mathbf{k}_i - \mathbf{P})\frac{1}{(E - \epsilon_{\mathbf{q}} - \epsilon_{\mathbf{q}'} - \epsilon_{\mathbf{k}_3} - \cdots - \epsilon_{\mathbf{k}_n})} \sim -\frac{a^{d-2}}{2t\, f_0},$$

where all the $\mathbf{k}$'s belong to the $U = 0$ FS. As a first approximation we just solve the equation $\hat{T}(E)^{(s)}\cdot\vec{J} = 0$ (as before, that implies $U \to \infty$ in $3d$, but not in $2d$). This again requires that the only J different from zero are those whose arguments k are part of the Fermi sphere of the unperturbed n electrons [their number N_j is $(n/2)^2$ for non-degenerate closed shells, counting the possible pairings of different spin states in the Fermi sphere. In the case of open shells this number is bigger, because the pairings involve all the degenerate possibilities which can be realized at the outer shell of the Fermi sea]. In

general the equations these J must satisfy look like an eigenvalue problem of the type seen earlier,

$$\hat{M} \cdot \vec{J} = \lambda \vec{J}, \tag{1.39}$$

where λ determines the unknown $\alpha(L)$ through

$$\lambda = \left(\frac{\alpha(L) a^{d-2} L^{d-2}}{2t f_0} \right) \tag{1.40}$$

and the ground–state energy expressed as a function of λ is

$$E = E_0 + \frac{\lambda 2t f_0}{a^{d-2} L^d}. \tag{1.41}$$

In (1.39) the matrix $\hat{M}$ is independent of E and has dimension N_j. The method for constructing $\hat{M}$ is very simple and can be deduced by inspection of (1.34) and by using the symmetry properties of the L's.

For the sake of physical clarity, we recall again the significance of the rows and columns. In this matrix $\hat{M}$, each vector represents a given configuration of the $n-2$ spectator electrons, while the remaining two are getting into a doubly excited state. Similar to what happened for three electrons, it turns out that, if $\alpha(L) \to 0$ for $L \to \infty$ (i.e., first class not empty), then in the limit *no spectators are allowed to lie outside of the unperturbed* FS. Since the number of ways N_j in which the spectator electrons can be assigned inside the FS is finite and small, the matrix $\hat{M}$ is always very simple, and can be diagonalized exactly.

First, suppose that the $U = 0$ Fermi surface to be non-degenerate (closed shell). Then $\hat{M}$ is the matrix

$$\hat{M} = \begin{pmatrix} 1 & -1 & 1 & -1 & 1 & -1 & \cdots \\ -1 & 1 & -1 & 1 & -1 & 1 & \cdots \\ 1 & -1 & 1 & -1 & 1 & -1 & \cdots \\ \vdots & \vdots & \vdots & \vdots & \vdots & \vdots & \vdots\vdots\vdots \end{pmatrix} \tag{1.42}$$

Table 1.1: Values of λ and of the total spin for the degenerate ground state of 4, 6 and 8 electrons.

# of electrons	λ	Total spin
4	3	0,1,1
6	7	0,2
8	15	0,1,1

of dimension $(n/2)^2 \times (n/2)^2$. The case in which the Fermi surface is degenerate (open shell) is a little more complicated. Let us suppose that it is m-fold degenerate. First we construct a block matrix made up of m boxes like (1.42) each of which is defined in a particular degenerate Fermi Surface. However some rows (columns) of different boxes correspond to the same J component. For this reason we move these rows (columns) in order to let them coincide with just one. The final matrix will look much more complicated than (1.42), and it will generally be more difficult to diagonalize. In this case we expect that the interaction partially removes the degeneracy. In table 1.1 we show the value of λ and the possible (degenerate) values of the total spin of the ground states of 4, 6 and 8 electrons. More details about the case of open k–shells, are given in Appendix A. For the non degenerate case however the solution is very simple. In fact the matrix (1.42) has only one physical solution, i.e. $\lambda \neq 0$, which is $\lambda = (n/2)^2$. For this solution the ground state energy is

$$E = E_0 + \frac{n^2 t f_0}{2a^{d-2}L^d} \tag{1.43}$$

and

$$\vec{J} = \begin{pmatrix} 1 \\ -1 \\ 1 \\ -1 \\ \vdots \\ 0 \\ 0 \\ \vdots \end{pmatrix}, \tag{1.44}$$

where, as was said before, the components different from zero correspond to the spectator electrons belonging to the unperturbed FS.

The expression of the momentum distribution can be easily derived from (1.33) and (1.36). Apart from a normalization factor, it is

$$n_{\mathbf{k}\uparrow} = \sum_{(\mathbf{k}_3,\cdots,\mathbf{k}_n)} L^2\left(\mathbf{k}, \mathbf{P} - \mathbf{k} - \sum_{i=3}^{n} \mathbf{k}_i,\, \mathbf{k}_3, \cdots, \mathbf{k}_n\right) \tag{1.45}$$

for spin up electrons, and analogously for spin down ones. The asymptotic solution of Eq. (1.43) and Eq. (1.44), implies that the only L's different from zero are

$$L^2(\{\mathrm{FS}\}) \simeq V^2/f_0^2 = \Delta, \tag{1.46}$$

$$L^2(\{\mathrm{FS} - \mathbf{k}_i - \mathbf{k}'_i + \mathbf{k}_o + \mathbf{k}'_o\}) \simeq \frac{1}{(\Delta E - \epsilon_{k_i} - \epsilon_{k'_i} + \epsilon_{k_o} + \epsilon_{k'_o})^2} = \Lambda(\mathbf{k}_i, \mathbf{k}'_i, \mathbf{k}_o, \mathbf{k}'_o), \tag{1.47}$$

where $\{\mathrm{FS}\}$ means the set of k vectors defining the Fermi sea, the $\mathbf{k}_i$ are wavevectors inside the FS while $\mathbf{k}_o$ are outside, and the prime refers to down spin electrons. Notice that $\mathbf{k}_i + \mathbf{k}'_i = \mathbf{k}_o + \mathbf{k}'_o$. As was said before, the asymptotic ground state is a linear combination of the unperturbed Fermi sea with the entire set of two–particle excitations. Let us consider first the case $\mathbf{k} \in \mathrm{FS}$. Then

$$\begin{aligned} n_{\mathbf{k}\uparrow} \;=\; & L^2(\{\mathrm{FS}\}) + \\ & \sum_{\mathbf{k}_i, \mathbf{k}'_i \in \mathrm{FS}, \mathbf{k}_i \neq \mathbf{k}} \\ & + \sum_{\mathbf{k}_o, \mathbf{k}'_o \notin \mathrm{FS}} L^2(\{\mathrm{FS} - \mathbf{k}_i - \mathbf{k}'_i + \mathbf{k}_o + \mathbf{k}'_o\}) \delta(\mathbf{k}_i + \mathbf{k}'_i - \mathbf{k}_o - \mathbf{k}'_o) = \end{aligned}$$

$$= \Delta + \sum_{\substack{\mathbf{k}_i,\mathbf{k}'_i\in FS \\ \mathbf{k}_o,\mathbf{k}'_o\notin FS}} \Lambda(\mathbf{k}_i,\mathbf{k}'_i,\mathbf{k}_o,\mathbf{k}'_o)\delta(\mathbf{k}_i+\mathbf{k}'_i-\mathbf{k}_o-\mathbf{k}'_o)+$$
$$- \sum_{\substack{\mathbf{k}'_i\in FS \\ \mathbf{k}_o,\mathbf{k}'_o\notin FS}} \Lambda(\mathbf{k},\mathbf{k}'_i,\mathbf{k}_o,\mathbf{k}'_o)\delta(\mathbf{k}+\mathbf{k}'_i-\mathbf{k}_o-\mathbf{k}'_o) = \Delta+\Omega-\Xi(\mathbf{k})^-, \quad (1.48)$$

which also serves as a definition for Ω and $\Xi(\mathbf{k})^-$. When $\mathbf{k}\notin$ FS then

$$n_{\mathbf{k}\uparrow} = \sum_{\substack{\mathbf{k}_i,\mathbf{k}'_i\in FS \\ \mathbf{k}'_o\notin FS}} L^2(\{FS+\mathbf{k}+\mathbf{k}'_o-\mathbf{k}_i-\mathbf{k}'_i\})\delta(\mathbf{k}_i+\mathbf{k}'_i-\mathbf{k}-\mathbf{k}'_o) = \Xi(\mathbf{k})^+, \quad (1.49)$$

where the $+$ or $-$ refers to $\mathbf{k}\notin$ FS or $\mathbf{k}\in$ FS respectively. It is easy to see that

$$\sum_{\mathbf{k}\in FS} n_{\mathbf{k}\uparrow} = \frac{n}{2}(\Delta+\Omega)-\Omega \quad (1.50)$$

and

$$\sum_{\mathbf{k}\notin FS} n_{\mathbf{k}\uparrow} = \Omega. \quad (1.51)$$

If we properly normalize the momentum distribution, i.e. we divide by

$$\frac{2\sum_{\mathbf{k}} n_{\mathbf{k}\uparrow}}{n} = \Delta+\Omega, \quad (1.52)$$

then we find

$$n_{\mathbf{k}} = \frac{\Delta+\Omega-\Xi(\mathbf{k})^-}{\Delta+\Omega} \simeq 1-\frac{\Xi(\mathbf{k})^-}{\Delta} \quad (1.53)$$

for $\mathbf{k}\in$ FS. Outside the Fermi surface, instead

$$n_{\mathbf{k}} = \frac{\Xi(\mathbf{k})^+}{\Delta+\Omega} \simeq \frac{\Xi(\mathbf{k})^+}{\Delta.} \quad (1.54)$$

To obtain (1.53)–(1.54) we have assumed $\Delta \gg \Omega$. This is actually true in our approximation (i.e. $L\to\infty$ while n is finite), because $\Omega \simeq n\cdot\Xi^-(\mathbf{k})$, where, as we are going to show, $\Xi^-(\mathbf{k})\sim L^4$, so that $\Omega\sim L^4 \ll \Delta$ ($\sim L^4\log^2 L$ in $d=2$ and $\sim L^6$ in $d=3$). It is possible to evaluate the asymptotic behaviour of $n_{\mathbf{k}}$ close to the Fermi surface. In this

case, orders of magnitude are

$$\Xi(\mathrm{k})^- \sim \Xi(\mathrm{k})^+ \sim \frac{n}{2} \sum_{\mathbf{q}\notin \mathrm{FS}} \frac{1}{(2\epsilon_{\mathbf{q}} - 2\epsilon_f)^2} \sim L^d n k_f^{d-4} \tag{1.55}$$

(the factor $n/2$ counts the down spin electrons, i.e k'_i, inside the FS). This means that

$$\frac{\Xi(\mathrm{k})^-}{\Delta} \sim k_f^{2(d-2)} f_0^2 \tag{1.56}$$

and that the jump Z in the momentum distribution scales to one when $k_f \sim n^{1/d}/L \to 0$ as

$$1 - Z = 1 - (n_{k_f - 0\uparrow} - n_{k_f + 0\uparrow}) \sim k_f^{2(d-2)} f_0^2 \sim \begin{cases} (k_f a)^2 & \text{in 3D} \\ \log^{-2} L & \text{in 2D.} \end{cases} \tag{1.57}$$

1.4 Extension to finite density

In the previous sections, we have presented a solution for the ground–state of n electrons in the $d = 2$ and $d = 3$ Hubbard model. The results are simple, analytical and formally exact. However, they are asymptotic in the sense that only the lowest order terms of an ordered expansion in powers of $1/\log L$ (for $d = 2$) and $1/L$ (for $d = 3$) is obtained. In particular, we have not yet shown that the coefficients of the higher orders in this expansion are all finite, for any finite number of particles n. With this only provision, the results presented are exact.

We have obtained the ground–state energy, total momentum, symmetry, wavefunction and momentum distribution. For a general closed shell in k-space (i.e. $n = 2, 10, 18, ...$ in $d = 2$) the ground–state is a $\mathbf{P} = \mathbf{0}$ singlet, with energy given by Eq. (1.43). The situation is considerably richer for open shells, which display degeneracy (see Appendix A). However, the basic physics should converge to that of closed shells for large n.

The momentum distribution $n(\mathbf{k})$ for the closed shell case yields a Fermi jump [Eq. (1.57)] which, modulo U-independent logarithmic corrections, scales asymptotically to 1 for $d = 2$ and zero density.

If we assume, reasonably but without proof, that our results can be extrapolated to small but finite densities $\rho = n/(aL)^d$, we obtain formally the same ground–state energy and momentum distribution obtainable by T-matrix technique in the low-density limit[12, 13, 14, 15]. The analogy between finite n, $\rho \to 0$ and finite ρ is direct in $d = 3$, where the low energy limit of the scattering amplitude is a constant. In this case, by substituting $f_0 = 4\pi a$ in Eq. (1.43), we obtain

$$E = E_0 + n2\pi\rho t a^3, \tag{1.58}$$

which is exactly the first order correction obtained by Galitskii[12]. In the same way, it is not difficult to realize that the momentum distribution as given by Eq. (1.53) and (1.54), coincides with the general expression obtained for example by Belyakov[25].

In $d = 2$ the generalization is not so straightforward because the low energy limit of the scattering amplitude does depend on the energy. The consequence is that the simple result (1.43) cannot be extrapolated at finite density simply because we have no *a priori* prescription to extend $f_0 = 2\pi/\log L$ to finite density. This problem can be solved by a little refinement of our calculations, which amounts to evaluate corrections up to second order in $1/\log L$. The second order correction to the ground–state energy, which is proportional to $1/\log^2 L$, can, as usual, be obtained simply through the first order correction to the eigenvector $\vec{J}$ given by Eq. (1.44). Unfortunately, the next order correction to the momentum distribution (proportional to $1/\log^3 L$) is more complicated, because it involves the second order correction to the eigenvector $\vec{J}$, which is harder to evaluate. For simplicity, let us consider for the moment only the next order correction to the ground–state energy. It is not difficult to show that Eq. (1.39) is the large size limit of another equation, namely

$$\hat{M} \cdot \vec{J} = L^{d-2}\alpha(L)\hat{\chi} \cdot \vec{J}, \tag{1.59}$$

where $\hat{M}$ and $\vec{J}$ are the same of Eq. (1.39), while $\hat{\chi}$ is a diagonal matrix in the "spectator electron" configurations of the unperturbed FS, whose diagonal elements are

$$\chi(\mathbf{k}_1, \mathbf{k}_2) = -\frac{1}{L^d} \sum_{\mathbf{q},\mathbf{q}' \notin \mathrm{FS}} \delta(\mathbf{q} + \mathbf{q}' - \mathbf{k}_1 - \mathbf{k}_2) \frac{1}{\epsilon_{\mathbf{k}_1} + \epsilon_{\mathbf{k}_2} - \epsilon_{\mathbf{q}} - \epsilon_{\mathbf{q}'}}. \tag{1.60}$$

In Eq. (1.60) $\mathbf{k}_1$ and $\mathbf{k}_2$ are the two states (one for a spin up electron, the other for a spin down) which belong to the unperturbed FS and are going to be excited to higher states

$\mathbf{q}$, $\mathbf{q}'$. In other words, all electrons inside the FS are spectators except $\mathbf{k}_1, \uparrow$ and $\mathbf{k}_2, \downarrow$. In the large–size, zero density limit $L \to \infty$, $n/L^d \to 0$, the matrix $L^{d-2}\alpha(L)\hat{\chi} \to \lambda \hat{I}$ where $\hat{I}$ is the identity operator and λ has the same meaning of Eq.(1.39) and Eq. (1.40), so that we recover all the results already quoted. It is important however to retain the full momentum dependence of $\hat{\chi}$. It is then easy to show that the solution of Eq. (1.59) (we restrict to closed shells, because the differences with the open shell case is expected not to survive in the thermodynamic limit) is now

$$\alpha(L) = L^{2-d} \sum_{\mathbf{k}_1, \mathbf{k}_2 \in \mathrm{FS}} \frac{1}{\chi(\mathbf{k}_1, \mathbf{k}_2)}. \tag{1.61}$$

From Eq. (1.59) it is also possible to calculate the second order correction to the components of the eigenvector $\vec{J}$ corresponding to the spectator electron configurations inside the FS. This is however not enough, because other spectator configurations are also allowed to that order (in particular those which refer to three- and four-particle correlations), and Eq. (1.59) is not sufficient to calculate these corrections, unlike it was the case for the energy. From Eq. (1.61) the ground–state energy turns out to be

$$E = E_0 + \frac{1}{L^d} \sum_{\mathbf{k}_1, \mathbf{k}_2 \in \mathrm{FS}} \frac{1}{\chi(\mathbf{k}_1, \mathbf{k}_2)} \tag{1.62}$$

which, in the limit $L \to \infty$, is just Eq. (1.43). In order to obtain self-consistent results, the sum in Eq. (1.62) must be expanded in powers of $1/\log L$ up to second order. Hence Eq. (1.62) provides the *formally correct generalization of the energy shift to small but finite density, in a way which is unique.*

One can immediately see that Eq.(1.62) coincides with the ground state energy obtainable by the T–matrix technique [see for example Ref. [14]]. However, the method we have presented here, allows to go systematically beyond the simple T–matrix approximation. By means of our technique, it is possible to generate a well ordered expansion of the

ground–state properties in terms of the scattering amplitude f_0, and, from this point of view, it is analogous to the approach described in Ref. [29].

The analytical expression of the function $\chi(\mathrm{k}_1, \mathrm{k}_2)$ at leading order in the low–density limit, is simply

$$\chi(\mathrm{P}/2+\mathrm{k}, \mathrm{P}/2-\mathrm{k}) = -\frac{1}{4\pi t}\left(\log(k_f a) + \frac{1}{2}\log\frac{[(k_f+P/2)^2-k^2]}{k_f^2}\right) \tag{1.63}$$

Equation (1.63) diverges both for $k_f a \to 0$ and for $P = 0$ and $k = k_f$. Hence there is strictly no contribution to $E-E_0$ of Eq. (1.62) from scattering at zero total momentum[26]. However, the error made by ignoring this cancellation, i.e. by ignoring the second term in Eq. (1.63), is small, of order $1/\log^2(k_f a)$ [27]. Therefore, if we are only interested in the first order in $1/\log(k_f a)$ corrections, then we can consistently take

$$\chi(\mathrm{k}_1, \mathrm{k}_2) \simeq -\frac{1}{4\pi t}\log(k_f a) \tag{1.64}$$

in Eq. (1.62) which yields finally

$$E = E_0 - n\frac{2\pi t \rho a^2}{\log(\rho a^2)}. \tag{1.65}$$

This is the same expression we would have obtained by simply substituting $f_0 = 2\pi/\log L$ in Eq. (1.43) with $-2\pi/\log(k_f a)$.

The same consideration holds for the momentum distribution, whose jump at the Fermi level turns out to be[28]

$$Z = 1 - \frac{4\log 2}{\log^2(\rho a^2)} \tag{1.66}$$

The next–order correction to the momentum distribution is harder to evaluate. However one can show that Eqs. (1.53) and (1.54) give the right result with the same definition of the functions $\Xi^+(\mathrm{k})$ and $\Xi^-(\mathrm{k})$, and with the only provision that the correct function

$\Lambda(\mathbf{k}_i, \mathbf{k}'_i; \mathbf{k}_o, \mathbf{k}'_o)$ to be used is

$$\begin{aligned}\Lambda(\mathbf{k}_i, \mathbf{k}'_i; \mathbf{k}_o, \mathbf{k}'_o) &= \frac{1}{(\epsilon_{\mathbf{k}_o} + \epsilon_{\mathbf{k}'_o} - \epsilon_{\mathbf{k}_i} - \epsilon_{\mathbf{k}'_i})^2} \left(\frac{1}{\chi^2(\mathbf{k}_i, \mathbf{k}'_i)} + \right. \\ &+ \frac{2(2tf_0)^3}{L^2} \sum_{\mathbf{k}\in \mathrm{FS}} \sum_{\mathbf{q}'\notin \mathrm{FS}} \delta(\mathbf{k}_o + \mathbf{q}' - \mathbf{k} - \mathbf{k}'_i) \frac{1}{\epsilon_{\mathbf{k}_o} + \epsilon_{\mathbf{q}'} - \epsilon_{\mathbf{k}} - \epsilon_{\mathbf{k}'_i}} + \\ &\left. + \frac{2(2tf_0)^3}{L^2} \sum_{\mathbf{k}'\in \mathrm{FS}} \sum_{\mathbf{q}\notin \mathrm{FS}} \delta(\mathbf{k}'_o + \mathbf{q} - \mathbf{k}' - \mathbf{k}_i) \frac{1}{\epsilon_{\mathbf{k}'_o} + \epsilon_{\mathbf{q}} - \epsilon_{\mathbf{k}_i} - \epsilon_{\mathbf{k}'}} \right). \end{aligned} \tag{1.67}$$

The first term inside curly brackets corresponds to the spectator configurations of the Fermi sea [it is simply the solution of Eq. (1.59)], while the second term derives from the three-particle correlations, which must also be included at this order. These corrections remain of higher order in $1/\log(k_f a)$, even when we generalize the results to finite density. This is not trivial, and was not *a priori* evident nor guaranteed. In particular, there might have been terms, e.g. like $n/\log L$, which are well ordered in $1/\log L$, but diverges when $n \to \infty$. However, *these types of terms turn out to be strictly absent, at least up to third order.* Let us see qualitatively, how this happens. The function $\Lambda(\mathbf{k}_i, \mathbf{k}'_i; \mathbf{k}_o, \mathbf{k}'_o)$ which gives the Fermi jump through Eqs. (1.48)–(1.54), is just the square of a function L, that is from Eq. (1.36)

$$L(\mathbf{k}_1, \mathbf{k}_2, \mathbf{k}_3, ..., \mathbf{k}_n) = \frac{J(\mathbf{k}_3, \mathbf{k}_4, ..., \mathbf{k}_n) - J(\mathbf{k}_3, \mathbf{k}_2 ..., \mathbf{k}_n) + \cdots}{(E - \epsilon_{\mathbf{k}_1} - ... - \epsilon_{\mathbf{k}_n})}.$$

We see that, in order to obtain consistent results to third order in $1/\log L$, it is necessary to expand up to first order the energy denominator in $\Delta E = E - E_0$. This expansion, however, yields terms proportional to $\Delta E \sim n\rho/\log\rho$, which is not well ordered at finite density, as discussed earlier. However, a consistent calculation shows that, at least up to third order in f_0, each time one of these dangerous terms appears, it is cancelled by an

identical one coming from the numerator. Thus, in the end, the net result is well ordered in $1/\log(k_f a)$ as well as in $1/\log L$. We have not evaluated explicitly the next order correction to the momentum distribution by means of Eq. (1.67), but it is not difficult to convince ourselves that this correction is finite.

Therefore, unless some yet undetected change of regime, or phase transition, takes place precisely for $n \to \infty$, there is every reason to believe that our results extended to very low-density, remain correct also in $d = 2$. We stress in particular that the formal coincidence with our extrapolated results for finite electron numbers of Eq. (1.43) was by no means expected from the start. It is interesting to note, as a side remark, that also in $d = 1$ the $\rho = 0$ point is non-singular, so that even there, the finite n, $n/L^d \to 0$ results extrapolate smoothly into the finite density, small ρ regime[24].

To conclude this section, we would like to point out the important role played in our calculation by the interaction correction $\Delta E/V$ to the energy density. We have shown how this quantity can be used as an effective expansion parameter, to be determined self–consistently. This allows a calculation of all the ground state properties of dilute short–range–interacting Fermi systems in more than one dimension. We have found that in $d \geq 2$ this expansion is well defined and the ground state does not show anomalous properties, with respect to the non–interacting case. For $d < 2$, $\Delta E/V$ is not a small parameter, and the same expansion does not hold. Even though the method does not work in this case, it allows to draw some important conclusions which are known to be valid in 1D, e.g. the absence of a finite jump in the momentum distribution.

The connection, suggested by our calculations, between $\Delta E/V$ and possible anomalies induced on the ground state by the interaction, might have its explanation in a simple

argument[24]. Let us consider a non interacting Fermi gas on a d–dimensional lattice. At low density, the energy is:

$$\left(\frac{E}{V}\right)_{U=0} \simeq -2dt\rho + c_d t \rho^{(d+2)/d} \tag{1.68}$$

where c_d is a constant depending just on dimensionality. The first term in (1.68) is just the energy density of a system of non interacting bosons. The second term is a pure effect of Pauli principle, and can be in a sense interpreted as a statistical interaction correction. If U is switched on, it can be shown, on very general grounds, that the energy density has to change by an amount:

$$\left(\frac{E}{V}\right)_{U\neq 0} - \left(\frac{E}{V}\right)_{U=0} \sim f_0(k_f)\rho^2 \tag{1.69}$$

where $f_0 \sim k_f \sim \rho$ in 1D, $f_0 \sim 1/\log\rho$ in 2D, while it is a constant in $d \geq 3$. Now, from Eqs. (1.68) and (1.69), it turns out that *while in $d \geq 2$ the interaction correction is, at low density, always negligible with respect to what we called the statistical correction, in 1D they are of the same order, i.e. ρ^3, in the density.* We conclude that the interaction not only is relevant in the latter case, but also its effects are comparable to those of Pauli principle, thus suggesting anomalous ground state behavior in 1D but not in $d \geq 2$. We have shown in more detail in the previous sections, that this type of qualitative argument is indeed correct. We have in fact demonstrated that, assuming the interaction correction negligible with respect to the statistical one, the ground state properties do not show anomalies with respect to the non interacting case. If that assumption is not true, the opposite scenario is realized. We have also shown that the former case does occur in $d \geq 2$, but does not in 1D, in agreement with available exact solutions.

1.5 Anderson's singular forward scattering and other open questions

Besides the ground state properties, which, as we have shown in the previous Sections, can be accurately calculated, at least in the very low–density regime, an equally important problem regards the nature of the low lying excitations of a 2D Fermi gas. Two different scenarios can be realized: either the Landau Fermi–liquid theory is valid and the elementary excitations are quasi–particles in a one–to–one correspondence with the excitations of a non interacting Fermi gas; or they have completely different properties, as it is the case in 1D.

In this Section, we will discuss some available results concerning this controversial problem, which are closely related to the kind of calculations presented in the previous Sections. Most of them support the point of view that Landau theory applies in 2D as well as in 3D. They are essentially based on very old studies of the dilute Fermi gases[12, 30, 13]. We present these results at the end of this Section, while we start by discussing the opposite point of view, according to which Landau quasiparticles are not stable excitations in 2D.

This scenario was originally proposed by Anderson[7], who pointed out that a non–Fermi liquid RVB–type state could explain some of the anomalous properties of the Cu–O planes in the High Tc superconductors. More recently, he has formulated[10] quite general arguments against the applicability of Landau theory in 2D. These arguments are based purely on dimensionality effects, independently from the specific details of each model.

1.5.1 Derivation of the singular forward scattering

The mechanism which is, according to Anderson, responsible for the breakdown of Landau theory, is based on the existence of a *singular forward scattering* between two opposite

spin electrons with almost equal momentum, and on the ability of this vertex to destroy Fermi–liquid behavior. Even though it is possible to identify such a singular interaction, the successive step of proving that it generates non Fermi liquid (FL) behavior, is still not completely clear. First of all we sketch our derivation of the singular forward scattering vertex.

Let us consider the correction to the total energy (1.62) at low density. From that expression, we can define the energy shift due to the interaction between a spin up electron of momentum $\mathbf{k}_1$ and a spin down electron of momentum $\mathbf{k}_2$, both belonging to the Fermi sea. It turns out to be simply:

$$\Delta E(\mathbf{k}_1, \mathbf{k}_2) = \frac{1}{L^d \chi(\mathbf{k}_1, \mathbf{k}_2)}. \tag{1.70}$$

By analogy with the problem of the scattering from an impurity, we can interpret (1.70) as due to a shift in the allowed momenta. This point of view has proved quite fruitful in 1D[31]. Let us assume that the interaction energy is indeed generated by a shift $\Delta\mathbf{k}/2$ to $\mathbf{k}_1$ and a corresponding shift $-\Delta\mathbf{k}/2$ to $\mathbf{k}_2$, due to momentum conservation. From the symmetry between the two momenta, the shift $\Delta\mathbf{k}$ is assumed to be parallel to $\mathbf{Q} \equiv \mathbf{k}_1 - \mathbf{k}_2$, and we can write the momentum shift in terms of a "phase shift" δ as:

$$\Delta\mathbf{k} = \frac{\delta}{L}\frac{\mathbf{Q}}{Q}. \tag{1.71}$$

We immediately obtain the equation for δ:

$$\frac{\Delta E(\mathbf{k}_1, \mathbf{k}_2)}{ta^2} = \left(\mathbf{k}_1 + \frac{\delta}{2L}\frac{\mathbf{Q}}{Q}\right)^2 + \left(\mathbf{k}_2 - \frac{\delta}{2L}\frac{\mathbf{Q}}{Q}\right)^2 - k_1^2 - k_2^2, \tag{1.72}$$

whose solution is:

$$\delta = \sqrt{(LQ)^2 + \frac{2L^{2-d}}{ta^2\chi(\mathbf{k}_1, \mathbf{k}_2)}} - LQ. \tag{1.73}$$

Notice that when $Q \sim 1/L$, this phase shift is finite in 2D, while is of order $O(1/L)$ in 3D. By means of Eq. (1.73), we can calculate the energy shift induced on the particle at momentum $\mathbf{k}_1$, by the electron at $\mathbf{k}_2$, which can be interpreted as an effective interaction potential $v_{\rm eff}(\mathbf{k}_1;\mathbf{k}_2)$ felt by $\mathbf{k}_1$

$$\begin{aligned} v_{\rm eff}(\mathbf{k}_1;\mathbf{k}_2) &= ta^2L^d\left[(\mathbf{k}_1+\Delta\mathbf{k}/2)^2-k_1^2\right]= \\ &= ta^2\left\{\frac{1}{2ta^2\chi(\mathbf{k}_1,\mathbf{k}_2)}+\frac{\delta L^{d-1}}{2}\frac{k_1^2-k_2^2}{Q}\right\}. \end{aligned} \tag{1.74}$$

The second term on the right hand side of Eq. (1.74) diverges as the linear size L both in 2D and 3D. However, this divergence does not affect the equal time properties, because it cancels with the analogous contribution coming from $v_{\rm eff}(\mathbf{k}_2;\mathbf{k}_1)$. From the expression of the phase shift Eq. (1.73), it comes out that the singular part of the effective potential Eq. (1.74) is strongly peaked at $Q = |\mathbf{k}_1 - \mathbf{k}_2| = 0$, and vanishes as $1/Q$ for large relative momenta. Equation (1.74) coincides with the *singular forward scattering* introduced by Anderson, even though we derived it in a different, but equivalent, way.

1.5.2 Physical consequences of the singular interaction

According to Anderson[10], who has originally derived Eq. (1.74), this interaction is the signature of the breakdown of Fermi liquid (FL) theory in 2D. This breakdown should manifest itself as in 1D, implying both power law decay of the correlation functions with exponents different from the non–interacting ones, and spin–charge decoupling. The arguments Anderson gives, are partly based on the analogy between the results of this calculation and the orthogonality catastrophe induced by a single impurity in a metal[32]. However, the infinite mass of the impurity is crucial in the original argument; in the present case, the finite electron mass allows for recoil. The "recoil effect", which naïvely

should prevent an analogous catastrophe in this problem, is claimed to be inhibited by the presence of the Fermi sea of occupied states. However, even though it is not difficult to derive the singular vertex (1.74), which, as we have shown, is perfectly compatible with all our results, we can not prove that it really gives rise in the end to genuine non Fermi–liquid behavior.

First of all, it is not obvious that the phase shifts (1.73) should play the same role of those which appear in the single impurity problem and are responsible for the orthogonality catastrophe. Secondly, even assuming that, we do not get the orthogonality catastrophe with the phase shifts defined as in Eq. (1.73)[33]. Let us suppose, in fact, that the consequence of adding one particle of spin up at the Fermi momentum, can indeed be absorbed in a phase–shift for the down–spin electrons. This means that, if a down–spin electron at momentum $\mathbf{k} = 2\pi\mathbf{m}/L$ ($\mathbf{m}$ is an integer vector in d–dimension), was previously represented by a wave–function

$$\psi_{\mathbf{k}}(\mathbf{r}) = \frac{1}{\sqrt{V}} e^{i\mathbf{q}\cdot\mathbf{r}}, \tag{1.75}$$

after an up–spin electron is added to the Fermi sea at momentum:

$$\mathbf{k}_f = 2\pi\mathrm{M}/L, \tag{1.76}$$

its wave–function will be modified into:

$$\phi_{\mathbf{k}}(\mathbf{r}) = \frac{1}{\sqrt{V}} e^{i(\mathbf{k}+\Delta\mathbf{k})\cdot\mathbf{r}}. \tag{1.77}$$

According to Eqs. (1.73) and (1.71), the momentum shift is approximately given by:

$$\Delta\mathbf{k} = \epsilon\frac{2\pi}{L}\frac{\mathbf{m}-\mathrm{M}}{(\mathbf{m}-\mathrm{M})^2} \equiv \frac{2\pi}{L}\delta, \tag{1.78}$$

with ϵ proportional to the scattering amplitude f_0. The residue Z, is proportional to the overlap between two Slater determinants, one with orbitals given by Eq. (1.75), the other with the modified plane–waves (1.77). It can be shown that this overlap is simply the determinant of the matrix

$$\Gamma_{\mathbf{k},\mathbf{q}} = \sum_{\mathbf{r}} \psi_{\mathbf{k}}(\mathbf{r})^* \phi_{\mathbf{q}}(\mathbf{r}), \tag{1.79}$$

where the matrix indices are the momenta $\mathbf{k}$ and $\mathbf{q}$, which lie inside the Fermi surface of N electrons. By summing the geometric series, one gets:

$$\Gamma_{\mathbf{k},\mathbf{q}} = \Pi_\alpha \frac{1 - e^{i2\pi\delta_\alpha}}{1 - e^{i2\pi(m_\alpha - n_\alpha + \delta_\alpha)/L}}, \tag{1.80}$$

with α labelling the components of the vectors ($\alpha = 1, ..., d$), and with the vectors $\mathbf{n}$ and $\mathbf{m}$ defined by $\mathbf{k} = 2\pi\mathbf{n}/L$, and $\mathbf{q} = 2\pi\mathbf{m}/L$. By definition, δ depends only on $\mathbf{m} - \mathbf{M}$ ($\mathbf{M}$ is the location of the added electron). At low density (when the number of electrons N is much smaller than the number of sites L^d), the matrix can be approximated to:

$$\Gamma_{\mathbf{k},\mathbf{q}} = \frac{1}{(\pi)^2} \Pi_\alpha \frac{\sin(\pi\delta_\alpha)}{m_\alpha - n_\alpha + \delta_\alpha}. \tag{1.81}$$

The determinant of this matrix can be exactly calculated in 1D, and, assuming constant phase–shifts, it is:

$$Z \equiv \det\Gamma \propto N^{-\delta^2}, \tag{1.82}$$

which is the well–known expression of the orthogonality catastrophe[32]. Unfortunately, in $d > 1$, the determinant can not be evaluated exactly. However, a numerical calculation can be easily performed up to a number of particles large enough to obtain a reliable size scaling. We have done this calculation in 2D[33], with the definition of δ given by Eq. (1.78), and we have found that the overlap saturates, for large number of particles, to a finite value, smaller than one but definitely nonzero. Therefore the phase–shifts, defined

as in (1.78), do not appear to produce an orthogonality catastrophe in 2D because, unlike those in the single impurity problem, they are strongly momentum dependent, and in particular, we suspect, because they vanish like $1/|\mathbf{m}-\mathbf{M}|$ for large $|\mathbf{m}-\mathbf{M}|$.

Therefore, even though the presence of a *singular forward scattering* is confirmed by our results, we still do not know if it causes a breakdown of ordinary FL theory. For example, in a perturbative treatment, e.g. the T–matrix technique, this singularity is completely invisible. This is because the pseudo–potential which enters in any perturbative expansion is, rather than each single $v_{\rm eff}$ of Eq. (1.74), the symmetrical combination $v_{\rm eff}(\mathbf{k}_1;\mathbf{k}_2)+v_{\rm eff}(\mathbf{k}_2;\mathbf{k}_1)$, which is not singular, unless the first term on the left hand side of Eq. (1.74), i.e. $1/\chi(\mathbf{k}_1,\mathbf{k}_2)$, diverges.

In a recent paper, Stamp[34], assuming the residual quasi–particle amplitude $f_{\mathbf{k}_1,\mathbf{k}_2}$ to have the singularity predicted by Anderson, has claimed that the quasi–particle residue Z vanishes at the Fermi energy, thus destroying the FL picture in 2D. In particular, he has shown that Z vanishes at the Fermi energy as a power law of $|k-k_F|$, with an exponent proportional to the square of the phase shift of Eq. (1.73), in agreement with what Anderson conjectured by analogy with the orthogonality catastrophe. The exponent he finds, is, however, not exactly that appearing in the single impurity problem, due to an additional factor ϵ_F/ω_0, ω_0 being an energy scale introduced as a cut–off of diverging integrals. He does not make any assumption on the origin of this scale, but, should ω_0 not depend on density, his results might also be reconciled with the low density perturbative calculations we have presented in the previous Sections.

On the other hand, we perfectly agree that non–Fermi liquid behavior in the form of spin–charge separation, may be easily derived if a strongly momentum dependent pseudo–

potential is used in place of the Hubbard interaction. In particular, should the pseudo–potential diverge as the linear size L, for small relative momentum $|\mathbf{Q}|$ ($\mathbf{Q}$ is the difference of the momenta of the two scattering electrons), and vanish for $|\mathbf{Q}| \to \infty$, as Anderson proposes, then it becomes possible for spin–charge decoupling to occur in 2D (but not in 3D). In this case, in fact, the interaction at small relative momentum is not any longer irrelevant in the renormalization group sense[35], and has to be considered at the same footing of the kinetic energy. This can be done by applying, for example, a bosonization technique in $d > 1$, derived long time ago by Luther[36] and recently re–formulated by Haldane[35]. It is then easy to see that such a singular forward scattering plays exactly the role of the g_4 interaction in the 1D g–ology models[18]. This interaction is well known to give rise to spin–charge decoupling, without generating anomalous exponents (see Section 2.4). The effective g_4, which should appear in the 1D–equivalent model, is approximately given by $v_{\rm eff} \times L^{1-d}$. In 2D, this turns out to be of order O(1), if the effective pseudo–potential diverges as the linear size L; on the contrary, in 3D, it is only of order $O(1/L)$, and therefore irrelevant.

We conclude that a forward scattering singularity, if it exists, does generate spin–charge decoupling in 2D, while it does not in 3D. Furthermore, the same line of argument would suggest its inability to give rise to anomalous exponents in any dimension greater than one. On the other hand, no convincing derivation of such interaction in realistic electronic models is available yet, and this problem remains open.

1.5.3 Low–density perturbation theory

Contrary to the strong coupling picture previously discussed, other approaches[13, 14, 16, 15] suggest that in 2D, at least in the low density regime, Landau Fermi–liquid theory is

valid. The claim is based on standard calculations of the single–particle Green function, obtained in the low–density regime after a T–matrix resummation[12]. This technique allows a perturbative expansion, even for strong short range repulsion, so it can be safely applied to the strong–coupling, but low–density, limit of the Hubbard model. All these studies find a quasi–particle decay rate which vanishes at the Fermi surface as $\omega^2 \log(1/|\omega|)$. This implies that the quasi–particles are well defined stable excitations, and, in turns, as a result of the Kramers–Kronig relations, that the jump in the momentum distribution is finite. Both these properties are usually considered as clear signatures that Landau Fermi–liquid theory holds. Once one assumes that the quasi–particles are well defined objects, then it is easy to derive, from the expansion of the total energy in Eq. (1.62) up to second order in f_0, all the Landau f–functions[16], following a method first applied in 3D by Abrikosov and Khalatnikov[30]. The resulting scattering amplitudes between the quasi–particles on the Fermi surface, turns out to be finite[16], and apart from some subtleties related to the presence of hole anti–bound states in the two–particle spectrum, nothing really special occurs. All these results, agree with our calculations, as we said in the preceeding Section, but contrast with Anderson's conjecture. However, we want to point out two aspects of these calculations, which, in our opinion, lead to the conclusion that some caution is still necessary to state definitively that Landau theory works in 2D.

The first is that, a ground state which does not show any anomalous property, does not necessarily imply that Landau Fermi–liquid theory is valid. In particular, a perfectly innocuous ground state, e.g. with a finite jump in the momentum distribution at the Fermi surface, is compatible with non FL excitations showing *spin–charge decoupling*, which is exactly what Anderson's singular forward scattering suggests, as we have just discussed.

This further implies that our calculations do not exclude such a possibility.

Specifically, *should spin–charge separation take place, the breakdown of FL theory would not be signaled by any logarithmic singularity in perturbation theory*, which is usually related to anomalous exponents, but it would rather appear as *an analytical property of the re–summed perturbation series*. In analogy to what happens in 1D (see Section 2.4), spin–charge separation is, in general, expected to manifest itself through the appearance of branch cut singularities in the single–particle Green function, replacing the usual quasi–particle pole. The change in the analytical properties of the Green function, can be recognized only away from the Fermi surface, both in frequency and in momentum, while no indication is found if either frequency or momentum are exactly at the Fermi surface. This can be easily realized by considering a simple 1D model where only spin–charge separation occurs (see Section 2.4). In absence of interaction, the 1D single–particle Green function is simply:

$$G(k_F + q, \omega) = \frac{1}{\omega - v_F q + i\eta \mathrm{sign} q} \tag{1.83}$$

while, once the interaction is switched on in this particular model, the Green function becomes:

$$G(k_F + q, \omega) = \frac{1}{\sqrt{(\omega - u_\rho q + i\eta \mathrm{sign} q)(\omega - u_\sigma q + i\eta \mathrm{sign} q)}} \tag{1.84}$$

where the holon and spinon velocities u_ρ and u_σ are simple linear functions of the interaction. Were one to expand (1.84) at $\omega = 0$, in powers of the interaction, i.e. in powers of $(u_\rho - v_F)$ and $(u_\sigma - v_F)$, then one could perfectly conclude that the interaction simply renormalizes the Fermi velocity. This conclusion is enforced by noting that, at $q = 0$, the Green function is not corrected at all by interaction. Only if the expansion is carried out both at q and ω different from zero, it is possible to realize that the interaction instead

really changes the analytical properties of the Green function, thus destroying Fermi liquid behavior.

To our knowledge, none of the available perturbative calculations of the 2D Green function[13, 14, 15], and of the Landau f–functions[16], has really looked into this aspect. We therefore believe that the problem of a possible occurrence of *spin–charge separation* in 2D interacting fermion systems, deserves more investigation, especially from the point of view of establishing the general features of such a behavior in more than one dimension, before concluding that Fermi liquid theory really works in 2D. What we can safely assert, is that, at low density, anomalous exponents are absent, which means that the asymptotic behavior of the correlation functions is not modified by the interaction and, consequently, that the jump of the momentum distribution at the Fermi surface, is finite.

There is also another reason why some caution on the low–density expansion results, has to be taken. It is not difficult to see that the value of the total energy which we obtained in the previous Sections, up to second order in the scattering amplitude $f_0 = -2\pi/\log(k_f a)$ [see Eq. (1.62)], (which coincides with that obtained in the low density limit by Ref. [14]), is not so accurate when compared to the energies of states with different symmetries, which are not expected to occur, at least at low density. In particular, if we compare the energy (1.62) with that of a fully ferromagnetically polarized system, we find that the two values cross at very low density, too low to believe that a real ferromagnetic transition takes place. According to our calculation, this should occur already at $f_0 = 2$, which according to our estimates of $f_0 \simeq -2\pi/\log(k_f/k_0)$ gives $k_f \simeq 0.043 k_0$, where k_0 is the inverse of the 2D scattering length, of order π/a. In terms of density, it means that already at $\rho_c \simeq 0.003$, the second order T–matrix results are not good enough, and higher

orders are needed. Moreover, one might compare the total energy of the paramagnetic state resulting from our calculation, with only partial polarized states. In this way the critical value $\rho_c \simeq 0.003$ can be much lowered. For example, let us consider, as a trial wave–function, the state where *only the outer shell of electrons is spin–polarized.* It is not difficult to apply the method we have discussed in the previous Sections to this state, and find that the difference ΔE between its total energy and that of the paramagnetic state (1.62) is simply:

$$\Delta E = ta^2 m \left[\left(k_F + \frac{2\pi}{La} \right)^2 - k_F^2 \right] - \frac{m^2}{L^2 \chi(k_F, k_F)} \tag{1.85}$$

where $m \simeq 2\pi k_F La$ is the total number of points on the Fermi surface. The polarized state acquires a lower energy than the paramagnetic one, if Eq. (1.85) vanishes, which happens at $f_0 = 1$. This value would correspond to a density $\rho = \mathrm{e}^{-2\pi}\rho_c \simeq 2 \times 10^{-3}\rho_c$, which is extremely low. Therefore, due to the peculiar 2D logarithmic dependence of f_0 upon the density, we find *a strong tendency of the Fermi surface towards spin–polarizing the outer shells.* It is still a controversial problem if Nagaoka's ferromagnetic state, which occurs when one hole is created in an otherwise half–filled 2D Hubbard model, might extend to finite density of holes, but is seem not plausible that it might extend up to such a high hole–density. We think therefore that this calculation does not imply that a phase transition towards ferrimagnetic states indeed occurs, but, more likely, it simply suggests that in 2D, the convergence of low–density expansion is not as good as in 3D, and therefore higher order terms need to be evaluated, before one can safely state that something or nothing anomalous really happens.

Chapter 2

Stability of 1D Luttinger liquid behavior in models of coupled chains

In this Chapter, we will discuss various aspects of the problem of 1D chains of interacting fermions, coupled by a transverse hopping.

In Section 2.1, we study the simple case of two coupled chains of spinless fermions. This problem is quite interesting, because it can be mapped onto a model describing a single chain of spin 1/2 fermions. In this representation, the transverse hopping plays the role of a magnetic field. Due to this mapping, the model can be analyzed in detail by making use of the known results on 1D chains in presence of a magnetic field. By means of renormalization group (RG) calculations and of the bosonization results, we derive a zero–temperature "phase diagram" of two coupled spinless chains, as a function of the intra–chain repulsion at infinitesimal transverse hopping.

In Section 2.2, we generalize the method to treat the case of spin 1/2 fermions. For this system, we have not found an analogous mapping onto known models. However, by making again use of RG, considerably more complicated than in the previous case, we show that the transverse hopping is actually a relevant perturbation, which modifies the

long–wavelength behavior of the two chains. We also show that this spinful case shares many aspects with the previous spinless model.

In Section 2.3, the RG is applied to calculate the phase diagram of two spinful chains with Hubbard on–site repulsion, for arbitrary transverse hopping. The phase diagram is further discussed by applying the bosonization technique directly to the fixed point hamiltonians identifying each different phase.

In Section 2.4, we study another simplified model of two coupled chains. The hamiltonian of each chain, in absence of transverse hopping, is defined in such a way as to exhibit spin–charge separation, but no anomalous exponent. We show how to solve exactly this model when an interchain hopping is applied.

The full model of Sections 2.2 and 2.3 in absence of transverse hopping, shows simultaneously anomalous exponents (as for the spinless chains of Section 2.1, but not for the model of Section 2.4) together with spin–charge separation (obviously absent in the spinless case, but present in the case of Section 2.4). Comparison between them is of greater help in elucidating what features in the phase diagram are due to what.

In Appendix B, it is shown the detailed derivation of the RG set of equations for arbitrary transverse hopping, in the spinless fermion case.

2.1 Relevance of the transverse hopping in a two spinless chain model

In this section we analyze the role of a single–electron interchain hopping in a simplified model of two spinless chains. We start with the hamiltonian of two coupled free spinless fermion chains.

$$\hat{H}_0 = -\sum_{<i,j>}(c^\dagger_{i,1}c_{j,1} + c^\dagger_{i,2}c_{j,2} + \text{H.c.}) - t_\perp \sum_i (c^\dagger_{i,1}c_{i,2} + \text{H.c.}), \tag{2.1}$$

where $c^\dagger_{i,1}(c^\dagger_{i,2})$ creates a spinless fermion at site i on chain 1(2). For $t_\perp < 1 - \cos(2\pi\rho)$ (ρ is the density) there are two branches, labelled 0 and π, of the non interacting Fermi surface (Fig. 2.1). Near ϵ_F, bands are linearized in the form $\epsilon^\mu_k = \pm v^\mu_F(k \mp k^\mu_F)$ ($\mu = 0, \pi$),

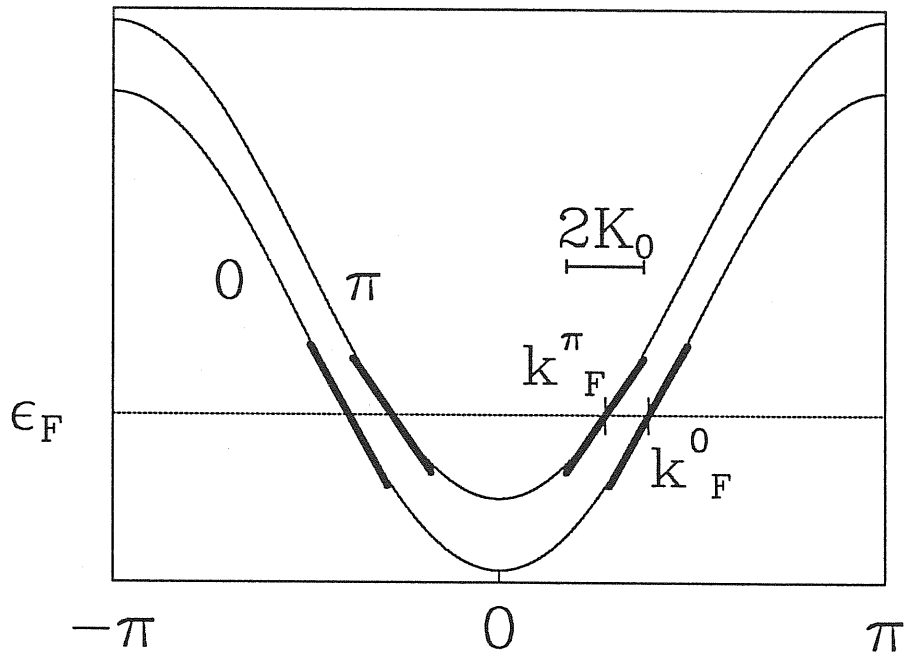

Figure 2.1: Band structure of two uncoupled chains: the two bands are labeled by the value of the transverse momentum $(0, \pi)$. Linearization around the Fermi points is also shown.

valid within some cutoff range of width K_0 around k^μ_F. The kinetic term therefore reduces

to two linear bands with different Fermi momenta and velocities. Let us further simplify it, by assuming equal Fermi velocities. This approximation is not so arbitrary, at least for small $t_\perp$, because, as we will show later, different Fermi velocities do not affect the asymptotic long wavelength behavior. The hamiltonian $\hat{H}_0$ is therefore rewritten as:

$$\begin{aligned}
\hat{H}_0 &= \sum_k v_F(k-k_F)(a^\dagger_{k0}a_{k0} + a^\dagger_{k\pi}a_{k\pi}) - v_F(k+k_F)(b^\dagger_{k0}b_{k0} + b^\dagger_{k\pi}b_{k\pi}) + \\
&- t_\perp(a^\dagger_{k0}a_{k0} - a^\dagger_{k\pi}a_{k\pi} + b^\dagger_{k0}b_{k0} - b^\dagger_{k\pi}b_{k\pi}) = \\
&= \sum_k v_F(k-k^0_F)a^\dagger_{k0}a_{k0} + v_F(k-k^\pi_F)a^\dagger_{k\pi}a_{k\pi} + \\
&- v_F(k+k^0_F)b^\dagger_{k0}b_{k0} - v_F(k+k^\pi_F)b^\dagger_{k\pi}b_{k\pi},
\end{aligned} \tag{2.2}$$

where the operator $a_{ki}(b_{ki})$ refers to the right(left) moving electrons, and the suffix 0 indicates the bonding band, while π the anti–bonding band. k_F is the Fermi momentum in the absence of transverse hopping, while $k^0_F = k_F + t_\perp/v_F$ and $k^\pi_F = k_F - t_\perp/v_F$ are the Fermi points for the two bands in presence of $t_\perp$.

The next step is to introduce the fermion–fermion interaction. We neglect all the scattering processes between two right–moving fermions or between two–left moving ones, because they do not generate logarithmic singularities. They are expected just to renormalize the sound velocities of the excitations. Moreover, we also ignore Umklapp scattering, which is important only for isolated commensurate fillings. Keeping into account the conservation of total transverse momentum, we can generate five different couplings[37, 38, 39] (see Fig. 2.2): $\tilde{g_0}$ (intra–bonding band scattering), $\tilde{g_\pi}$ (intra–anti–bonding band scattering), $\tilde{g_f}$ (inter–band forward scattering), $\tilde{g_t}$ (inter–band tunnelling) and $\tilde{g_b}$ (inter–band backward scattering). Physically, if we allow only intra–chain fermion–fermion repulsive interactions, then all these couplings are equal and positive. By *confinement* in this model, we will mean that, due to the interaction, *the transverse hopping is not able to shift the*

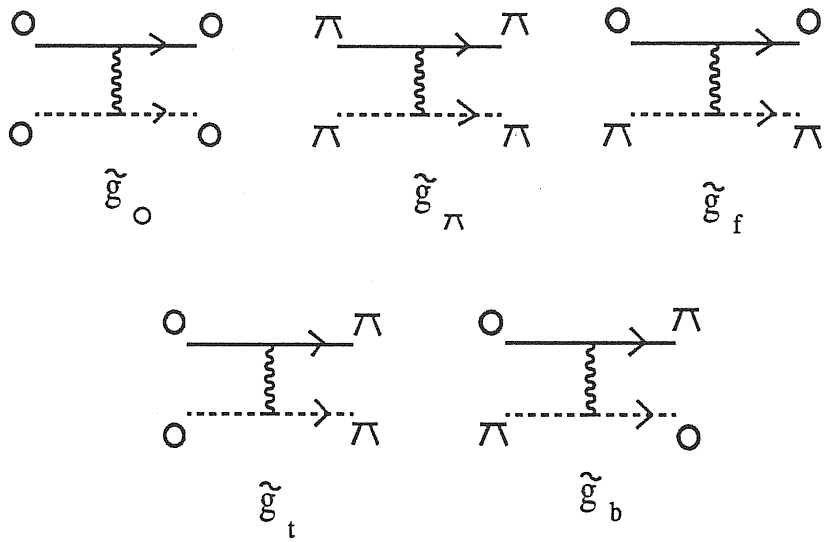

Figure 2.2: Coupling constants which can be generated for two chains of spinless fermions, compatibly with the conservation of total momentum. Solid lines represent right–moving fermions, whereas dashed lines denote left–moving particles.

bonding band with respect to the antibonding one, thus leaving the two distinct Fermi points k_F^0 and k_F^π degenerate, i.e. $k_F^0 = k_F^\pi$ means confinement.

This model is clearly equivalent to a single chain of fermions with spin $1/2$ in a magnetic field. It is enough to consider the band indices (0 or π) as pseudo–spin indices ($\uparrow$ or $\downarrow$) to build the mapping. In this representation, the transverse hopping plays the same role of a magnetic field in the z–direction, while the difference between the occupation numbers of the bonding band and the anti–bonding one, corresponds to the magnetization. The hamiltonian, in this representation, turns out to have spin–anisotropic interactions. Such a model has been studied in detail by Giamarchi and Schulz[37] (GS), by means of the renormalization group applied to the bosonized version of that hamiltonian. In the absence of a magnetic field, they find a critical plane, away from which there is always one variable scaling towards strong coupling. In particular, the hamiltonian we are considering, where all the couplings $\tilde{g}_i$ $(i = 0, \pi, f, t, b)$ are equal and positive, lies just on that critical plane,

simply reflecting the Luttinger liquid nature of two uncoupled spinless chains. What we want to show here, is that a transverse hopping induces a further pseudo–spin–anisotropy in the model, capable by itself to move the system away from criticality and towards strong coupling regimes. This result demonstrates that the two uncoupled Luttinger chain fixed point is unstable against switching on a transverse hopping [this was already implicit in the RG equations (3.15) of GS]. In particular, GS predict that, starting from the critical plane with all the couplings equal and positive, only one regime is reached, characterized by strong–coupling and by a finite magnetization. It corresponds to phase 2) of section 3.2 in Ref. [37]. In the chain representation, this result implies that two spinless chains coupled by a transverse hopping are always driven towards a unique strong coupling regime, which does not show confinement. Instead our RG calculations suggest a richer phase diagram, and, while we agree with the results of GS for small values of the bare couplings, other different phases are found for larger values.

2.1.1 The Method and the RG Equations

The method we have adopted to study the model described by the kinetic term Eq. (2.2) and by the couplings in Fig. 2.2, is the Wilson renormalization group. This amounts to integrate out fermionic degrees of freedom in a momentum shell of width δK_0 around the edges of the bands. The momenta are then rescaled by $(1+\delta K_0/K_0)$ and, at the same time, also the wave functions Ψ_0 and Ψ_π, the couplings $\tilde{g}_i$, the Fermi velocity and the Fermi momenta k_F^0 and k_F^π are scaled, in order to reproduce the original model with renormalized parameters. More precisely, we require that the Green function keeps, after rescaling, the same form, apart from an overall multiplicative factor. At first order in the coupling constants, neither wave–function nor Fermi velocity and momentum renormalization are

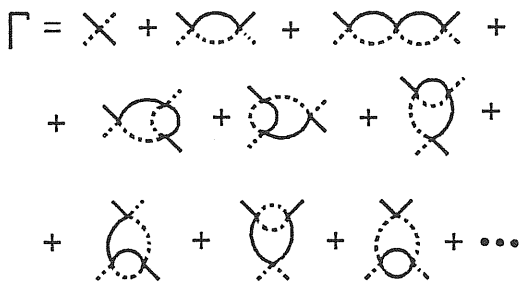

Figure 2.3: Low–order diagrams for the vertex.

found. In order to study the Fermi–liquid properties, we need therefore to evaluate the RG equations at least up to second order in the coupling constants. For the vertex corrections, this amounts to calculate the diagrams of Fig. 2.3, where the vertices may be anyone of the five scattering processes described earlier. Let us consider for example the particle–particle bubble of Fig. 2.4a. It is straightforward to calculate its value at first order in δK_0, which is

$$-\frac{1}{2\pi v_F}\frac{\delta K_0}{K_0}. \tag{2.3}$$

All the particle–particle bubbles (the particle–hole ones simply give an opposite contribution) which can be generated without the coupling $\tilde{g}_b$, give the same result. The other elementary bubble (Fig. 2.4b), where the coupling on the left vertex is $\tilde{g}_b$, gives a different contribution, which is

$$-\frac{1}{2\pi v_F}\frac{\delta K_0}{K_0}\frac{K_0}{K_0-\Delta k_F}, \tag{2.4}$$

when $K_0 > 2\Delta k_F = 2(k_F^0 - k_F^\pi)$, while it is strictly zero when $K_0 < 2\Delta k_F$. The reason for the difference between (2.3) and (2.4) is that the coupling $\tilde{g}_b$ with all the incoming and outgoing electron lines precisely at the Fermi energy, does not conserve momentum as soon as $\Delta k_F \neq 0$. For this reason, the logarithmic singularities generated by these processes, are shifted up in energy by an amount $2v_F\Delta k_F$. Then, at the beginning of the RG flow, i.e. in the high energy region, these scattering processes dominate the vertex

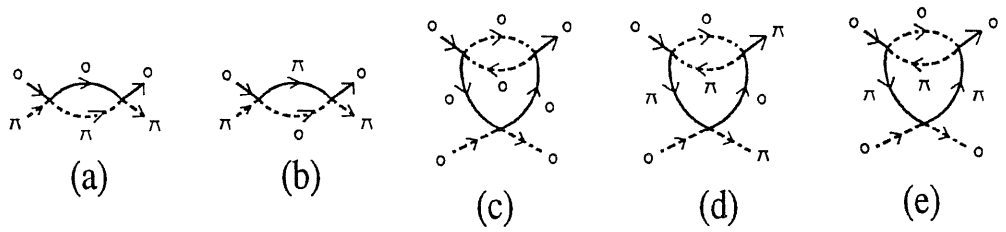

Figure 2.4: Elementary bubbles which are needed to evaluate leading and next–to–leading order corrections.

corrections, i.e. the term (2.4) is greater than (2.3). This occurs until the bandwidth cutoff K_0 is larger than $2\Delta k_F$. Below this value, these processes stop contributing to the scaling at all. This sharp change is the consequence of the bandwidth cut–off scheme, and it generates automatically a two–cut–off scaling theory. A similar behaviour occurs for the next–to–leading corrections. For example the diagram in Fig. 2.4c gives

$$-\frac{1}{2}\left(\frac{1}{2\pi v_F}\right)^2 \frac{\delta K_0}{K_0}, \tag{2.5}$$

while the diagram in Fig. 2.4d, to leading order in $\Delta k_F/K_0$, is

$$-\frac{1}{2}\left(\frac{1}{2\pi v_F}\right)^2 \frac{\delta K_0}{K_0}\left(1+\frac{\Delta k_F}{K_0}+\mathrm{O}(\Delta k_F^2)\right), \tag{2.6}$$

and remains finite [and different from Eq. (2.5)] until $K_0 = \Delta k_F$, while it vanishes for smaller K_0. The same happens for the diagram in Fig. 2.4e, even though it remains equal to (2.5) up to $\mathrm{O}(\Delta k_F^2)$. The calculation of the bubbles in Figs. 2.4a–2.4e, is enough to calculate the vertex corrections. As we said before, we have to generate all the possible diagrams like in Fig. 2.3 with the five different vertices, taking into account they can give different contributions according to Eqs. (2.3)–(2.6). The explicit expression of the diagrams in Fig. 2.4d–2.4e, at any order in Δk_F, is given in Appendix B. The next ingredient necessary to write down the RG equations, is the self–energy correction. In Fig. 2.5 we show the leading contribution to the self energy of the right moving electrons.

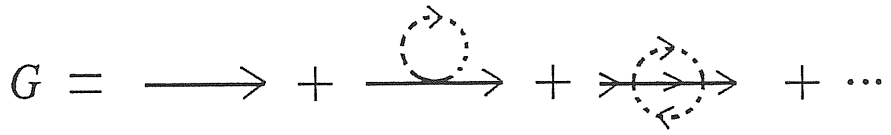

Figure 2.5: Low–order diagrams for the Green function.

The bare Green function is

$$G^{(0)}_{R,0(\pi)}(k,\omega) = \frac{1}{\omega - v_F(k - k_F^{0(\pi)}) + i\eta \mathrm{sign}(k - k_F^{0(\pi)})}, \tag{2.7}$$

while the correction at first order in Δk_F (the expression valid at any order is given in Appendix B) is

$$\begin{aligned}
\delta G^{(0)}_{R,0(\pi)}(k,\omega) &= G^{(0)}_{R,0(\pi)}(k,\omega)\left[-\frac{1}{2}\left(\frac{1}{2\pi v_F}\right)^2 (\tilde{g_{0(\pi)}}^2 + \tilde{g_t}^2 + \tilde{g_f}^2 + \tilde{g_b}^2)\frac{\delta K_0}{K_0}\right] + \\
&+ G^{(0)}_{R,0(\pi)}(k,\omega)^2\left[\pm\left(\frac{\tilde{g_b}}{2\pi v_F}\right)^2 v_F \Delta k_F \frac{\delta K_0}{K_0} + \right. \\
&+ \left.\left(\frac{\tilde{g_b}}{2\pi v_F}\right)^2 v_F(k - k_F^{0(\pi)})\frac{2\Delta k_F}{K_0}\frac{\delta K_0}{K_0}\right],
\end{aligned} \tag{2.8}$$

where the $+(-)$ refers to $0(\pi)$. This correction can be interpreted in the framework of RG if we introduce a wave–function renormalization, given by the first term in the right hand side, a Fermi momentum renormalization, given by the second term, and a Fermi velocity renormalization, given by the last term. Notice that the *Fermi momenta of the two bands renormalize oppositely, so that their sum is conserved*, in agreement with Luttinger theorem. Due to the coupling g_b, the interaction tends to deplete the bonding band in favor of the anti–bonding one, thus decreasing the bare value of Δk_F. Similar corrections are obtained for the left moving electrons. The final result is:

$$\delta z_0 = -\frac{1}{2}\left(\frac{1}{2\pi v_F}\right)^2 (\tilde{g_0}^2 + \tilde{g_t}^2 + \tilde{g_f}^2 + \tilde{g_b}^2)\frac{\delta K_0}{K_0} \tag{2.9}$$

$$\delta z_\pi = -\frac{1}{2}\left(\frac{1}{2\pi v_F}\right)^2 (\tilde{g_\pi}^2 + \tilde{g_t}^2 + \tilde{g_f}^2 + \tilde{g_b}^2)\frac{\delta K_0}{K_0} \tag{2.10}$$

$$\delta v_F = v_F \left(\frac{\tilde{g}_b}{2\pi v_F}\right)^2 \frac{2\Delta k_F}{K_0} \frac{\delta K_0}{K_0} \tag{2.11}$$

$$\delta \Delta k_F = -2\Delta k_F \left(\frac{\tilde{g}_b}{2\pi v_F}\right)^2 \frac{\delta K_0}{K_0} \tag{2.12}$$

where z_0 and z_π are the wave–function renormalization factors, or equivalently the quasi–particle residues, of the bonding and anti–bonding electrons. By means of Eqs. (2.9)–(2.12), we can write down the renormalization group equations for all the invariant couplings, in a manner similar to that outlined in Ref. [18]. Notice that the equality $\tilde{g}_0 = \tilde{g}_\pi = \tilde{g}$, satisfied by the initial condition, is conserved by the RG flow. Therefore, from now on, we consider just one $\tilde{g}$ as representative of both $\tilde{g}_0$ and $\tilde{g}_\pi$. Then, in order to simplify the notations, it is better to define the energy scale $\omega_0 = 2v_F^{(0)}K_0$ and the following dimensionless couplings:

$$g_\rho = \frac{\tilde{g} + \tilde{g}_f}{2\pi v_F^{(0)}} \tag{2.13}$$

$$g_\sigma = \frac{\tilde{g} - \tilde{g}_f}{2\pi v_F} \tag{2.14}$$

$$g_t = \frac{\tilde{g}_t}{2\pi v_F} \tag{2.15}$$

$$g_b = \frac{\tilde{g}_b}{2\pi v_F} \tag{2.16}$$

$$h = \Delta k_F / K_0, \tag{2.17}$$

where $v_F^{(0)}$ is the bare Fermi velocity, while v_F is the renormalized one. The RG equations calculated to first order in h and to second order in the coupling constants, are (a detailed derivation, valid at any order in $\Delta k_F/K_0$, is in the Appendix B):

$$\frac{\mathrm{d}g_\rho}{\mathrm{d}\log\omega_0} = 0 \tag{2.18}$$

$$\frac{\mathrm{d}g_\sigma}{\mathrm{d}\log\omega_0} = 2(g_t - g_b)(g_t + g_b) + 2g_\sigma(g_t^2 + g_b^2) + \\ - 2hg_b^2 + 2hg_\sigma g_b^2 \tag{2.19}$$

$$\frac{dg_t}{d\log\omega_0} = 2g_t g_\sigma + g_t g_\sigma^2 + g_t(g_t^2 - g_b^2) \tag{2.20}$$

$$\frac{dg_b}{d\log\omega_0} = -2g_b g_\sigma + g_b g_\sigma^2 - g_b(g_t^2 - g_b^2) + - hg_b g_\sigma - 2hg_b(g_t^2 - g_b^2) \tag{2.21}$$

$$\frac{dh}{d\log\omega_0} = h\left[2(1+h)g_b^2 - 1\right] \tag{2.22}$$

$$\frac{dz}{d\log\omega_0} = \frac{1}{4}(g_\rho^2 + g_\sigma^2 + 2g_t^2 + 2g_b^2) \tag{2.23}$$

$$\frac{dv_F}{d\log\omega_0} = -2v_F h g_b^2. \tag{2.24}$$

We have introduced the two couplings g_ρ and g_σ in order to show explicitly the pseudo–spin pseudo–charge separation, which occurs once the model is mapped onto a single chain of fermions with spin. In that representation g_ρ is indeed the coupling related to the charge degrees of freedom[37], which must be unaffected by the magnetic field. The RG correctly reproduces this important feature, and in fact, from Eq. (2.18) it turns out that g_ρ is not renormalized. The pseudo–spin sector is represented by all the other couplings, and it is obviously affected by the pseudo–magnetic field. Notice that the velocity renormalization affects only the pseudo–spinon velocity, as it is obvious from Eq. (2.13) compared with Eqs. (2.14)–(2.16).

2.1.2 Instability of the Luttinger Liquid: spinless case

The RG equations (2.18)–(2.24) allow to study the stability of the two uncoupled (spinless) Luttinger chain fixed point [characterized by $g_\sigma = 0 = h$ and $g_t = g_b = g^{(0)} > 0$], upon turning on a small transverse hopping ($h_0 = 4t_\perp/\omega_0 \neq 0$). In order to do it, first of all we linearize the RG equations near this fixed point to find the scaling variables. They turn out to be:

$$X_1(\omega_0) = g_\sigma(\omega_0) + (g_t(\omega_0) - g_b(\omega_0)) + \frac{\gamma+1}{\gamma-\alpha}h(\omega_0) =$$

$$= \frac{\gamma+1}{\gamma-\alpha} h_0 \omega_0^{\alpha}, \tag{2.25}$$

$$\begin{aligned} X_2(\omega_0) &= g_\sigma(\omega_0) - (g_t(\omega_0) - g_b(\omega_0)) + \frac{\gamma+1}{\gamma-\beta} h(\omega_0) \\ &= \frac{\gamma+1}{\gamma-\beta} h_0 \omega_0^{\beta}, \end{aligned} \tag{2.26}$$

$$X_3(\omega_0) = g_t(\omega_0) + g_b(\omega_0) = 2g^{(0)}, \tag{2.27}$$

together with

$$h(\omega_0) = h_0 \omega_0^{\gamma}, \tag{2.28}$$

where the scaling exponents are given by $\alpha = 4g^{(0)}(1 + g^{(0)})$, $\beta = 4g^{(0)}(g^{(0)} - 1)$ and $\gamma = 2g^{(0)2} - 1$. The two uncoupled Luttinger chain fixed point is stable if, in the $\omega_0 \to 0$ limit, no scaling variable grows. This requires all the exponents α, β and γ to be positive. The exponent α is always positive for repulsive interactions, while, for the exponents γ and β to be both greater than zero, we must have $g^{(0)} > 1$. Let us notice that h scales with the exponent of the wave–function renormalization factor of the two uncoupled chains minus one[40], and the condition $\gamma > 0$ [which implies $g^{(0)} > 1/\sqrt{2}$], simply means that the quasi–particle residue vanishes faster than ω_0. However this requirement is not enough for the two uncoupled Luttinger chain fixed point being stable, as we need also $\beta > 0$, which gives the more restrictive condition $g^{(0)} > 1$.

Let us study the RG flow equations when $g^{(0)} < 1$, that is when the transverse hopping is relevant and it drives the system away from the two uncoupled Luttinger chain fixed point. This analysis is instructive because it clearly shows how different regimes appear, depending on the strength of the interaction. At the beginning of the RG flow, the couplings g_σ, g_b and h increase with respect to their initial values, while g_t decreases. In

fact, from the expression of X_1, X_2 and X_3 in terms of the g_i's, it is possible to show that for $\omega_0 \ll 1$

(i) when $\gamma < \beta < 0$, that is $g^{(0)} < 1 - 1/\sqrt{2}$, then

$$g_\sigma = \frac{h_0(\gamma+1)}{2}\left(\frac{1}{\alpha-\gamma}+\frac{1}{\beta-\gamma}\right)\omega_0^\gamma \tag{2.29}$$

$$g_b = g^{(0)} + \frac{h_0(\gamma+1)(\alpha-\beta)}{4(\alpha-\gamma)(\beta-\gamma)}\omega_0^\gamma, \tag{2.30}$$

(ii) instead, when $\beta < 0$ and $\gamma > \beta$, i.e. $1 - 1/\sqrt{2} \leq g^{(0)} < 1$

$$g_\sigma = \frac{h_0(\gamma+1)}{2(\gamma-\beta)}\omega_0^\beta \tag{2.31}$$

$$g_b = g^{(0)} + \frac{h_0(\gamma+1)}{4(\gamma-\beta)}\omega_0^\beta, \tag{2.32}$$

while $g_t = 2g^{(0)} - g_b$. Eventually g_b grows up to the value $g_1 \simeq 1/\sqrt{2}$, beyond which the pseudo–magnetic field h begins decreasing, as implied by Eq. (2.22), and the system flows towards the fixed point $g_\sigma^* = 1$, $g_t^* = 0$, $g_b^* = 1$ and $h^* = 0$. Therefore, once the cut–off is reduced up to the value $\omega_0 = \omega_c$ at which $g_b(\omega_c) = g_1$, the model flows towards a confined phase with $h^* = 0$. On the other hand, the inter–band backward scattering g_b contributes to the scaling equations only until $h = h_0\omega_0^\gamma \leq h_1 \simeq 1/2$, that is until $\omega_0 \geq (h_0/h_1)^{-1/\gamma}$. This implies that confinement can occur only if the condition $\omega_c > (h_0/h_1)^{-1/\gamma}$ is verified. When $h_0 \ll 1$ this requires

$$\frac{h_1(\gamma+1)(\alpha-\beta)}{4(g_1-g^{(0)})(\alpha-\gamma)(\beta-\gamma)} > 1, \tag{2.33}$$

which means $g^{(0)} > 0.2775....$ Thus we have shown that RG can indeed flow towards a confined phase for infinitesimal transverse hopping, if the bare coupling constant is larger than some critical value $g_c^{(1)} \simeq 0.2775...$ (to leading order $g_c^{(1)} = 1 - 1/\sqrt{2} = 0.2929...$).

Notice that this critical value is smaller than that required to have the exponent of the wave–function renormalization larger than one, i.e. $\gamma > 0$, which means $g^{(0)} > 1/\sqrt{2} = 0.7071....$ However, even though this confined regime is shown to exist for the RG set of Eqs. (2.18)–(2.24), we must be very cautious about the possibility that a realistic model could exhibit this kind of behavior. First of all, we have shown that the model behaves in two different ways, depending on the energy region we are exploring, and processes which dominate in the high energy regime ($\omega_0 \gg t_\perp$), may be negligible at low energies. Such a situation is delicate to treat by means of RG. In addition, the high energy region turns out to be important only for sufficiently large values of the bare coupling, where higher order contributions might be important. In fact, we will show that, a more accurate analysis, obtained by means of the bosonization technique, suggests a partially different interpretation of this strong–coupling phase.

If the bare value of the coupling is not large enough to drive the system towards a confined phase, then the contribution to the RG flow coming from g_b disappears, and the RG equations reduce to:

$$\frac{\mathrm{d}g_\rho}{\mathrm{d}\log\omega_0} = 0 \tag{2.34}$$

$$\frac{\mathrm{d}g_\sigma}{\mathrm{d}\log\omega_0} = 2g_t^2 + 2g_\sigma g_t^2 \tag{2.35}$$

$$\frac{\mathrm{d}g_t}{\mathrm{d}\log\omega_0} = 2g_t g_\sigma + g_t g_\sigma^2 + g_t^3. \tag{2.36}$$

These equations are identical to those of a 1D Fermi gas, once we identify $g_t = g_{1\perp}$ and $g_\sigma = g_{1\parallel}$[18]. The scaling trajectories of this equations are well known and depend on the values of the couplings $\bar{g}_t$ and $\bar{g}_\sigma$ at the point where the contribution of g_b disappears from the equations. If $\bar{g}_\sigma > |\bar{g}_t|$ the system scales towards weak coupling with $g_t^* = 0$ and $g_\sigma^* > 0$. This fixed point represents a simple Luttinger liquid, even though the transverse

hopping remains finite. On the other hand, if $\bar{g}_\sigma < |\bar{g}_t|$ the RG flows to strong coupling with fixed point interactions $g_\sigma^* = -1$ and $g_t^* = 1$. Both these phases are characterized by a finite residual Δk_F, that is they are not confined. The separatrix between the weak and the strong coupling regimes can be approximately calculated. As we said, g_b disappears from the equation when $h = h_0\omega_0^\gamma = 1/2$. At this value of the cut–off, the equation $\bar{g}_\sigma = \bar{g}_t$, identifying the transition from one phase to the other, is

$$\frac{(\gamma+1)}{4}\left(\frac{1}{\alpha-\gamma}+\frac{1}{\beta-\gamma}\right) = g^{(0)} - \frac{(\gamma+1)(\alpha-\beta)}{8(\alpha-\gamma)(\beta-\gamma)}, \tag{2.37}$$

whose solution gives $g^{(0)} = g_c^{(2)} \simeq 0.2321....$

2.1.3 Phase diagram of two coupled spinless chains

We are now able to discuss the phase diagram of two chains of spinless fermions, at least for very small transverse hopping (see Fig. 2.6). First of all, let us recall the mapping of

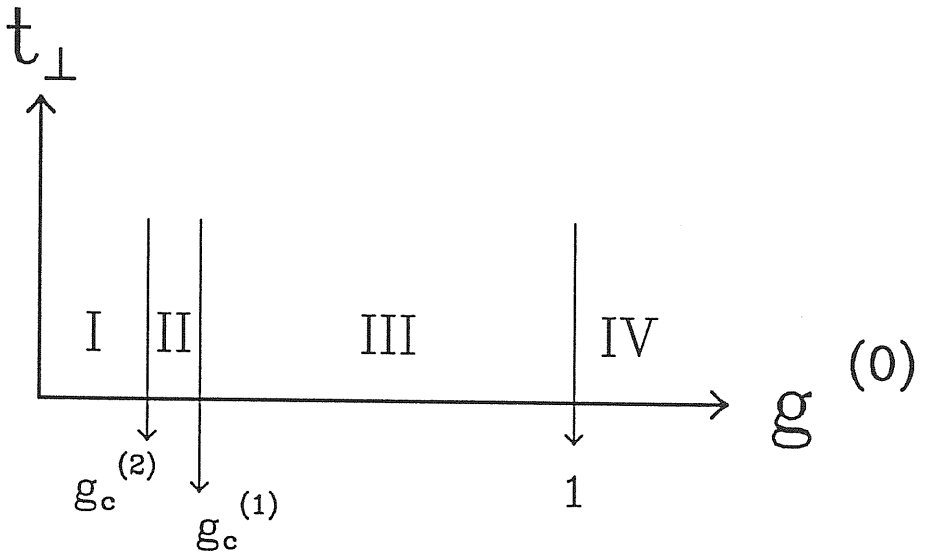

Figure 2.6: Phase diagram of two coupled chains of spinless fermions, as a function of the intra–chain interaction, calculated at infinitesimal transverse hopping.

this model onto a single chain of fermions with spin 1/2. This mapping makes it possible to apply to this case, all the exact results known for the 1D electron gas. The mapping is:

$$\begin{aligned} a_{k0} &\mapsto a_{k\uparrow} \\ b_{k0} &\mapsto b_{k\uparrow} \\ a_{k\pi} &\mapsto a_{k\downarrow} \\ b_{k\pi} &\mapsto b_{k\downarrow}. \end{aligned} \tag{2.38}$$

According to the usual g–ology jargon[18], the couplings map into:

$$\begin{aligned} g &\mapsto -g_{\|} = g_{2\perp} - g_{1\|} \\ g_f &\mapsto g_{2\perp} \\ g_b &\mapsto -g_{1\perp}, \end{aligned} \tag{2.39}$$

with a new coupling g_t[37, 38, 39], induced by spin–anisotropy and describing scattering processes where two parallel spins are flipped at the same time. In this representation, as we noticed, the transverse hopping plays the role of a magnetic field in the z–direction, and *confinement* means zero magnetization in presence of an applied magnetic field. The physical behavior of a 1D spin–anisotropic Fermi gas, can be characterized through the asymptotic behavior of the correlation functions, whose general expression is

$$R(k,\omega) = -i \int \mathrm{d}t e^{i\omega t} < T\{O(k,t)O^{\dagger}(k,0)\} > . \tag{2.40}$$

In practice, the operators $O(k,t)$ can describe charge–density wave (CDW), spin–density wave (SDW_X, SDW_Y and SDW_Z), singlet (SS) or triplet (TS) superconductive fluctuations[18], or others. In terms of the original two–chain model

(1) the CDW and SDW_Z correspond to the operators

$$O(k,t) = \frac{1}{L^{1/2}} \sum_q \left[b^\dagger_{q0}(t) a_{q+k0}(t) \pm b^\dagger_{q\pi}(t) a_{q+k\pi}(t) \right], \tag{2.41}$$

which describe respectively in–phase CDW and charge density fluctuations between the bonding and anti–bonding bands;

(2) SDW_X and SDW_Y operators correspond to

$$O(k,t) = \frac{1}{L^{1/2}} \sum_q \left[b^\dagger_{q0}(t) a_{q+k\pi}(t) \pm b^\dagger_{q\pi}(t) a_{q+k0}(t) \right], \tag{2.42}$$

and represent respectively the out–of phase CDW and some orbital antiferromagnetic correlations[39, 41];

(3) SS and TS susceptibilities correspond to pair fluctuations.

According to the mapping (2.39), the original two chain model translates into a single chain of interacting electrons with bare couplings $g_{1||} = 0$ and $g_{2\perp} = -g_{1\perp} = g_t = g^{(0)} > 0$, in presence of a magnetic field. It is well known that this hamiltonian can be written in terms of bosonic operators representing the charge and spin density fluctuations[42], $\rho(q) = 1/\sqrt{2}[\rho_\uparrow(q) + \rho_\downarrow(q)]$ and $\sigma(q) = 1/\sqrt{2}[\rho_\uparrow(q) - \rho_\downarrow(q)]$. In the original two chain model, $\rho(q) = 1/\sqrt{2}[\rho_0(q) + \rho_\pi(q)]$ is the symmetric while $\sigma(q) = 1/\sqrt{2}[\rho_0(q) - \rho_\pi(q)]$ is the antisymmetric combination of the densities of the two bands. The charge degree of freedom $\rho(q)$ is obviously unaffected by the magnetic field and simply describes a Luttinger liquid with sound velocity

$$u_\rho = \left(v_F^2 - \frac{(g_{1||} - 2g_{2\perp})^2}{4\pi^2} \right)^{1/2} \tag{2.43}$$

and with the coefficient K_ρ determining the long–distance decay of the charge part of the correlation functions[50], given by

$$K_\rho = \left(\frac{2\pi v_F + g_{1||} - 2g_{2\perp}}{2\pi v_F - g_{1||} + 2g_{2\perp}} \right)^{1/2}, \tag{2.44}$$

always smaller than one. This means that, from the point of view of the charge degrees of freedom, the most divergent correlation functions are CDW or SDW[50].

Let us study now what happens to the spin degrees of freedom.

We have shown that, for small initial couplings, $0 < g^{(0)} < g_c^{(2)} \simeq 0.2321$ the RG equations flow towards a strong coupling regime [indicated as phase I in Fig. 2.6] with $g_t^* = 1$, $g_{1\perp}^* = 0$ and $g_{1||}^* = 1$, characterized by the presence of a spin–gap in the y-direction and by a residual Δk_F (no confinement). It corresponds to the spin–flopped phase introduced by GS[37], where the dominant fluctuation is of SDW_X type. In the original two–chain model this means that the most divergent susceptibility is an out–of phase CDW.

Above the critical value $g_c^{(2)}$ and below $g_c^{(1)} \simeq 0.2775$, we find a weak coupling fixed point [II in Fig. 2.6] with $g_t^* = 0$, $g_{1\perp}^* = 0$ and $g_{1||}^* < 0$, which describes a regular Luttinger liquid. As in the previous phase, we find no confinement. The parameter K_σ^* governing the spin part of the correlation function asymptotic decay is

$$K_\sigma^* = \left(\frac{2\pi v_F + g_{1||}^*}{2\pi v_F - g_{1||}^*} \right)^{1/2}, \tag{2.45}$$

also smaller than one. This implies that in phase II the most divergent correlation functions are of the CDW and SDW_Z type (being $g_{1\perp} < 0$ a CDW should be favoured), which translated in the true chain language, means dominant in–phase CDW fluctuations as well as strong charge fluctuations between the bonding and anti–bonding bands.

Above $g_c^{(1)}$, a strong coupling regime (III in Fig. 2.6) is found. It is characterized by the fixed point couplings $g_t^* = 0$, $g_{1\perp}^* = -1$ and $g_{1||}^* = -1$, and by the presence of a spin–gap in the z-direction, which sets to zero the value of the magnetization, i.e. this fixed point describes a confined phase. The dominant fluctuations in this regime are of CDW type,

which for the two chains means an in–phase regular CDW. Therefore, even though single–particle hopping is asymptotically irrelevant, nevertheless the two chains get strongly correlated, and in particular, they show divergent in–phase CDW susceptibilities. The transition between the phases II and III is equivalent to a commensurate–incommensurate transition, for which exact results are known[43]. We can therefore make use of these results to better analyze phase III. Let us suppose we follow the RG flow until it crosses the Luther–Emery line, i.e. until $g_{1||} = -g_\sigma = -3/5$. Actually, when this occurs, weak coupling RG has already lost its justification, but anyway this procedure should be more reliable than the RG alone. On this line, we make use of the Luther–Emery solution, and map the hamiltonian of the spin degrees of freedom into a spinless fermion model[44]. If the coupling g_t is small enough, the resulting hamiltonian will correspond exactly to the Luther–Emery model, with a gap Δ_σ proportional to the cut–off ω_{LE} at which the crossing occurs[45]. From Eqs. (2.29) and (2.31), it follows that this cut–off, and consequently the gap, vanishes when $h_0 \to 0$ as

$$\omega_{LE} \sim \Delta_\sigma \sim h_0^\nu, \tag{2.46}$$

where the crossover exponent ν is (see also Ref. [43])

$$\nu = \begin{cases} -1/\gamma & \text{if } g^{(0)} < 1 - 1/\sqrt{2} \\ -1/\beta & \text{if } 1 - 1/\sqrt{2} \leq g^{(0)} < 1, \end{cases}$$

always greater than one. In order to find the ground state, one has to compare the value of the gap with the starting magnetic field h_0[43], which now plays the role of a chemical potential. For $h_0 \ll 1$, we find $h_0 \gg \Delta_\sigma \sim h_0^\nu$, therefore the chemical potential lies above the gap. The low energy excitations are obtained by simply linearizing the conduction band around the chemical potential, and thus we recover an usual Luttinger liquid behavior. The magnetization is given by the occupation of the conduction band,

and therefore it is simply proportional to h_0. According to this simple argument and contrary to the prediction of RG, phase III should not be really confined. Rather it should exhibit properties analogous to phase II. In fact, both describe a Luttinger liquid with dominant CDW fluctuations, which in terms of the chains means a proper in phase CDW. The difference between k_F^0 and k_F^π remains finite, and therefore both these phases are "not confined". This scenario seems to us more realistic that the one predicted by the RG alone. First of all, second order RG loses its validity when it flows towards strong coupling. Therefore, being the confinement only a feature of the system strictly at the fixed point III, we are not sure it really occurs. Secondly, the way confinement is generated, is very interesting, but hard to justify. In fact, it would imply that a chain of spin 1/2 fermions, massless in absence of magnetic field, prefers, at strong coupling and in a magnetic field, to open a spin gap rather than acquiring a finite magnetization. Since this seems quite unlikely to us, we tend to believe more in the combined RG plus bosonization result than in the RG alone, even though we have no rigorous proof for that.

Lastly, above $g^{(0)} = 1$, the transverse hopping becomes irrelevant, and the two uncoupled Luttinger chain fixed point is stable (IV in Fig. 2.6). This phase is therefore the only confined region we find, in the sense that $\Delta k_f = k_F^0 - k_F^\pi$ remains zero upon application of a transverse hopping.

This result is also compatible with the observation, valid for any number of chains, that no confined phase, having $k_F^0 = k_F^\pi$ in presence of a transverse hopping, exists but that describing completely uncoupled Luttinger chains[1].

[1]The statement for any number of chains is: if the Fermi surface in presence of $t_\perp$ is equal to that in absence, i.e. if the Fermi surface is simply two parallel straight lines in the transverse direction, then the asymptotic behaviour of the system is equivalent to that of completely uncoupled chains. In fact if the Fermi surface does not change by switching on a transverse hopping, this implies that on this state the

To conclude this section, we compare our results with those obtained by Giamarchi and Schulz[37] (GS). We recall that, using the method of GS, the phase diagram of our model, would have shown only phase I. The origin of this discrepancy in the predictions of two different implementations of RG, is not clear to us. GS first bosonize the model and then they apply a real space version of the RG, to treat the effect of the interactions which can not be trivially diagonalized. We already said that the existence of phase II, and maybe III, crucially depends on the fact that $t_\perp$ shifts up some logarithmic singularities, which, in absence of $t_\perp$, occur at zero frequency. The consequence is that two energy regimes appear: for high frequencies the poles which are shifted up by $t_\perp$, play the most relevant role and they tend to suppress the effect of the transverse hopping, whereas for small energies they are irrelevant and only the other poles, those which are unaffected by $t_\perp$, contribute to the RG equations. It is just the high energy behavior which causes phases II and III to occur. However, the equivalent low distance regime, as comes out from the real space calculations of GS, does not play the same crucial role, probably because the real space representation washes out partly this peculiar behavior.

In summary, both formulations of RG show that the model considered in this section scales towards strong coupling, where the flow equations lose their validity. The fact that real vs. momentum space RG, predict different phase diagrams, further suggests that the results must be taken with caution because, at this stage, it is not clear which formulation

average value of the transverse hopping operator $O_\perp$, i.e.

$$< O_\perp >= -2t_\perp \sum_{k_\perp \in BZ} \cos k_\perp a < \hat{n}_{k\perp} >$$

is zero, because $< \hat{n}_{k\perp} >$, i.e. the total number of electrons with transverse momentum $k_\perp$, is a constant independent from $k_\perp$. Therefore only the term of the hamiltonian which describes the set of uncoupled 1D chains, contributes to the total energy. This contribution is clearly minimized if the ground state is exactly equal to the product of the ground states of each isolated chain, which in our case simply describes a Luttinger liquid. Thus we have demonstrated the initial statement.

of weak coupling RG is more accurate in reproducing the physics of this model.

2.2 Two spinful chains with inter–chain hopping

The same technique we have just used to study the effect of single particle tunnelling between two Luttinger chains, can be applied also to the more general spinful case. This model is described by a non interacting hamiltonian equal, for each spin species, to that we defined for spinless fermions in Eqs. (2.1) and (2.2). Without interaction, the band structure is therefore the same as in Fig. 2.1, where each branch is now doubly degenerate due to the spin. We still assume equal Fermi velocities of the bonding ($k_\perp = 0$) and antibonding bands ($k_\perp = \pi$). Later, we will discuss the consequences of different Fermi velocities, and we will present some results obtained in this general case.

Similarly to the spinless case, we can think of this model as describing 1D Fermions with spin 1/2 and with an additional flavour index (0 or π). The transverse hopping acts for the different flavor as a magnetic field for different spins, i.e. it splits the energy of the two flavor by an amount $2t_\perp$.

The coupling constants, in this model, must conserve both total transverse momentum and spin. Thus, for each scattering process we introduced in the spinless case, represented by the couplings $\tilde{g}_0$, $\tilde{g}_\pi$, $\tilde{g}_f$, $\tilde{g}_t$ and $\tilde{g}_b$ (see Fig. 2.2), three possible spin orientations are allowed. Therefore, out of a single $\tilde{g}_i$ ($i = 0, \pi, f, t, b$), we can now define three different coupling constants[18]: $\tilde{g}_i^{(1)}$ and $\tilde{g}_i^{(2)}$, describing respectively backward and forward scattering processes between opposite spin electrons, and $\tilde{g}_i^{||}$, which couples parallel spin electrons (see Fig. 2.7). The elementary bubbles, which appear in the diagrammatic expansion, are obviously the same encountered in the spinless case. In particular, the remarks on the role played by $t_\perp$ in shifting up in energy some singularities, occurring at zero frequency when $t_\perp = 0$, still hold. This allows to write the RG set of equations,

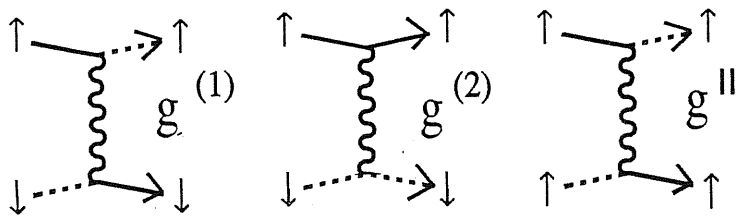

Figure 2.7: Interaction vertices for spinful fermions. As in Fig. 2.2, solid(dashed) lines denote right(left)–moving particles.

which for spin–isotropic interactions, implying $g_i^{||} = g_i^{(1)} - g_i^{(2)}$, are:

$$\frac{\mathrm{d}g^{(1)}}{\mathrm{d}\log\omega_0} = 2g^{(1)2} + 2g_t^{(1)}g_t^{(2)} + 2Ig_b^{(1)}\left(g_b^{(1)} - g_b^{(2)}\right) + 2g^{(1)}\left(g^{(1)2} + g_f^{(1)2} + g_t^{(1)2} + D_2 g_b^{(1)2}\right) + \\ -2\left(g^{(1)} - g_f^{(1)}\right)\left[g_t^{(2)}\left(g_t^{(1)} - g_t^{(2)}\right) + D_2 g_b^{(2)}\left(g_b^{(1)} - g_b^{(2)}\right)\right]$$

$$\frac{\mathrm{d}g^{(2)}}{\mathrm{d}\log\omega_0} = g^{(1)2} + g_t^{(1)2} + g_t^{(2)2} - Ig_b^{(2)2} + g^{(1)3} + g^{(1)}g_f^{(1)2} + g_f^{(1)}g_t^{(1)2} + D_2 g_f^{(1)}g_b^{(1)2} + \\ +2\left(g^{(2)} - g_f^{(2)}\right)\left[g_t^{(1)2} - g_t^{(1)}g_t^{(2)} + g_t^{(2)2} + D_2\left(g_b^{(1)2} - g_b^{(1)}g_b^{(2)} + g_b^{(2)2}\right)\right]$$

$$\frac{\mathrm{d}g_f^{(1)}}{\mathrm{d}\log\omega_0} = 2g_f^{(1)2} + 2Ig_b^{(1)}g_b^{(2)} + 2g_t^{(1)}\left(g_t^{(1)} - g_t^{(2)}\right) + 2g_f^{(1)}\left(g^{(1)2} + g_f^{(1)2} + g_t^{(1)2} + D_2 g_b^{(1)2}\right) + \\ -2\left(g_f^{(1)} - g^{(1)}\right)\left[g_t^{(2)}\left(g_t^{(1)} - g_t^{(2)}\right) + D_2 g_b^{(2)}\left(g_b^{(1)} - g_b^{(2)}\right)\right]$$

$$\frac{\mathrm{d}g_f^{(2)}}{\mathrm{d}\log\omega_0} = g_f^{(1)2} + Ig_b^{(1)2} + Ig_b^{(2)2} - g_t^{(2)2} + g_f^{(1)3} + g_f^{(1)}g^{(1)2} + g^{(1)}g_t^{(1)2} + D_2 g^{(1)}g_b^{(1)2} + \\ +2(g_f^{(2)} - g^{(2)})\left[g_t^{(1)2} - g_t^{(1)}g_t^{(2)} + g_t^{(2)2} + D_2\left(g_b^{(1)2} - g_b^{(1)}g_b^{(2)} + g_b^{(2)2}\right)\right]$$

$$\frac{\mathrm{d}g_t^{(1)}}{\mathrm{d}\log\omega_0} = 2g_t^{(1)}g^{(2)} + 2g^{(1)}g_t^{(2)} + 2g_t^{(1)}\left(g_f^{(1)} - g_f^{(2)}\right) + 2g_f^{(1)}\left(g_t^{(1)} - g_t^{(2)}\right) + \\ +2g_t^{(1)}\left[\left(g^{(2)} - g_f^{(2)}\right)^2 - \left(g^{(1)} - g_f^{(1)}\right)\left(g^{(2)} - g_f^{(2)}\right) + g^{(1)2} + g_f^{(1)2}\right] + \\ +2D_1 g_b^{(1)}\left[\left(g_t^{(1)} - g_t^{(2)}\right)g_b^{(2)} + g_t^{(2)}\left(g_b^{(1)} - g_b^{(2)}\right)\right] + \\ +2g_t^{(1)}\left[g_t^{(1)2} - g_t^{(1)}g_t^{(2)} + g_t^{(2)2} + D_2\left(g_b^{(1)2} - g_b^{(1)}g_b^{(2)} + g_b^{(2)2}\right)\right]$$

$$
\begin{aligned}
\frac{\mathrm{d}g_t^{(2)}}{\mathrm{d}\log\omega_0} &= 2g_t^{(2)}\left(g^{(2)}-g_f^{(2)}\right)+2g_t^{(1)}g^{(1)}+2g_t^{(1)}g_f^{(1)}g^{(1)}+\\
&+2g_t^{(2)}\left[\left(g^{(1)}-g_f^{(1)}\right)^2-\left(g^{(1)}-g_f^{(1)}\right)\left(g^{(2)}-g_f^{(2)}\right)+\left(g^{(2)}-g_f^{(2)}\right)^2\right]+\\
&+2D_1\left[\left(g_b^{(1)}-g_b^{(2)}\right)g_t^{(1)}g_b^{(1)}-g_b^{(2)}\left(g_t^{(1)}-g_t^{(2)}\right)\left(g_b^{(1)}-g_b^{(2)}\right)-g_b^{(2)2}g_t^{(2)}\right]+\\
&+2g_t^{(2)}\left[g_t^{(1)2}-g_t^{(1)}g_t^{(2)}+g_t^{(2)2}+D_2\left(g_b^{(1)2}-g_b^{(1)}g_b^{(2)}+g_b^{(2)2}\right)\right]
\end{aligned}
$$

$$
\begin{aligned}
\frac{\mathrm{d}g_b^{(1)}}{\mathrm{d}\log\omega_0} &= 2g_b^{(1)}g_f^{(2)}+2g_f^{(1)}g_b^{(2)}+2g_b^{(1)}\left(g^{(1)}-g^{(2)}\right)+2g^{(1)}\left(g_b^{(1)}-g_b^{(2)}\right)+\\
&+2g_b^{(1)}\left[\left(g^{(2)}-g_f^{(2)}\right)^2-\left(g^{(1)}-g_f^{(1)}\right)\left(g^{(2)}-g_f^{(2)}\right)+g^{(1)2}+g_f^{(1)2}\right]+\\
&+2D_1g_t^{(1)}\left[\left(g_b^{(1)}-g_b^{(2)}\right)g_t^{(2)}+g_b^{(2)}\left(g_t^{(1)}-g_t^{(2)}\right)\right]+\\
&+2g_b^{(1)}\left[g_t^{(1)2}-g_t^{(1)}g_t^{(2)}+g_t^{(2)2}+D_2\left(g_b^{(1)2}-g_b^{(1)}g_b^{(2)}+g_b^{(2)2}\right)\right]
\end{aligned}
\tag{2.47}
$$

$$
\begin{aligned}
\frac{\mathrm{d}g_b^{(2)}}{\mathrm{d}\log\omega_0} &= 2g_b^{(2)}\left(g_f^{(2)}-g^{(2)}\right)+2g_b^{(1)}g_f^{(1)}+2g_b^{(1)}g^{(1)}g_f^{(1)}+\\
&+2g_b^{(2)}\left[\left(g^{(1)}-g_f^{(1)}\right)^2-\left(g^{(1)}-g_f^{(1)}\right)\left(g^{(2)}-g_f^{(2)}\right)+\left(g^{(2)}-g_f^{(2)}\right)^2\right]+\\
&+2D_1\left[\left(g_t^{(1)}-g_t^{(2)}\right)g_b^{(1)}g_t^{(1)}-g_t^{(2)}\left(g_b^{(1)}-g_b^{(2)}\right)\left(g_t^{(1)}-g_t^{(2)}\right)-g_t^{(2)2}g_b^{(2)}\right]+\\
&+2g_b^{(2)}\left[g_t^{(1)2}-g_t^{(1)}g_t^{(2)}+g_t^{(2)2}+D_2\left(g_b^{(1)2}-g_b^{(1)}g_b^{(2)}+g_b^{(2)2}\right)\right]
\end{aligned}
$$

$$
\frac{\mathrm{d}h}{\mathrm{d}\log\omega_0} = h\left[4C_2\left(g_b^{(1)2}-g_b^{(1)}g_b^{(2)}+g_b^{(2)2}\right)-1\right]
$$

$$
\begin{aligned}
\frac{\mathrm{d}z}{\mathrm{d}\log\omega_0} &= \left(g^{(1)2}-g^{(1)}g^{(2)}+g^{(2)2}\right)+\left(g_f^{(1)2}-g_f^{(1)}g_f^{(2)}+g_f^{(2)2}\right)+\\
&+\left(g_t^{(1)2}-g_t^{(1)}g_t^{(2)}+g_t^{(2)2}\right)+D_2\left(g_b^{(1)2}-g_b^{(1)}g_b^{(2)}+g_b^{(2)2}\right)
\end{aligned}
$$

$$
\frac{\mathrm{d}v_F}{\mathrm{d}\log\omega_0} = -4v_FhC_3\left(g_b^{(1)2}-g_b^{(1)}g_b^{(2)}+g_b^{(2)2}\right)
$$

where for small h, the functions $I(h)\simeq 1+h$, $D_2(h)\simeq 1$, $D_1(h)\simeq 1+h$, $C_2(h)\simeq 1+2h$,

and $C_3(h) \simeq 1$ (see Appendix B). The dimensionless invariant couplings appearing in Eq. (2.47), are now defined, as $g_i = \tilde{g}_i/(2\pi v_F^{(0)})$, instead of Eqs. (2.13)–(2.16). Analogously to the spinless case, we can identify a particular combination of couplings:

$$g^{(1)} + g_f^{(1)} - 2\left(g^{(2)} + g_f^{(2)}\right) \tag{2.48}$$

which remains invariant under RG. This combination corresponds to the total charge sector, which is again unaffected by the transverse hopping, and remains gapless as it was in absence of $t_\perp$.

The model describing only intra–chain interactions is obtained by assuming:

$$\begin{aligned} g_i^{(1)} &= g_j^{(1)} = g_0^{(1)} \\ g_i^{(2)} &= g_j^{(1)} = g_0^{(2)} \end{aligned} \qquad \forall i,j \tag{2.49}$$

In the absence of $t_\perp$ and for $g_0^{(1)} > 0$, the RG flow of this model (two uncoupled chains) is well known to scale to a Tomonaga–Luttinger liquid, characterized by the fixed point coupling constants:

$$\begin{aligned} g_i^{(1)*} &= 0 \\ g_i^{(2)*} &= g^{(2)0} - \frac{g^{(1)0}}{2} \end{aligned} \qquad \forall i \tag{2.50}$$

In order to analyse the role played by $t_\perp$, we start by studying the stability of this fixed point, upon switching on a small transverse hopping. This analysis is still meaningful, even though the model we are considering is not exactly at the fixed point (2.50). This can be realized by considering, for example, the popular case of a Hubbard interaction, which in the g–ology language, corresponds to $g_0^{(1)} = g_0^{(2)}$. A typical RG flow of Hubbard–like interactions in presence of $t_\perp$, is shown in Fig. 2.8. We notice that, at high energy, the system behaves as if $t_\perp$ were absent. In fact, the trajectory of the different $g_i^{(2)}$'s are almost indistinguishable, and the same occurs for the $g_i^{(1)}$'s. Furthermore, the former couplings correctly saturates to a finite value, whereas the latter ones scale down to zero. Only at

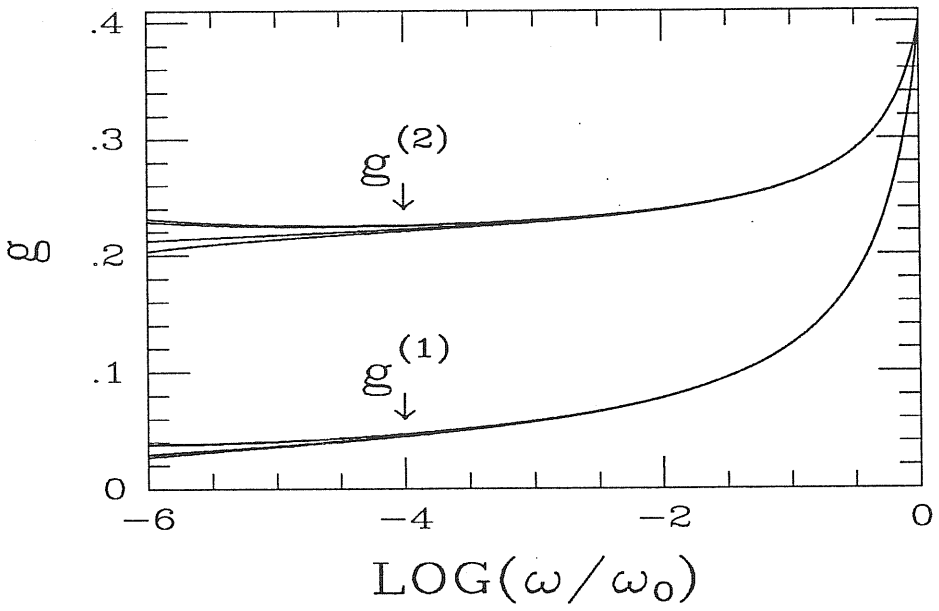

Figure 2.8: Typical RG flow for Hubbard–like interactions. The upper curves correspond to the $g_i^{(2)}$'s, the lower ones to the $g_i^{(1)}$'s

energies of order $t_\perp$, the system notices the presence of inter–chain hopping, and the RG trajectories begin deviating from their $t_\perp = 0$ limit. The smaller is $t_\perp$, the closer is the system to the fixed point (2.50). As a consequence, instead of the original two Hubbard chains, we can equivalently consider two Tomonaga–Luttinger chains, defined by the fixed point coupling constants (2.50), and study their stability upon switching small $g_i^{(1)}$'s and $t_\perp$. A non zero, but small, value of the couplings $g_i^{(1)}$, contributes to the RG flow only via non–linear terms, as it can be realized from (2.47). Then, to linear order, the $g^{(1)}$'s disappear from the RG equations, and the analysis of the stability of RG trajectories towards the Luttinger liquid fixed point, reduces to studying a set of linear first order differential equations, very similar to that encountered in the spinless case. This result, however, does not imply that non zero $g_i^{(1)}$'s do not affect at all the asymptotic physical behavior of the model, as we shall see. It simply suggests that the physical origin of the

instability of Luttinger liquid behavior of two spinful chains once $t_\perp$ is switched on, is, similarly to the spinless case, the flavor anisotropy induced on the model by the transverse hopping, independently from the presence of the spin.

2.2.1 Instability of the Luttinger liquid: spinful case

Therefore, let us begin by considering a two–spinful–chain model characterized by the coupling constants $g_i^{(1)} = 0$ and $g_i^{(2)} = -g_i^{||} = g_0$, for all $i = 0, \pi, f, t, b$. In the absence of $t_\perp$, this model is a fixed point, invariant under RG. Let us switch on a small $t_\perp$ and linearize the RG set of equations around the starting fixed point hamiltonian. The same analysis carried out for the spinless chains, can be also applied to this case. For example, the scaling variables are now:

$$\begin{aligned} X_1(\omega) &= \left(g^{(2)}(\omega) - g_f^{(2)}(\omega)\right) + \left(g_t^{(2)}(\omega) - g_b^{(2)}(\omega)\right) + \frac{\gamma+1}{2(\gamma-\alpha)}h(\omega) = \\ &= \frac{\gamma+1}{2(\gamma-\alpha)}h_0\omega^\alpha \qquad (2.51) \\ X_2(\omega) &= \left(g^{(2)}(\omega) - g_f^{(2)}(\omega)\right) - \left(g_t^{(2)}(\omega) - g_b^{(2)}(\omega)\right) + \frac{\gamma+1}{2(\gamma-\beta)}h(\omega) = \\ &= \frac{\gamma+1}{2(\gamma-\beta)}h_0\omega^\beta \qquad (2.52) \\ X_3(\omega) &= g_t^{(2)}(\omega) + g_b^{(2)}(\omega) = 2g_0 \qquad (2.53) \\ h(\omega) &= h_0\omega^\gamma \qquad (2.54) \end{aligned}$$

with the exponents:

$$\begin{aligned} \alpha &= 4g_0(2g_0+1) \qquad (2.55) \\ \beta &= 4g_0(2g_0-1) \qquad (2.56) \\ \gamma &= 4g_0^2 \qquad (2.57) \end{aligned}$$

Analogously to spinless fermions, roughly two different regimes of the RG flow can be identified:

(1) for $0 < g_0 < 0.21...$:

$$\begin{aligned} g^{(2)} - g_f^{(2)} &\to -\infty \\ g_t^{(2)} &\to \infty \\ g_b^{(2)} &\to 0 \end{aligned}$$

(2) for $0.21... < g_0 < 0.5$:

$$\begin{aligned} g^{(2)} - g_f^{(2)} &\to \infty \\ g_t^{(2)} &\to 0 \\ g_b^{(2)} &\to \infty \end{aligned}$$

For $g_0 > 0.5$, the transverse hopping is irrelevant and the two uncoupled Tomonaga–Luttinger chain fixed point is stable. This simplified model does not show, contrary to the spinless case, any tendency towards confinement and the phase III of Fig. 2.6 is absent. However non–zero $g_i^{(1)}$'s can stabilize a confined phase, even though its physical interpretation is still ambiguous, as we discussed in the previous Section. If we start from a more general spin–isotropic model, characterized by non zero $g_i^{(1)} = g_0^{(1)}$ and $g_i^{(2)} = g_0^{(2)}$ for all i, the analysis of the RG flow, predicts a behavior analogous to the $g_i^{(1)} = 0$ case, with a renormalized g_0 approximately given by the fixed point value of $g_i^{(2)}$ at $t_\perp = 0$, that is $g_0 = g_0^{(2)} - g_0^{(1)}/2$. For example, in the specific case of an Hubbard model, with $g_0^{(2)} = g_0^{(1)}$, at small $t_\perp$, different regimes are expected for small and intermediate couplings, the transition occurring at

$$g_0 = \frac{g_0^{(2)}}{2} = \frac{1}{2}\frac{U}{4\pi v_F} \simeq 0.21... \tag{2.58}$$

This result is not far from what we have obtained by direct numerical integration of the RG equations for two Hubbard chains, as we are going to show.

2.3 Phase diagram of two Hubbard chains with interchain hopping

We have shown that RG predicts an instability of the Luttinger liquid asymptotic behavior, which occurs for isolated Hubbard chains, as soon as an infinitesimal $t_\perp$ is switched on (see also Ref. [6]). In particular, the two chains flow towards strong coupling, and at least two or possibly three different regimes occur.

This scenario, which was obtained through a simple stability analysis of of the Luttinger liquid fixed point upon switching $t_\perp$, can be further confirmed by direct numerical integration of the RG set of differential equations[46]. By means of a numerical approach, moreover, arbitrary values of $t_\perp$ and also the additional complications induced by taking different Fermi velocities of the two bands, can be handled without much effort, thus allowing a more detailed analysis of the model.

The non interacting hamiltonian we consider is the same of Eq. (2.1), generalized to spinful fermions. For $t_\perp < 1-\cos(\pi\rho)$ the Fermi energy crosses the two bands, and the low energy physics can be again described by two linear bands with different Fermi velocities and momenta.

The Hubbard interaction is:

$$\hat{H}_{\rm int} = U \sum_i (\mathrm{n}_{i,1,\uparrow}\mathrm{n}_{i,1,\downarrow} + \mathrm{n}_{i,2,\uparrow}\mathrm{n}_{i,2,\downarrow}),$$

where, let us recall, the labels 1 and 2 refer to the two chains, $\mathrm{n}_{i,1(2),\sigma} = c^\dagger_{i,1(2),\sigma} c_{i,1(2),\sigma}$, and $U > 0$. As before, we neglect both scattering processes between two right or two left moving electrons, and Umklapp scatterings. This leaves just the 10 coupling constants we introduced in the previous sections, i.e. $g_0^{(l)}$, $g_\pi^{(l)}$, $g_f^{(l)}$, $g_t^{(l)}$ and $g_b^{(l)}$, with $l = 1, 2$, [see Figs. (2.2) and (2.7)]. The relation between these coupling constants and the on–site repulsion

is simply $\tilde{g}_i^{(1)} = \tilde{g}_j^{(2)} = U/2 > 0$ for all $i, j = 0, \pi, f, t, b$. As discussed, we then adopt a standard Wilson Renormalization Group (RG) procedure. The only difference with the models we discussed previously, is that we now allow different Fermi velocities (v_F^0 and v_F^π) between the two bands. This generates another scaling parameter, related to v_F^0/v_F^π, which is left free to renormalize in the RG process[47]. The RG equations depend on this parameter, and therefore they look more cumbersome than Eq. (2.47). However, as we are going to show, at small $t_\perp$ this difference does not play any relevant role in the asymptotic regime. It is however important at large transverse hopping, because it tends to decouple the two bands, and eventually it produces a two uncoupled band model, each single band behaving as a Luttinger liquid. We have solved the second order RG equations numerically, starting from initial Hubbard values, i.e. with the positive invariant couplings defined as[47] $g_0^{(i)} = U/(4\pi v_F^0)$, $g_\pi^{(i)} = U/(4\pi v_F^\pi)$, and $g_f^{(i)} = g_t^{(j)} = g_b^{(k)} = U/[2\pi(v_F^0 + v_F^\pi)]$. Useful checks are provided by (a) the $t_\perp = 0$ limit[18] (independent chains); (b) zero inter–band backward scattering[47] $g_b^{(1)} = g_b^{(2)} = 0$.

The resulting phase diagram is presented in Fig. 2.9, and the main fixed points further described by Table 2.1. In this Table, the parameter x characterizing each phase, is related to the total charge mode, whose asymptotic behavior is not affected by the transverse hopping and therefore remains gapless. We now discuss in detail each phase. When $t_\perp$ is very large, $t_\perp \gg 1 - \cos(\pi\rho)$, only one band is occupied ($k_F^\pi = 0$) and a standard one band Luttinger Liquid, denoted as $LL1$[48], should be recovered. By decreasing $t_\perp$, we enter a two–band region (both k_F^0 and $k_F^\pi \neq 0$). Here we find a weak–coupling two–component Luttinger Liquid[18] fixed point ($LL2$). In this state, the "effective interchain hopping",

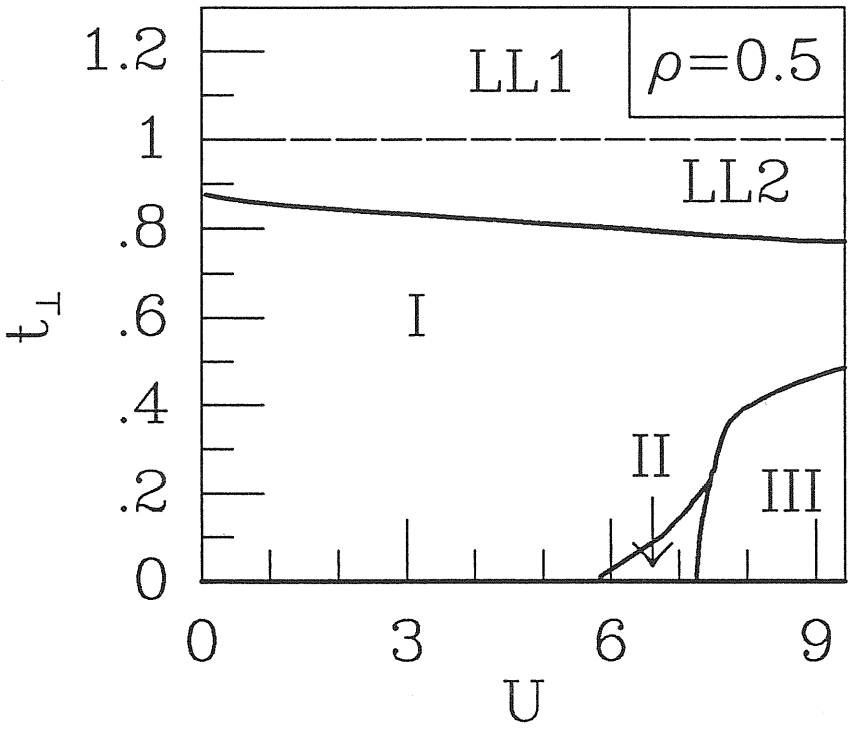

Figure 2.9: Phase diagram at density $\rho = 0.5$. LL1, LL2, and the line $t_\perp = 0$ are Luttinger liquids. I, II, and III are strong–coupling phases. Similar phase diagrams are found for different (noncommensurate) densities.

which we define as

$$t_\perp^{eff} = (v_F^0 + v_F^\pi)(k_F^0 - k_F^\pi)/2,$$

remains finite (no confinement in $LL2$). Things become very different for small $t_\perp$ where the RG flow scales to different strong coupling regimes, depending on the strength of U. These regimes correspond to those we predicted by simply linearizing the RG equations around the Luttinger liquid, and they have their exact counterpart in the two spinless chain model. For this reason, we will denote them using the same labels, i.e. I, II and III. Needless to say, since our approach is based on weak coupling assumptions, any strong–coupling outcome must be taken with great caution. On the other hand, instability of the

weak coupling state, which is suggested by the RG flow, should give reliable informations on the physical behaviour at long wavelength, as is common experience with other 1D problems[18].

The first strong–coupling phase we find (III), appears at large U. It is characterized by $t_\perp^{eff}/K_0 \to 0$, i.e., confinement. The fixed point III can be described as two Luttinger chains with zero interchain hopping and strong interchain particle–hole pair hopping. The generation of pair hopping in the RG process has been discussed earlier[19]. Turning to correlations, we consider the charge and spin susceptibilities $N(q_x, q_y, \omega)$ and $\chi(q_x, q_y, \omega)$, as well as the most singular pair susceptibilities,

$$\Pi^\alpha(q_x, q_y, \omega) = -i \int dt e^{i\omega t} \langle T\{\Delta^\alpha(q_x, q_y, t)\Delta^{\alpha\dagger}(q_x, q_y, 0)\}\rangle,$$

where α =I, II, III refers to phases I, II and III, and

$$\Delta^{\rm I}(0,0,t) = \sum_{\sigma,|k|<K_0} \sigma c_{k+k_F^0,0,\sigma}(t) c_{-k-k_F^0,0,-\sigma} - \sigma c_{k+k_F^\pi,\pi,\sigma}(t) c_{-k-k_F^\pi,\pi,-\sigma},$$

$$\Delta^{\rm III}(k_F^0 - k_F^\pi, \pi, t) = \sum_{\sigma,|k|<K_0} \sigma c_{k+k_F^0,0,\sigma}(t) c_{-k-k_F^\pi,\pi,-\sigma} - \sigma c_{k+k_F^\pi,\pi,\sigma}(t) c_{-k-k_F^0,0,-\sigma}, \quad (2.59)$$

while $\Delta^{\rm II}(0,0,t)$ is the ordinary s–wave Cooper pair. All correlations show a power–law behavior as a function of frequency at the fixed point (again we stress that only trends are to be taken seriously). As shown in Table 2.1, the most divergent correlation in III is a pairing of the $\Pi^{\rm III}$ type. In $\Delta^{\rm III}(0,\pi,t)$ (at the III fixed point, $k_F^0 - k_F^\pi = 0$) the $[(k_F,0),(-k_F,\pi)]$ pair combines with opposite sign with the "90° rotated pair" $[(k_F,\pi),(-k_F,0)]$. Among the spin–spin correlation functions, only $\chi(2k_F,0,\omega)$ is singular (less than $\Delta^{\rm III}$ though) while $\chi(2k_F,\pi,\omega)$ is non–singular, suggesting a tendency of the two renormalized chains to couple ferromagnetically. By contrast, for $t_\perp = 0$ (truly decoupled Luttinger chains) both χ's simultaneously diverge. III is further characterized by an

Table 2.1: The fixed point values of the invariant couplings at the Fermi points and the exponents of various susceptibilities. The divergent susceptibilities have negative exponents and are indicated by "div.". Here $0 < x < 1$ is a dimensionless non–universal constant increasing with U.

	III	I	$LL2$	II
v^0/v^π	1	1	const.	1
$t_\perp^{eff}$	0	const.	const.	const.
$g_0^{*(1)}$	0	-1	0	0
$g_0^{*(2)}$	x	-1+x	x^0	-x
$g_\pi^{*(1)}$	0	-1	0	0
$g_\pi^{*(2)}$	x	-1+x	x^π	-x
$g_t^{*(1)}$	0	1	0	-1
$g_t^{*(2)}$	0	1	0	0
$g_f^{*(1)}$	-1	0	0	-1
$g_f^{*(2)}$	-1+x	x	x	-x
$g_b^{*(1)}$	1	0	0	0
$g_b^{*(2)}$	1	0	0	0
$N(2k_F^\mu, 0, \omega)$	2(1-x)	-2(1+x) (div.)	$-2x^\mu$ (div.)	2x
$N(k_F^0 + k_F^\pi, \pi, \omega)$	-2(1+x) (div.)	2(1-x)	-2x (div.)	-2(4-x) (div.)
$\chi(2k_F^\mu, 0, \omega)$	-2(1+x) (div.)	2(1-x)	$-2x^\mu$ (div.)	2x
$\chi(k_F^0 + k_F^\pi, \pi, \omega)$	2(1-x)	-2(1+x) (div.)	-2x (div.)	2x
$\Pi^{III}(k_F^0 - k_F^\pi, \pi, \omega)$	-2(4-x) (div.)	—	—	—
$\Pi^{I}(0, 0, \omega)$	2x	-2(4-x) (div.)	x^0+x^π	2(1-x)
$\Pi^{II}(0, 0, \omega)$	2x	2x	x^0+x^π	-2(1+x)(div.)

interaction–induced depletion of the lowest band (0) in favour of the higher one (π). This leads to an effective Luttinger Fermi surface formally coincident with that at $t_\perp = 0$, which implies confinement. In this case, it is perhaps more instructive to envisage pairing in real space. We rewrite Eq. (2.59) as

$$\Delta^{\rm III}(0,\pi,t) = \sum_{\sigma,|k|<K_0} \sigma c_{k+k_F,1,\sigma}(t) c_{-k-k_F,2,-\sigma} - \sigma c_{k+k_F,2,\sigma}(t) c_{-k-k_F,1,-\sigma}, \qquad (2.60)$$

Hence, the two electrons live on different chains [labeled 1 and 2 in Eq. (2.60)]. Pairing occurs via crossed hopping of each electron to the other chain.

The other strong coupling phase I is very different. It still describes two strongly interacting chains, but this time with a residual $t_\perp^{eff} \neq 0$ (no confinement). Correlations show that the strongest singularity occurs for $\Pi^{\rm I}(0,0,\omega)$, again a pair susceptibility. However $\Delta^{\rm I}$ now combines the $[(k_F^0,0),(-k_F^0,0)]$ pair with that at $[(k_F^\pi,\pi),(-k_F^\pi,\pi)]$ with opposite relative sign[49]. In I, $\chi(k_F^0+k^\pi,\pi,\omega)$ diverges while $\chi(2k_F^i,0,\omega)$ does not, signaling antiferromagnetic coupling between the two chains.

Finally, the narrow region between III and I denoted by II, is again a strong coupling phase, with non zero $t_\perp^{eff}$ and dominant out–of–phase CDW fluctuations and s–wave pair fluctuations.

The phase diagram of Fig. 2.9 has been obtained within weak coupling RG which cannot be justified *a priori* in the strong coupling phases. A rough check of the level of accuracy of second order RG follows from the analysis of the single Hubbard chain, where exact results are now available[50]. The problem is that the approximate critical exponents obtained to $O(g^2)$ grow indefinitely with g while the exact ones quickly saturate at finite (and small) values. This might in principle induce unphysical features in the resulting behavior of the RG flow. However, we argue that in the whole region of the phase diagram

shown in Fig. 2.9, second order RG is still qualitatively correct, at least for $t_\perp = 0$, although the accuracy depends on the physical property in consideration. For instance, RG predicts a smoothing of the momentum distribution characterized by an exponent $\alpha = (U/4\pi v_F)^2$, which, at $U = 8t$ and $v_F = \sqrt{2}ta$ (corresponding to $\rho = 0.5$)[2], gives $\alpha \sim 0.2$, to be compared to the correct value $\alpha \sim 0.1$. This guarantees that, even within weak coupling RG, single particle hopping is definitely more relevant than pair hopping, to lowest order in $t_\perp$[6], and no spurious result should follow from our approximate treatment. However, we stress once more that only the tendencies towards different strong coupling regimes and their general features, have to be taken seriously, while neither the values of the fixed point couplings, nor those of the correlation function exponents, are reliable. However, the information we extracted from the RG, combined with the bosonization technique, provides an efficient tool to better analyze the different phases.

2.3.1 Bosonization of the strong coupling fixed points

Let us start, once more, with the two chain model (2.2), keeping for the moment only the couplings $g^{(2)}$, $g_f^{(2)}$, $g^{||}$ and $g_f^{||}$, which can be easily treated by means of bosonization technique. The kinetic part of the hamiltonian is rewritten in terms of the charge and spin density operators of each chain, as[18]:

$$\begin{aligned}\hat{H}_0 \;=\; \frac{2\pi v_F}{L}\sum_{q>0}\Big(&\rho_{1\sigma}(q)\rho_{1\sigma}(-q)+\rho_{2\sigma}(q)\rho_{2\sigma}(-q)+\sigma_{1\sigma}(q)\sigma_{1\sigma}(-q)+\sigma_{2\sigma}(q)\sigma_{2\sigma}(-q)+\\&+\rho_{1\pi}(q)\rho_{1\pi}(-q)+\rho_{2\pi}(q)\rho_{2\pi}(-q)+\sigma_{1\pi}(q)\sigma_{1\pi}(-q)+\sigma_{2\pi}(q)\sigma_{2\pi}(-q)\Big)\end{aligned} \tag{2.61}$$

[2]Notice that the value $U = 8t$ at which approximately phase II occurs, is in a quite good agreement with that we predicted, by means of very simple arguments, in the previous Section, i.e. $U \simeq 0.21 \times 8\pi v_F \simeq 7.5t$.

where the indices 1 and 2 refer to right and left moving particles, while 0 or π refer to the two different bands. We keep once again equal Fermi velocities v^0 and v^π. The RG flow at small $t_\perp$, as can be seen by Table 2.1, suggests that their difference is irrelevant in the asymptotic long wave–length regime. In terms of these operators, the interaction terms we are considering, can be written as the sum of two pieces $\hat{H}_\rho$ and $\hat{H}_\sigma$, involving separately the charge and the spin degree of freedom. In short notation,

$$\begin{aligned}\hat{H}_\nu &= \frac{2\pi}{L}\sum_q \Big[g\Big(\nu_{10}(q)\nu_{20}(-q) + \nu_{1\pi}(q)\nu_{2\pi}(-q)\Big) + \\ &\quad + g_f\Big(\nu_{10}(q)\nu_{2\pi}(-q) + \nu_{1\pi}(q)\nu_{20}(-q)\Big)\Big],\end{aligned} \tag{2.62}$$

where $\nu(q) = \rho(q), \sigma(q)$ and the couplings are defined as:

	charge	spin
$g =$	$2g^{(2)} - g^{(1)}$	$-g^{(1)}$
$g_f =$	$2g_f^{(2)} - g_f^{(1)}$	$-g_f^{(1)}$

In each sector we apply a Bogoliubov rotation of the density operators, defined in general as:

$$\begin{pmatrix} \nu_{10}(q) \\ \nu_{1\pi}(q) \\ \nu_{20}(q) \\ \nu_{2\pi}(q) \end{pmatrix} = \begin{pmatrix} \hat{C}_\nu & \hat{S}_\nu \\ \hat{S}_\nu & \hat{C}_\nu \end{pmatrix} \begin{pmatrix} \nu_{1c}(q) \\ \nu_{1s}(q) \\ \nu_{2c}(q) \\ \nu_{2s}(q) \end{pmatrix}$$

where the 2×2 matrices $\hat{C}_\nu$ and $\hat{S}_\nu$ must satisfy the conditions:

$$\begin{aligned} \hat{C}_\nu \hat{C}_\nu^T - \hat{S}_\nu \hat{S}_\nu^T &= \hat{\mathrm{I}}, \\ \hat{C}_\nu \hat{S}_\nu^T - \hat{S}_\nu \hat{C}_\nu^T &= 0. \end{aligned} \tag{2.63}$$

The indices c and s labelling the eigenvectors, clearly refer to the symmetric (pseudo–charge) and anti–symmetric (pseudo–spin) combinations of the densities of the two bands. By means of this rotation, the Hamiltonian can be easily diagonalized, the two eigenvalues

being:

$$v_c = \sqrt{v_F^2 - (g + g_f)^2}, \tag{2.64}$$

$$v_s = \sqrt{v_F^2 - (g - g_f)^2}, \tag{2.65}$$

and the rotation matrices:

$$\hat{C} = \frac{1}{\sqrt{2}} \begin{pmatrix} \cosh\psi_c & \cosh\psi_s \\ \cosh\psi_c & -\cosh\psi_s \end{pmatrix}, \tag{2.66}$$

$$\hat{S} = \frac{1}{\sqrt{2}} \begin{pmatrix} \epsilon_c \sinh\psi_c & \epsilon_s \sinh\psi_s \\ \epsilon_c \sinh\psi_c & -\epsilon_s \sinh\psi_s \end{pmatrix}, \tag{2.67}$$

where $\epsilon_c = \text{sign}(g + g_f)$ and $\epsilon_s = \text{sign}(g - g_f)$ while

$$\begin{aligned} \cosh\psi_c &= \sqrt{\frac{v_F + v_c}{2v_c}}, \\ \cosh\psi_s &= \sqrt{\frac{v_F + v_s}{2v_s}}. \end{aligned} \tag{2.68}$$

We have dropped everywhere the index $\nu = \rho, \sigma$, indicating in which sector, spin or charge, we are making the rotation. We will re–introduce it later.

Let us now specialize to the cases under consideration. The fixed points I, II and III, are characterized by a conserved quantity:

$$2\left(g^{(2)} + g_f^{(2)}\right) - g^{(1)} - g_f^{(1)} = 2g_0, \tag{2.69}$$

and by a unique strong coupling parameter $g_1 = v_F$. It is not difficult to show that for each of the three fixed points:

$$v_{\rho c} = \sqrt{v_f^2 - 4g_0^2} \tag{2.70}$$

and

$$v_{\rho s} = v_{\sigma c} = v_{\sigma s} = \sqrt{v_f^2 - g_1^2}, \tag{2.71}$$

while

	I	II	III
$\epsilon_{\rho c}$	1	1	1
$\epsilon_{\rho s}$	-1	-1	1
$\epsilon_{\sigma c}$	1	1	1
$\epsilon_{\sigma s}$	1	-1	-1

It is interesting to notice that the three fixed points share the same symmetry property, i.e. the degrees of freedom related to the densities ρ_s, σ_c and σ_s are completely equivalent. If we now introduce the couplings, which we left aside, i.e.

$$\begin{aligned} &\bullet \text{ Phase I } : g^{(1)} = -g_1,\ g_t^{(1)} = g_1, \quad g_t^{(2)} = g_1; \\ &\bullet \text{ Phase II} : g_f^{(1)} = -g_1,\ g_t^{(1)} = -g_1,\ g_t^{||} = -g_1; \\ &\bullet \text{ Phase II} : g_f^{(1)} = -g_1,\ g_b^{(1)} = g_1, \quad g_b^{(2)} = g_1, \end{aligned} \tag{2.72}$$

we find that they give origin to non quadratic terms in the hamiltonian, which can not be analytically diagonalized any more. Even in this case, the symmetry among ρ_s, σ_c and σ_s remains unchanged. No interaction couples these modes with ρ_c, which remains gapless. As we have repeatedly said, this symmetric charge mode is not affected by the transverse hopping, being related to the total charge of the two chains. Instead, the anti–symmetric charge mode get strongly coupled to the spin modes, implying that complete decoupling of charge and spin, does not occur anymore. The parameter g_1 characterizing the three strong coupling fixed points, coincides with v_F in second order of RG. However, its precise value is not important in the following, the only relevant thing being that it is shown to flow towards strong coupling under RG. In order to write these interactions in a bosonized form, we have to introduce the phase fields which allow the fermions to be written in terms of density operators. These fields are defined as[42]:

$$\phi_\nu(x),\ \theta_\nu(x) = \mp\frac{\mathrm{i}}{\sqrt{4\pi}}\sum_q \frac{2\pi}{qL}\mathrm{e}^{-\mathrm{i}qx-\alpha|q|/2}\left(\nu_1(q) \pm \nu_2(q)\right), \tag{2.73}$$

the upper(lower) sign referring to $\phi_\nu(\theta_\nu)$. According to this definition, $\Pi_\nu(x) = \partial_x\theta_\nu(x)$ is the conjugate momentum of ϕ_ν. Using these new variables, we can show that the

interactions (2.72) generate coupling between the modes ρ_s, σ_c and σ_s. The fixed point hamiltonians for these three equivalent modes, have the same functional form:

$$\hat{H}^* = \int \mathrm{d}x \Big\{ \sum_{i=1}^{3} \frac{1}{2} \left[\Pi_i^2(x) + (\partial_x \phi_i(x))^2 \right] + \\ + \frac{4g_1}{(2\pi\alpha)^2 v} \sum_{i<j} \cos\beta\phi_i(x) \cos\beta\phi_j(x) \Big\}, \tag{2.74}$$

in all the three phases I, II and III. Here v is given by Eq. (2.71) and $\beta = \sqrt{4\pi}\mathrm{e}^{\psi}$, where ψ is the angle defining the Bogoliubov rotation of the three equivalent fields [see Eq. (2.68)]. These fields turn out to be, for the three different fixed points:

I	II	III
$\theta_{s\rho}$, $\phi_{c\sigma}$, $\phi_{s\sigma}$	$\theta_{s\rho}$, $\phi_{c\sigma}$, $\theta_{s\sigma}$	$\phi_{s\rho}$, $\phi_{c\sigma}$, $\theta_{s\sigma}$

(2.75)

The RG predicts that the coupling constant g_1 flows towards strong coupling. The consequence is that, for each fixed point, one has long–range order in the correspondent phase fields (2.75), while the correlations of the dual fields decay exponentially at large distance. The remaining fields, associated to ρ_c, have no gap, and their correlation functions decay as power law.

It is then possible to determine more precisely the asymptotic behavior of the correlation functions we defined in the previous section. Most of them are shown to decay exponentially, even though weak coupling RG predicts a power law decay. For example, the $2k_F$–spin susceptibility at transverse momentum $k_\perp = \pi$, can be written in terms of the combinations of densities $(\rho_{10} + \rho_{2\pi})$ and $(\sigma_{10} + \sigma_{2\pi})$, thereby involving the correlation functions of the phase fields $(-\phi_{c\rho} + \theta_{s\rho})$ and $(-\phi_{c\sigma} + \theta_{s\sigma})$. The latter term has a field whose correlation decay exponentially, which implies that the spin susceptibility $\chi(k_F^0 + k_F^\pi, \pi, \omega)$ is not singular, contrary to the RG prediction. In fact, one can show that the dominant fluctuations in phase I are indeed the pair fluctuations represented by the

correlation function Π^{I}, which at large distance decays as:

$$\Pi^{I}(x) \sim \frac{1}{x^{\delta}}, \tag{2.76}$$

with

$$\delta = e^{-2\psi_{\rho c}}/4. \tag{2.77}$$

Analogously, phase II has dominant out of phase CDW fluctuations, which for $x \gg 1$, decay as:

$$N(x) \sim \frac{\sin(k_F^0 + k_F^\pi)x}{x^{\gamma}}, \tag{2.78}$$

with

$$\gamma = e^{2\psi_{\rho c}}/4. \tag{2.79}$$

Finally, in phase III, as predicted by RG, the dominant singularity occurs for the pair susceptibility Π^{III}, which decays asymptotically as a power law with the exponent δ of Eq. (2.77).

Therefore, the bosonization of the fixed points allows to determine the character of the dominant fluctuations and all correlation exponents. The comparison with weak coupling RG analysis shows that, while the RG correctly establishes which is the most singular susceptibility, it fails in predicting both the other singular susceptibilities and all the exponents. This discrepancy is likely to be due to the strong coupling nature of the fixed point hamiltonians, which can not be properly handled by weak coupling RG. However, other problems may arise, due to the complicated scaling properties of this two band model. The usual way of defining scaling susceptibilities in the single band 1D problems[18], is not fully consistent in our model, because these functions do not have the correct scaling properties, as we checked by calculating the leading second order corrections for some

of these correlation functions. Instead, the invariant couplings do scale, as Penc and Solyom[47] have shown, and the RG for these parameters is hopefully well defined.

2.4 Spin–charge separation in a two chain model

A central problem in the theory of strongly correlated systems is whether the mechanism leading to the breakdown of Fermi liquid (FL) theory in one dimensional models can be generalized to higher dimensions[10]. In most 1D systems, it is known that non FL behavior manifests itself in two distinct ways: the correlation functions show power law behavior with coupling dependent anomalous exponents[5] leading, in particular, to the smoothing of the Fermi surface which is often considered as the key signature of non FL behavior. An independent, but equally effective mechanism which induces the breakdown of FL without generating anomalous exponents, is the well known *spin–charge decoupling*[6] which originates from the *dynamical* independence of charge and spin excitations. Schulz[6] has given a very nice and transparent picture of spin–charge decoupling. Let us imagine to induce a spin– and charge–density fluctuation by adding an extra particle, e.g. a right moving one, at time $t = 0$ and at spatial coordinate x_0. Initially these fluctuations will be obviously centered at x_0, that is:

$$\begin{aligned} \langle 0|\psi_1(x_0)\rho(x)\psi_1^\dagger(x_0)|0\rangle &= \delta(x - x_0), \\ \langle 0|\psi_1(x_0)\sigma(x)\psi_1^\dagger(x_0)|0\rangle &= \delta(x - x_0). \end{aligned}$$

Due to spin–charge separation, the two density fluctuations will asymptotically propagate independently, with different velocities u_ρ and u_σ. Therefore for $t \gg 1$ it is expected that:

$$\begin{aligned} \langle 0|\psi_1(x_0)\rho(x,t)\psi_1^\dagger(x_0)|0\rangle &= \delta(x - x_0 - u_\rho t), \\ \langle 0|\psi_1(x_0)\sigma(x,t)\psi_1^\dagger(x_0)|0\rangle &= \delta(x - x_0 - u_\sigma t). \end{aligned}$$

This kind of behavior should be common to a large variety of 1D models of spinful fermions, and it has been clearly shown to occur in the Hubbard model[52]. In an ordinary Fermi

liquid, the same hypothetical experiment would have shown the two fluctuations mostly centered at the single space coordinate $x = x_0 + v_F t$.

Many unsuccessful attempts have been made in the past years to search for a breakdown of FL theory in 2D through the study of the discontinuity in the momentum distribution, i.e. by looking for anomalous exponents. Some of them have been discussed in Chapter 1. On the contrary, very little effort[21, 51] has been focused on the alternative possible realization of non–Fermi liquid behavior in 2D through spin–charge decoupling but without anomalous exponents. The RG approach to weakly coupled chains, which we have applied to the simple two–chain model in the previous sections, is not suited to tackle this problem. Even though we have shown (see Section 2.1) that RG correctly reproduces the spin–charge decoupling at the level of the scaling equations, the detailed physical consequences of this decoupling, like e.g. those we have shown before, do not come up naturally from RG. On the contrary, bosonization technique is a very powerful method to deal with this problem, as we are going to show.

A simple 1D model which shows spin–charge decoupling without anomalous power–law decay in the correlation functions, can be obtained by including only forward scattering processes between electrons on the same branch of the Fermi surface (usually referred to as g_4 interactions). The hamiltonian of this model is[18]:

$$\begin{aligned}\hat{H}_0 &= \sum_{k,\sigma} v_F(k-k_F)a^\dagger_{k\sigma}a_{k\sigma} + \sum_{k,\sigma} v_F(-k-k_F)b^\dagger_{k\sigma}b_{k\sigma} + \\ &+ \frac{1}{2L}\sum_{k_1,k_2,p}\sum_{\alpha,\beta}(g_{4\|}\delta_{\alpha\beta} + g_{4\perp}\delta_{\alpha-\beta})(a^\dagger_{k_1\alpha}a^\dagger_{k_2\beta}a_{k_2+p\beta}a_{k_1-p\alpha} + b^\dagger_{k_1\alpha}b^\dagger_{k_2\beta}b_{k_2+p\beta}b_{k_1-p\alpha})\end{aligned} \tag{2.80}$$

where the operator $a^\dagger_{k\sigma}(b^\dagger_{k\sigma})$ creates an electron of momentum k and spin σ belonging to the branch with positive(negative) slope $v_F(-v_F)$. Due to the linear dispersion relation

of the hamiltonian[3] (2.80), this model can be solved by use of standard bosonization technique being a special case of the well known Tomonaga–Luttinger model. While this interaction does not affect the ground state properties, the excitations are profoundly different. Two low–lying gapless excitations with linear dispersion, are found, describing charge and spin collective modes with different sound velocities $u_\rho = v_F + (g_{4||} + g_{4\perp})/2\pi$ and $u_\sigma = v_F + (g_{4||} - g_{4\perp})/2\pi$. No quasi–particle excitation exists and, as a consequence, the Green function does not have simple poles but branch cut singularities. The bosonization method allows to calculate the exact form of the Green function in real space and time:

$$G(x,t) = \frac{1}{2\pi}\left\{ \frac{e^{ik_F x}}{\sqrt{(x - u_\rho t + i\eta \mathrm{sign}t)(x - u_\sigma t + i\eta \mathrm{sign}t)}} + \right.$$
$$\left. - \frac{e^{-ik_F x}}{\sqrt{(x + u_\rho t - i\eta \mathrm{sign}t)(x + u_\sigma t - i\eta \mathrm{sign}t)}} \right\}. \qquad (2.81)$$

After Fourier transforming, the spectral weight, e.g. for the right moving electrons, can be easily obtained (for more general 1D models see Ref. [53]):

$$A(k_F + q, \omega) = \frac{[\theta(q)\theta(\omega - u_\sigma q)\theta(u_\rho q - \omega) + \theta(-q)\theta(\omega - u_\rho q)\theta(u_\sigma q - \omega)]}{\pi\sqrt{|\omega - u_\sigma q||\omega - u_\rho q|}}. \qquad (2.82)$$

In the particular case $g_{4||} = g_{4\perp} = 0$ the spin and charge velocities u_σ and u_ρ coincide and the branch cut merges in a simple pole reproducing the standard free particle Green function. In this simple model, although the low lying excitations can not be described in terms of the Landau Fermi liquid theory, *all the equal time correlation functions at zero temperature, including the momentum distribution, coincide with the non–interacting ones.* The form of the spectral function (2.82) explicitly shows that non FL behavior can occur even without anomalous exponents. In this case, the breakdown of FL is related to a change in the analytic structure of $A(k,\omega)$ which does not generate the logarithmic singularities in perturbation theory present in many 1D models.

This model is an ideal prototype to study the relevance of spin–charge decoupling in a system of chains coupled by transverse hopping. As a first step let us consider the simple case of two chains[54]. The total hamiltonian will be the sum of two terms like Eq. (2.80), one for each chain, plus an hopping term between the two chains:

$$H_\perp = -t_\perp \sum_{k\sigma} \left(a^\dagger_{k\sigma,1} a_{k\sigma,2} + b^\dagger_{k\sigma,1} b_{k\sigma,2} + \text{H.c.} \right), \tag{2.83}$$

where the suffixes 1 or 2 refer to the two chains. We will now show how it is possible to solve exactly this problem by bosonization technique. As there is no term in the Hamiltonian which couples right to left moving electrons, we treat only the case of the right moving electrons. The hamiltonian Eq. (2.80) can be easily rewritten in terms of the density operators of the electrons on the positive branch[18]:

$$\begin{aligned} \hat{H}_0 \;=\; & \frac{2\pi}{L} u_\rho \sum_{q>0} \left[\rho_1(q)\rho_1(-q) + \rho_2(q)\rho_2(-q) \right] + \\ & + \frac{2\pi}{L} u_\sigma \sum_{q>0} \left[\sigma_1(q)\sigma_1(-q) + \sigma_2(q)\sigma_2(-q) \right], \end{aligned} \tag{2.84}$$

where $\rho_1(q)(\sigma_1(q))$ is the charge(spin) density operator of the right moving electrons on chain 1. In order to write the transverse hopping Eq. (2.83) in terms of the density operators, it is necessary to introduce the boson representation of fermion operators[42]. Then one obtains:

$$H_\perp = 2it_\perp \frac{1}{2\pi\alpha} \int \mathrm{d}x \left[\sin\left(\phi_{\rho s}(x) + \phi_{\sigma s}(x)\right) + \sin\left(\phi_{\rho s}(x) - \phi_{\sigma s}(x)\right) \right], \tag{2.85}$$

where the operator ϕ_i's are the phase fields related to the densities:

$$\begin{array}{ll} \rho_c = \frac{1}{\sqrt{2}}(\rho_1 + \rho_2) & \rho_s = \frac{1}{\sqrt{2}}(\rho_1 - \rho_2) \\ \sigma_c = \frac{1}{\sqrt{2}}(\sigma_1 + \sigma_2) & \sigma_s = \frac{1}{\sqrt{2}}(\sigma_1 - \sigma_2) \end{array} \tag{2.86}$$

and they are defined as[42, 18]:

$$\phi_i(x) = \mathrm{i} \sum_{q>0} \frac{2\pi}{qL} \mathrm{e}^{-\alpha q/2} \left(\mathrm{e}^{-\mathrm{i}qx} \rho_i(q) - \mathrm{e}^{\mathrm{i}qx} \rho_i(-q) \right).$$

The suffix i labels any of the four densities in Eq. (2.86), and the factor $\exp(-\alpha q/2)$ plays the role of an ultraviolet cutoff for divergent integrals. In terms of the densities (2.86), the hamiltonian (2.84) remains diagonal. Let us introduce the fermionic fields corresponding to the densities (2.86). Then, the hopping term (2.85) acquires a very simple form:

$$-t_\perp \int \mathrm{d}x \left(\Psi^\dagger_{\rho s}(x)\Psi_{\sigma s}(x) + \mathrm{H.c.}\right) + \left(\mathrm{e}^{2ik_F x}\Psi^\dagger_{\rho s}(x)\Psi^\dagger_{\sigma s}(x) + \mathrm{H.c.}\right). \tag{2.87}$$

Equation (2.87) shows that the transverse hopping $t_\perp$ affects only the ρ_s and σ_s sector, which is equivalent to the pseudo–spin sector in the representation of the bonding and anti–bonding combination of the two chains. In this representation, as we said in Section 2.1, the transverse hopping plays the role of a magnetic field, in splitting the energies of the bonding combination from the anti–bonding one. By defining the Fourier transform $c_\rho(k)$ ($c_\sigma(k)$) of the field operator $\Psi_{\rho s}$ ($\Psi_{\sigma s}$),

$$\begin{aligned}
\Psi_{\rho s}(x) &= \frac{1}{\sqrt{L}}\sum_k \mathrm{e}^{\mathrm{i}kx} c_\rho(k) \\
\Psi_{\sigma s}(x) &= \frac{1}{\sqrt{L}}\sum_k \mathrm{e}^{\mathrm{i}kx} c_\sigma(k)
\end{aligned}$$

the total hamiltonian, i.e. Eqs. (2.84) plus (2.87), can be rewritten as:

$$\begin{aligned}
\hat{H} &= \sum_k \left(u_\rho(k-k_F)c^\dagger_\rho(k)c_\rho(k) + u_\sigma(k-k_F)c^\dagger_\sigma(k)c_\sigma(k)\right) + \\
&- t_\perp \sum_k \left(c^\dagger_\rho(k)c_\sigma(k) + \mathrm{H.c.}\right) + \\
&- t_\perp \sum_{k>0} \left(c^\dagger_\rho(k+k_F)c^\dagger_\sigma(k-k_F) + \mathrm{H.c.} + c^\dagger_\rho(k-k_F)c^\dagger_\sigma(k+k_F) + \mathrm{H.c.}\right).
\end{aligned} \tag{2.88}$$

This hamiltonian is the sum of bilinear terms of fermion operators, therefore it can be easily diagonalized. First of all, we perform the particle–hole transformation:

$$\begin{array}{ll}
c^\dagger_\rho(k+k_F) \to c^\dagger_\rho(k) & c^\dagger_\rho(k_F-k) \to d_\rho(k) \\
c^\dagger_\sigma(k+k_F) \to c^\dagger_\sigma(k) & c^\dagger_\sigma(k_F-k) \to -d_\sigma(k)
\end{array} \tag{2.89}$$

where $k > 0$, then Eq. (2.88) becomes:

$$\begin{aligned}\hat{H} &= \sum_{k>0}\Big\{u_\rho\left(c_\rho^\dagger(k)c_\rho(k)+d_\rho^\dagger(k)d_\rho(k)\right)+u_\sigma\left(c_\sigma^\dagger(k)c_\sigma(k)+d_\sigma^\dagger(k)d_\sigma(k)\right)+\\ &\quad -t_\perp\left(c_\rho^\dagger(k)c_\sigma(k)+\text{H.c.}+d_\rho^\dagger(k)d_\sigma(k)+\text{H.c.}\right)+\\ &\quad +t_\perp\left(c_\rho^\dagger d_\sigma+\text{H.c.}+c_\sigma^\dagger d_\rho+\text{H.c.}\right)\Big\},\end{aligned} \tag{2.90}$$

which can be further simplified to:

$$\begin{aligned}\hat{H} &= \sum_{k>0}\Big\{u_\rho\left(a_\rho^\dagger(k)a_\rho(k)+b_\rho^\dagger(k)b_\rho(k)\right)+u_\sigma\left(a_\sigma^\dagger(k)a_\sigma(k)+b_\sigma^\dagger(k)b_\sigma(k)\right)+\\ &\quad -2t_\perp\left(b_\rho^\dagger(k)b_\sigma(k)+\text{H.c.}\right)\Big\},\end{aligned} \tag{2.91}$$

by using the operators:

$$\begin{aligned}a_{\rho(\sigma)} &= \frac{1}{\sqrt{2}}\left(c_{\rho(\sigma)}+d_{\rho(\sigma)}\right)\\ b_{\rho(\sigma)} &= \frac{1}{\sqrt{2}}\left(c_{\rho(\sigma)}-d_{\rho(\sigma)}\right).\end{aligned}$$

The hamiltonian (2.91) is already diagonal in the modes $a_{\rho(\sigma)}$, and can be easily diagonalized in the other modes $b_{\rho(\sigma)}$, by means of the unitary transformation:

$$\begin{aligned}b_\rho(k) &= \cos\theta_k b_3(k)+\sin\theta_k b_4(k)\\ b_\sigma(k) &= -\sin\theta_k b_3(k)+\cos\theta_k b_4(k)\end{aligned}$$

with:

$$\tan 2\theta_k = \frac{4t_\perp}{(u_\rho-u_\sigma)k} \tag{2.92}$$

The hamiltonian, written in terms of these eigenmodes, is:

$$\hat{H}=\sum_{q>0}\Big[\epsilon_1(q)a_\rho^\dagger(q)a_\rho(q)+\epsilon_2(q)a_\sigma^\dagger(q)a_\sigma(q)+\epsilon_3(q)b_3^\dagger(q)b_3(q)+\epsilon_4(q)b_4^\dagger(q)b_4(q)\Big] \tag{2.93}$$

with the four eigenvalues:

$$\begin{aligned}
\epsilon_1(q) &= u_\rho q \\
\epsilon_2(q) &= u_\sigma q \\
\epsilon_3(q) &= \tfrac{1}{2}(u_\rho + u_\sigma)q + \sqrt{\left(\tfrac{1}{2}(u_\rho - u_\sigma)q\right)^2 + 4t_\perp^2} \\
\epsilon_4(q) &= \tfrac{1}{2}(u_\rho + u_\sigma)q - \sqrt{\left(\tfrac{1}{2}(u_\rho - u_\sigma)q\right)^2 + 4t_\perp^2}
\end{aligned} \tag{2.94}$$

Having set the chemical potential equal to zero, the ground state is obtained by filling the branch $\epsilon_4(q)$ up to a momentum $Q = 2t_\perp/\sqrt{u_\rho u_\sigma}$ corresponding to $\epsilon_4(Q) = 0$.

We have checked that, although this spinless fermion excitation spectrum seems quite complicated, it correctly reproduces all known results, in particular the charge– and spin–density normal modes in the trivial limits *a*) $g_{4\|} = 0 = g_{4\perp}$ for $t_\perp \neq 0$; *b*) $g_{4\|} \neq 0$, $g_{4\perp} \neq 0$ for $t_\perp = 0$.

From the ground state and the excitation spectrum several physical properties of the system can be calculated. The ground state energy is given by twice the integral of $\epsilon_4(q)$ from $q = 0$ up to $q = Q$. This accounts for both right and left moving electrons, giving:

$$\frac{\Delta E}{L} = -\frac{1}{2\pi}\frac{4t_\perp^2}{(u_\rho - u_\sigma)}\log(\frac{u_\rho}{u_\sigma}). \tag{2.95}$$

Notice that Eq. (2.95) reproduces the correct result in the non–interacting case, i.e. when $u_\rho = u_\sigma = v_F$. The energy correction (2.95) being proportional to $t_\perp^2$ implies a non zero value of the transverse hopping operator averaged on the ground state, which in turns means that *spin–charge decoupling is not sufficient to generate confinement of the electrons within each chain[21].* In order to analyse this issue more deeply, we calculate the difference of the occupation numbers between the bonding and the anti–bonding band. By labelling the two bands according to the correspondent transverse momenta, i.e. $k_\perp = 0$

for the bonding combination, and $k_\perp = \pi$ for the anti–bonding one, we get:

$$\frac{\langle N_0 - N_\pi \rangle}{L} = \frac{4t_\perp}{2\pi} \frac{1}{u_\rho - u_\sigma} \log\left(\frac{u_\rho}{u_\sigma}\right) \tag{2.96}$$

which, again, does not show confinement in the two chain problem. As a further probe for confinement, we have evaluated the number fluctuations between the two chains. This quantity is easily related to the long wavelength limit of the density structure factor, which can be calculated by the bosonization method, and it turns out to be

$$\begin{aligned} S_{12}(q) &= \sum_r e^{-iqr} \langle n_r^1 n_0^2 \rangle = -\frac{\theta(Q-q)t_\perp}{2\pi(u_\rho - u_\sigma)} \times \\ &\quad \times \left[I\left(Q\frac{u_\rho - u_\sigma}{4t_\perp}\right) - I\left(q\frac{u_\rho - u_\sigma}{4t_\perp}\right)\right] \\ S_{11}(q) &= -S_{12}(q) + \frac{q}{2\pi} \end{aligned}$$

where the function $I(x) = 1 + x - \sqrt{1+x^2}$. By means of the structure factor, the number fluctuation is shown to be:

$$\frac{1}{2}\frac{\langle (N_1 - N_2)^2 \rangle}{L} = \lim_{q\to 0}[S_{11}(q) - S_{12}(q)] = \frac{t_\perp}{\pi(u_\rho - u_\sigma)}\left(1 - \sqrt{\frac{u_\sigma}{u_\rho}}\right).$$

This expression, apart from the trivial dependence upon $t_\perp$, is a function of the interaction through u_ρ and u_σ. In the simple case of spin–isotropic interaction, i.e. $g_{4||} = g_{4\perp}$, the number fluctuation is a monotonic decreasing function of the interaction, which goes to zero only when the coupling tends to infinity. Another quantity easy to calculate, is the spin–spin correlation between the two chains, which measures the strength of the magnetic coupling between the chains. In particular, we have shown that

$$\langle \sigma_1(x)\sigma_2(x)\rangle = -\frac{t_\perp^2}{2\pi^2(u_\rho - u_\sigma)^2}\left[\frac{u_\rho - u_\sigma}{u_\sigma} - \log\left(\frac{u_\rho}{u_\sigma}\right)\right] \tag{2.97}$$

where 1(2) is the chain label. From Equation (2.97) it appears that the two chains couple

antiferromagnetically. When the interaction is strong [$u_\rho \to g_4/\pi$ for $g_4 \gg v_F$, while $u_\sigma = v_F$, in the spin–isotropic model], (2.97) correctly scales as $J_\perp \sim t_\perp^2/g_4$.

It is now interesting to investigate the effects of transverse hopping on the spin–charge decoupling of the elementary excitations. From a simple inspection of the excitation spectrum in Eq. (2.94), one can argue that for large momentum the standard 1D picture is recovered, together with spin–charge decoupling. In fact, for large q, $\epsilon_3(q) \to \epsilon_1(q) = u_\rho q$, $\epsilon_4(q) \to \epsilon_2(q) = u_\sigma q$, and the spectrum tends to the $t_\perp = 0$ case. On the other hand, new excitations appear at low energy, centered around $q = 2t_\perp/\sqrt{u_\rho u_\sigma}$, with an almost linear spectrum and velocity $2u_\rho u_\sigma/(u_\rho + u_\sigma)$. The length scale which separates the two regimes is given by

$$\xi = (u_\rho - u_\sigma)/4t_\perp. \tag{2.98}$$

This form of the excitation spectrum leads to important consequences in the spin and charge density–density correlation functions. On chain 1 the latter is defined as

$$-\mathrm{i}\theta(t)\langle[\rho_1(q,t),\rho_1(-q)]\rangle = -\frac{\mathrm{i}\theta(t)}{2}\{\langle[\rho_c(q,t),\rho_c(-q)]\rangle + \langle[\rho_s(q,t),\rho_s(-q)]\rangle\}$$

The first term on the right hand side is not affected by $t_\perp$ and contributes to the spectral weight $A(\omega,q)$ with a delta–function centered at $\omega = -u_\rho q$. For $q\xi \gg 1$, the $t_\perp \sim 0$ regime is recovered and most of the spectral weight of the second term lies in the sharp peak at $\omega \simeq -u_\rho q$ as in the case of two independent chains (Fig. 2.10). In the opposite limit $q\xi \ll 1$ the effect of transverse hopping dominates over interaction and the system behaves like in the non interacting case where the ρ_s term contributes to the spectral weight with two delta–peaks centered respectively at $\omega = -v_F q + 2t_\perp$ and at $\omega = -v_F q - 2t_\perp$ (see Fig. 2.11). In both limits, the interplay between the transverse hopping and the interaction, has the effect of broadening the peaks in $A(k,\omega)$, which now acquire a finite width. A

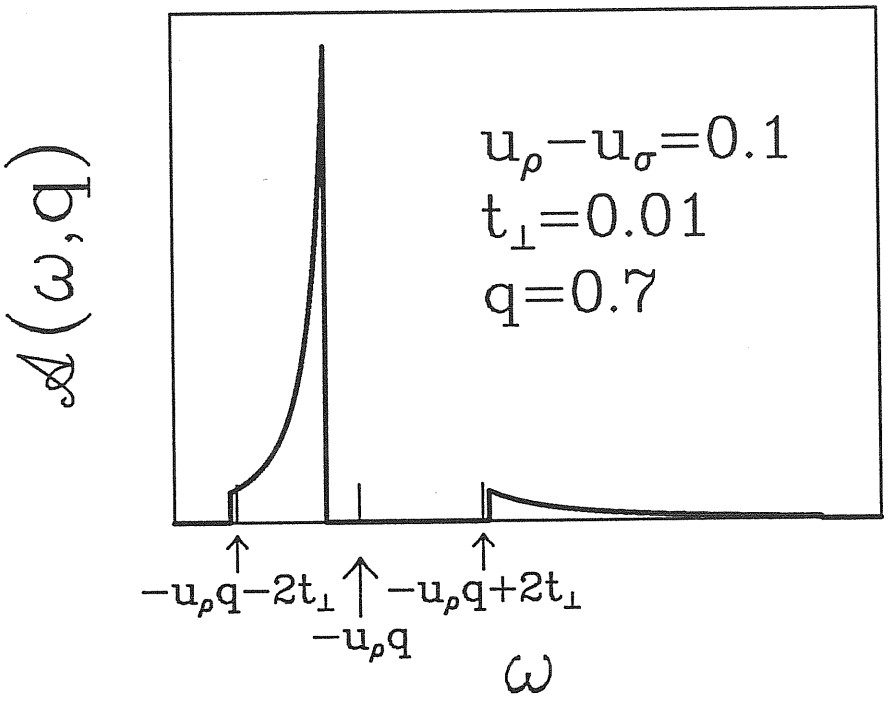

Figure 2.10: Charge density–density spectral function in the channel $\rho_s = 1/\sqrt{2}(\rho_1 - \rho_2)$. The calculation has been performed setting $u_\rho - u_\sigma = 0.1$, $t_\perp = 0.01$ and $q = 0.7$ in units of $v_F = 1$.

direct probe of spin–charge decoupling can be obtained through the single–particle Green function. This correlation function is difficult to extract from our solution, because the fermionic operators have a very complicated expression in terms of the normal modes which diagonalize the hamiltonian. However, it is possible to obtain its asymptotic behavior at large distance which contains the relevant information regarding FL behavior. In this regime, we approximate the excitation branch $\epsilon_4(q)$ in Eq. (2.94) near $q = 2t_\perp/\sqrt{u_\rho u_\sigma}$ with a linear spectrum having velocity $u_r = 2u_\rho u_\sigma/(u_\rho + u_\sigma)$. This simplification allows to calculate the real space Green function at fixed transverse momentum ($k_\perp = 0, \pi$):

$$\langle \Psi_0(x,t)\Psi_0^\dagger(0,0)\rangle \sim e^{i(k_F+\Delta k_F)x}(x-u_\rho t)^{-\frac{3}{8}}(x-u_\sigma t)^{-\frac{3}{8}}(x-u_r t)^{-\frac{1}{4}} \qquad (2.99)$$

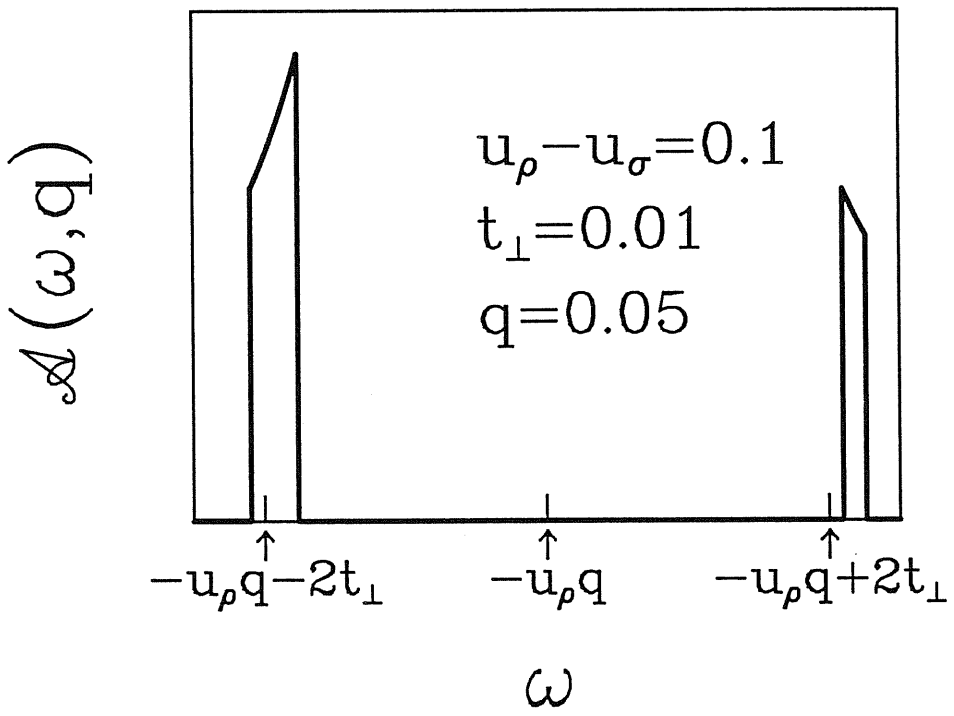

Figure 2.11: The same as the Fig. 2.10, but at momentum $q = 0.05$.

where

$$\Delta k_F = \frac{t_\perp}{u_\rho - u_\sigma} \log(u_\rho/u_\sigma). \tag{2.100}$$

An analogous expression can be derived for the anti-bonding combination of the two chains ($k_\perp = \pi$) by reversing the sign of Δk_F. Equation (2.100) shows that the transverse hopping does move the Fermi points of the bonding with respect to the anti-bonding band. The asymptotic expression Eq. (2.99) is valid in the region $x, v_F t \gg \xi$, while for smaller separation we expect to recover the single chain limit Eq. (2.81). Therefore, we find a crossover between two regimes. On a scale $x < \xi$ fluctuations between the two chains are suppressed and the model essentially behaves like two independent chains. At long distance ($x > \xi$), the coupling between the chains is reintroduced but interaction

still plays a crucial role. An electron excitation now decays into a *triplet* of elementary excitations, and not just a holon and a spinon.

Encouraged by the absence of singularities in the transverse hopping as it comes out from the exact solution, we have checked the bosonization results against perturbation theory in $t_\perp$. The first order correction to the single particle Green function can be easily obtained up to first order in $t_\perp$:

$$G_{0(\pi)}(k,\omega) = G^{(0)}(k,\omega) \mp t_\perp \left[G^{(0)}(k,\omega)\right]^2 \tag{2.101}$$

where the $-(+)$ corresponds to $k_\perp = 0(\pi)$, and the unperturbed Green function $G^{(0)}(k,\omega)$ is just the Fourier transform of Eq. (2.81). From Eq. (2.101) we can calculate the correction to the bare momentum distribution $n_0^{(0)}(k) = n_\pi^{(0)}(k) = \theta(k_F - k)$:

$$\delta n_0(k) = -\delta n_\pi(k) = \mathrm{i}t_\perp \int \frac{\mathrm{d}\omega}{2\pi} \mathrm{e}^{\mathrm{i}\omega 0^+} \left[G^{(0)}(k,\omega)\right]^2 .$$

This integral gives apparently zero due to a well known anomaly of the $T = 0$ perturbation theory[55]. This problem can be avoided by working at finite temperature. In this way the momentum distribution becomes:

$$\delta n_0(k_F + q) = t_\perp \frac{1}{(u_\rho - u_\sigma)q} \left[f(\beta u_\sigma q) - f(\beta u_\rho q)\right]$$

where the function $f(x)$ is the Fermi distribution. By taking the $T \to 0$ limit, we get:

$$\delta n_0(k) = \frac{t_\perp}{u_\rho - u_\sigma} \log(u_\rho/u_\sigma)\delta(k - k_F)$$

which can be interpreted as a shift of Fermi momenta given by Eq. (2.100). Analogously, we can easily check that the total energy correction induced by this shift coincides with Eq. (2.95). Therefore, at least up to lowest order in $t_\perp$, perturbation theory agrees with the exact solution.

It is straightforward to generalize these perturbative results to the case of an array of N chains. The relevant equations remain unchanged, the only difference being that the inter–chain hopping operator acting at transverse momentum $k_\perp$ is formally replaced by $-t_\perp \cos(k_\perp)$. For example the correction to the longitudinal Fermi momentum with transverse momentum $k_\perp$ is:

$$\Delta k_F(k_\perp) = \frac{t_\perp \cos(k_\perp)}{u_\rho - u_\sigma} \log(u_\rho/u_\sigma).$$

to first order in $t_\perp$. This equation gives the shape of the Fermi surface for a strongly anisotropic 2D system as a function of the spin and charge velocities. However, we have not been able to find an exact solution of the N-chain problem to all orders in $t_\perp$ and the crucial issue of the breakdown of FL behavior in two dimensions is still open.

Conclusions

The properties of a two dimensional (2D) interacting electron gas, have become a central problem in condensed matter since the suggestion that the normal state of HTc superconductors might require new concepts which go beyond ordinary Landau Fermi liquid (FL) theory, and that such a behavior might be intrinsic to interacting 2D models, much as it does in 1D. In the work leading to, and summerized in this thesis, we have analyzed two distinct aspects of this problem

In the first part, we have shown how it is possible to calculate the ground–state wave–function of the N–site Hubbard model in dimensions greater than one, for any finite number of electrons n, in the extremely dilute limit $n/N \to 0$. The method is simple and allows to obtain the exact and consistent expansion of any ground–state property in powers of $(n/N)^{1/3}$ in 3D, and $1/\log(n/N)$ in 2D. Through this calculation, we have established an interesting connection between the functional dependence upon the density n/N, of the correction to the total energy induced by the interaction, and the ground–state properties. The method makes use of this relation, to solve self–consistently the Schrœdinger equation and to calculate the ground–state energy and wave–function. All the results agree in lowest order, with the perturbative calculations in the low–density

limit both in 3D[12] and in 2D[13, 14, 15]. In particular, we have shown that in $d \geq 2$, the interacting ground state shows no anomalous behavior compared to the non–interacting one. The method does not allow to determine the ground–state wave function in $d < 2$, nevertheless, or rather as a consequence, it predicts anomalous ground–state properties, in agreement with the known results in 1D.

However this result does not necessarily prove that FL theory is valid in these systems. In fact, even if the ground state is adiabatically connected to the free Fermi gas, the low–lying excitations might be quite different from those of an ordinary Fermi liquid, and in particular might show the phenomenon of spin–charge separation. This possibility has not been much investigated in the literature and we believe that further analysis of the perturbative expansion of the single–particle Green function is needed.

In the second part of the thesis, we have studied another aspect of the same problem: the effects of the anomalous ground state properties and of spin–charge decoupling, on the dynamics of fermions in an array of weakly coupled 1D chains. Several scenarios are in principle possible. For instance, it might happen that all the chains asymptotically behave as they were still uncoupled. This case in usually referred to as intra–chain *confinement*[21]. Furthermore, even if confinement does not occur, two more routes are still possible. The transverse correlation might be sustained either by single–particle hopping, or, even, by pair–hopping processes. By applying the renormalization group (RG) technique, we have shown that *confinement*, in a strict sense, can never occur, at least for realistic models, e.g. the Hubbard model. Instead, transverse hopping is always a relevant perturbation, which modifies completely the long wave–length behavior of the coupled chains. This occurs both for spinless and spinful fermions, and, in fact, we have shown that the mechanism

responsible for the instability of un–coupled Luttinger chains, is the same in both cases, independently from the presence of the spin. Furthermore, for spinful fermions, whether single–particle hopping is asymptotically irrelevant or relevant, dominant pair fluctuations may arise, in spite of the interaction being repulsive.

Finally, we have defined and exactly solved a two–chain model, where the role and the stability of spin–charge separation, can be investigated, without the complications introduced by the anomalous exponents. We have shown that spin–charge separation alone is not able to give rise to confinement. However, we have demonstrated that Fermi liquid behavior never occurs, because spin–charge decoupling does partly survive, even though further excitations carrying both spin and charge are generated.

Appendix A

Four electrons, and other open shells

In this appendix we solve the asymptotic set of equations (1.39) for an open shell, in particular two extra electrons added to an otherwise closed shell. As an exemplification we consider first the case of $n = 4$ electrons. A generic $S_z = 0$ wave function of four electrons is

$$|\Psi\rangle = \sum L(\mathrm{k}_1, \mathrm{k}_2, \mathrm{k}_3, \mathrm{k}_4) c^\dagger_{\mathrm{k}_1\uparrow} c^\dagger_{\mathrm{k}_2\downarrow} c^\dagger_{\mathrm{k}_3\uparrow} c^\dagger_{\mathrm{k}_4\downarrow} |0\rangle, \tag{A.1}$$

where $L(\mathrm{k}_1, \mathrm{k}_2, \mathrm{k}_3, \mathrm{k}_4) = -L(\mathrm{k}_3, \mathrm{k}_2, \mathrm{k}_1, \mathrm{k}_4) = -L(\mathrm{k}_1, \mathrm{k}_4, \mathrm{k}_3, \mathrm{k}_2)$. The Schrœdinger equation for the coefficients is

$$\begin{aligned} &(E - \epsilon_{\mathrm{k}_1} - \epsilon_{\mathrm{k}_2} - \epsilon_{\mathrm{k}_3} - \epsilon_{\mathrm{k}_4}) L(\mathrm{k}_1, \mathrm{k}_2, \mathrm{k}_3, \mathrm{k}_4) = \\ &= \frac{U}{L^d} \textstyle\sum_{\mathbf{q}} [L(\mathrm{k}_1 + \mathrm{q}, \mathrm{k}_2 - \mathrm{q}, \mathrm{k}_3, \mathrm{k}_4) + L(\mathrm{k}_1 + \mathrm{q}, \mathrm{k}_2, \mathrm{k}_3, \mathrm{k}_4 - \mathrm{q}) + \\ &\quad + L(\mathrm{k}_1, \mathrm{k}_2 - \mathrm{q}, \mathrm{k}_3 + q, \mathrm{k}_4) + L(\mathrm{k}_1, \mathrm{k}_2, \mathrm{k}_3 + \mathrm{q}, \mathrm{k}_4 - \mathrm{q})]. \end{aligned} \tag{A.2}$$

If we define the function

$$J(\mathrm{k}_1, \mathrm{k}_2) = \frac{U}{L^d} \sum_{\mathbf{q}} L(\mathrm{q}, \mathrm{P} - \mathrm{q}, \mathrm{k}_1, \mathrm{k}_2), \tag{A.3}$$

then the coefficients L are

$$L(\mathbf{k}_1,\mathbf{k}_2,\mathbf{k}_3,\mathbf{k}_4)=\frac{J(\mathbf{k}_3,\mathbf{k}_4)-J(\mathbf{k}_3,\mathbf{k}_2)-J(\mathbf{k}_1,\mathbf{k}_4)+J(\mathbf{k}_1,\mathbf{k}_2)}{E-\epsilon_{\mathbf{k}_1}-\epsilon_{\mathbf{k}_2}-\epsilon_{\mathbf{k}_3}-\epsilon_{\mathbf{k}_4}}. \tag{A.4}$$

The self consistent set of equations the J's have to satisfy is

$$\begin{aligned} J(\mathbf{k}_1,\mathbf{k}_2) &= J(\mathbf{k}_1,\mathbf{k}_2)\frac{U}{L^d}\sum_{\mathbf{q}}\frac{1}{E-\epsilon_{\mathbf{k}_1}-\epsilon_{\mathbf{k}_2}-\epsilon_{\mathbf{q}}-\epsilon_{\mathbf{P}-\mathbf{k}_1-\mathbf{k}_2-\mathbf{q}}}+ \\ &\quad -\frac{U}{L^d}\sum_{\mathbf{q}}\frac{J(\mathbf{k}_1,\mathbf{q})+J(\mathbf{q},\mathbf{k}_2)}{E-\epsilon_{\mathbf{k}_1}-\epsilon_{\mathbf{k}_2}-\epsilon_{\mathbf{q}}-\epsilon_{\mathbf{P}-\mathbf{k}_1-\mathbf{k}_2-\mathbf{q}}}+ \\ &\quad +\frac{U}{L^d}\sum_{\mathbf{q}}\frac{J(\mathbf{q},\mathbf{P}-\mathbf{q}-\mathbf{k}_1-\mathbf{k}_2)}{E-\epsilon_{\mathbf{k}_1}-\epsilon_{\mathbf{k}_2}-\epsilon_{\mathbf{q}}-\epsilon_{\mathbf{P}-\mathbf{k}_1-\mathbf{k}_2-\mathbf{q}}}. \end{aligned} \tag{A.5}$$

Let us define the functions

$$A(\mathbf{k}_1,\mathbf{k}_2,\mathbf{k}_3,\mathbf{k}_4)=\frac{U}{L^d}\frac{1}{E-\epsilon_{\mathbf{k}_1}-\epsilon_{\mathbf{k}_2}-\epsilon_{\mathbf{k}_3}-\epsilon_{\mathbf{k}_4}}, \tag{A.6}$$

$$I(\mathbf{k}_1,\mathbf{k}_2)=-\frac{U}{L^d}\sum_{\mathbf{q}}\frac{1}{E-\epsilon_{\mathbf{k}_1}-\epsilon_{\mathbf{k}_2}-\epsilon_{\mathbf{q}}-\epsilon_{\mathbf{P}-\mathbf{k}_1-\mathbf{k}_2-\mathbf{q}}}\simeq\frac{Ua^{d-2}}{2tf_0} \tag{A.7}$$

and the wave vectors (for simplicity we work in $2d$)

$$\mathbf{0}=(0,0)\quad \mathbf{1}=(0,\frac{2\pi}{La})\quad \mathbf{2}=(0,-\frac{2\pi}{La})\quad \mathbf{3}=(\frac{2\pi}{La},0)\quad \mathbf{4}=(-\frac{2\pi}{La},0). \tag{A.8}$$

Let us look for the $\mathbf{P}=\mathbf{0}$ ground state (for $\mathbf{P}\neq\mathbf{0}$ the problem becomes effectively closed shell, and is solved as in Section 1.3). The unperturbed Fermi sea for total momentum zero is fourfold degenerate. If we assume the asymptotic condition $\alpha(L)=(E-E_0)L^2\to 0$ where, as usual, $E_0=2\epsilon_{\mathbf{0}}+2\epsilon_{\mathbf{1}}$ is the $U=0$ ground state energy, then the value of A is more singular when the arguments belong to one of the possible Fermi surfaces i.e.

$$A(\mathbf{0},\mathbf{0},\mathbf{1},\mathbf{2})=A(\mathbf{0},\mathbf{0},\mathbf{2},\mathbf{1})=A(\mathbf{0},\mathbf{0},\mathbf{3},\mathbf{4})=A(\mathbf{0},\mathbf{0},\mathbf{4},\mathbf{3})=\cdots=\frac{U}{\alpha(L)}, \tag{A.9}$$

while in the other cases A does not diverge when $L\to\infty$. As it happened for closed shells, just the J whose arguments (the two spectator electron momenta for this $n=4$ problem)

belong to the degenerate Fermi surfaces are non-zero, to leading order. The number of spectator configurations is 13. The peculiarity of the general case $n = n_0$ (closed shell)+2 (of which $n = 4$ is an example), is that the spectator configuration of the electrons which belong to the n_0-Fermi Surface mixes with all the others. Let us show how this happens for $n = 4$. We can write explicitly the set of Eq. (A.5) as

$$
\begin{aligned}
&J(0,0) = \\
&= J(0,0)(-I + A(0,0,1,2) + A(0,0,2,1) + A(0,0,3,4) + A(0,0,4,3)) + \\
&- A(0,0,1,2)(J(0,2) + J(1,0)) - A(0,0,2,1)(J(0,1) + J(2,0)) + \\
&+ A(0,0,1,2)J(1,2) + A(0,0,2,1)J(2,1) + A(0,0,3,4)J(3,4) + \\
&+ A(0,0,4,3)J(4,3),
\end{aligned}
$$

$$
\begin{aligned}
&J(0,1) = \\
&= J(0,1)(-I + A(0,1,0,2) + A(0,1,2,0)) - A(0,1,0,2)(J(0,2) + J(0,1)) \\
&- A(0,1,2,0)(J(0,0) + J(2,1)) + A(0,1,2,0)J(2,0) + A(0,1,0,2)J(0,2),
\end{aligned}
$$

$$
\begin{aligned}
&J(1,2) = \\
&= J(1,2)(-I + A(1,2,0,0)) - A(1,2,0,0)(J(1,0) + J(0,2)) + \\
&+ A(1,2,0,0)J(0,0).
\end{aligned}
\tag{A.10}
$$

All the other ten equations can be easily obtained by these ones. Again, since both A and I are logarithmically divergent we can set the left hand side terms equal to zero. Then we can divide the equations by the term $U/\alpha(L)$ of Eq. (A.9), so that the resulting set of equations look like an eigenvalue problem, where the eigenvalue is

$$
\lambda = \frac{I}{A} \simeq \frac{\alpha(L)}{2tf_0}, \tag{A.11}
$$

and the 13×13 matrix $\hat{M}$ is

$$\hat{M} = \begin{pmatrix} 4 & -1 & 1 & -1 & -1 & 1 & -1 & -1 & 1 & -1 & -1 & 1 & -1 \\ -1 & 1 & -1 & 1 & 0 & 0 & 0 & 0 & 0 & 0 & 0 & 0 & 0 \\ 1 & -1 & 1 & -1 & 0 & 0 & 0 & 0 & 0 & 0 & 0 & 0 & 0 \\ -1 & 1 & -1 & 1 & 0 & 0 & 0 & 0 & 0 & 0 & 0 & 0 & 0 \\ -1 & 0 & 0 & 0 & 1 & -1 & 1 & 0 & 0 & 0 & 0 & 0 & 0 \\ 1 & 0 & 0 & 0 & -1 & 1 & -1 & 0 & 0 & 0 & 0 & 0 & 0 \\ -1 & 0 & 0 & 0 & 1 & -1 & 1 & 0 & 0 & 0 & 0 & 0 & 0 \\ -1 & 0 & 0 & 0 & 0 & 0 & 0 & 1 & -1 & 1 & 0 & 0 & 0 \\ 1 & 0 & 0 & 0 & 0 & 0 & 0 & -1 & 1 & -1 & 0 & 0 & 0 \\ -1 & 0 & 0 & 0 & 0 & 0 & 0 & 1 & -1 & 1 & 0 & 0 & 0 \\ -1 & 0 & 0 & 0 & 0 & 0 & 0 & 0 & 0 & 0 & 1 & -1 & 1 \\ 1 & 0 & 0 & 0 & 0 & 0 & 0 & 0 & 0 & 0 & -1 & 1 & -1 \\ -1 & 0 & 0 & 0 & 0 & 0 & 0 & 0 & 0 & 0 & 1 & -1 & 1 \end{pmatrix}. \quad \text{(A.12)}$$

The first row (column) corresponds to $J(\mathbf{0},\mathbf{0})$, while the others in order to $J(\mathbf{0},\mathbf{1})$, $J(\mathbf{2},\mathbf{1})$, $J(\mathbf{2},\mathbf{0})$, $J(\mathbf{0},\mathbf{2})$, $J(\mathbf{1},\mathbf{2})$, $J(\mathbf{1},\mathbf{0})$, $J(\mathbf{0},\mathbf{3})$, $J(\mathbf{4},\mathbf{3})$, $J(\mathbf{4},\mathbf{0})$, $J(\mathbf{0},\mathbf{4})$, $J(\mathbf{3},\mathbf{4})$ and $J(\mathbf{3},\mathbf{0})$. We see that the matrix has the form we anticipated in Section IV. However, in the present open shell case, the $(\mathbf{0},\mathbf{0})$ spectator configuration mixes with all others. The matrix can be easily diagonalized to find two physical (i.e. non-zero) eigenvalues, $\lambda = 3$ (threefold degenerate), and $\lambda = 7$ (nondegenerate), and nine unphysical $\lambda = 0$ eigenvalues [unphysical eigenvalues of $\hat{M}$ are generally caused by the transformation from Eq. (A.2) to Eq. (A.4), which is singular for $\lambda = 0$]. The $\lambda = 3$ eigenvectors are

$$\vec{J}_1 = \begin{pmatrix} 0 \\ 1 \\ -1 \\ 1 \\ -1 \\ 1 \\ -1 \\ 0 \\ 0 \\ 0 \\ 0 \\ 0 \\ 0 \end{pmatrix} \quad \vec{J}_2 = \begin{pmatrix} 0 \\ 0 \\ 0 \\ 0 \\ 0 \\ 0 \\ 1 \\ -1 \\ 1 \\ -1 \\ 1 \\ -1 \end{pmatrix} \quad \vec{J}_3 = \begin{pmatrix} 0 \\ 1 \\ -1 \\ 1 \\ 1 \\ -1 \\ 1 \\ -1 \\ 1 \\ -1 \\ -1 \\ 1 \\ -1 \end{pmatrix}. \quad \text{(A.13)}$$

$\vec{J}_1$ and $\vec{J}_2$ correspond to triplet states, while $\vec{J}_3$ is a singlet, as is seen by direct inspection of the relative sign of e.g. J(0,1) [second from top in (A.13)], and J(1,0) [seventh from top in (A.13)]. The eigenvector corresponding to $\lambda = 7$ is

$$\vec{J}_4 = \begin{pmatrix} 4 \\ -1 \\ 1 \\ -1 \\ -1 \\ 1 \\ -1 \\ -1 \\ 1 \\ -1 \\ -1 \\ 1 \\ -1 \end{pmatrix} \tag{A.14}$$

and is a singlet.

We note that the lowest singlet J_3 has a rotational d symmetry, while the highest J_4 s symmetry.

We further note that for the lowest eigenvalues, J_1, J_2, J_3, the component $J(\mathbf{0},\mathbf{0})$ is zero. This result, inserted in the Eq. (A.4) for the coefficients L, implies that in the lowest energy states, it is not possible to excite a pair of electrons keeping the "core" of the Fermi sea frozen. In other words, the coefficient of the states with two spectator electrons at $\mathbf{k} = \mathbf{0}$ and the other two excited out of the FS are rigorously zero in the four electron ground state.

The results just found for $n = 4$ can be immediately generalized to the case $n = n_0$ (closed shell) +2-electrons. Let us suppose that there are $2m$ degenerate states in the outer k-space shell. The matrix $\hat{M}$ will be similar to the matrix (A.12), the only differences being that now there are $2m$ boxes of dimension $((n/2)^2 - 1) \times ((n/2)^2 - 1)$ instead of $2 \cdot 2 = 4$

boxes of dimension 3×3, and that the first diagonal element is $2m$ instead of 4. The first (top left) $\hat{M}$ matrix element corresponds to the J whose arguments belong to the "core", that is to the case where n_o spectator electrons rigidly occupy the $(n-2)$ closed-shell FS. It is easy to show that the lowest eigenvalue is

$$\lambda = \frac{n^2}{4} - 1 \tag{A.15}$$

and it is $2m-1$ times degenerate. Of the lowest eigenvectors, m are triplets and $m-1$ d–like singlets. As before, for all these eigenvectors the component corresponding to the J of the "core", is zero. This again implies that the ground state has exactly no components in which the spectator electrons are in the "core". The other non-degenerate eigenvalue is

$$\lambda = \frac{n^2}{4} + (2m-1) \tag{A.16}$$

and corresponds to an s–like singlet (in this case the component corresponding to the J of the core is $2m$ times bigger than the others).

For the sake of completeness, we report here also the ground state energy for $P = 2k_f + 4\pi/La$. In that case, we have a singlet with

$$\lambda = \frac{n^2}{4}, \tag{A.17}$$

which is higher than the true $2m-1$ degenerate ground state (A.15).

Appendix B

RG equations at arbitrary $t_\perp$

In this Appendix we derive the RG equations at any order in Δk_F and at next to leading logarithmic approximation. First of all let us recall the expression of the diagram in Fig. 2.4b,

$$\text{Fig.2.4b} = -\frac{1}{2\pi v_F}\frac{\delta\omega_0}{\omega_0} I,$$

where

$$I = \begin{cases} \dfrac{\omega_0}{\omega_0 - 2v_F\Delta K_F} & \text{if } \omega_0 > 4v_F\Delta k_F \\ 0 & \text{if } \omega_0 < 4v_F\Delta k_F \end{cases}$$

and $\omega_0 = 2v_F K_0$. Secondly, we write down the expression of the diagrams in Fig. 2.4d–2.4e, at any order in Δk_F. Let us denote as D_1 the ratio between the diagrams Fig. 2.4d and 2.4c, and D_2 that between Fig. 2.4e and Fig. 2.4c, where

(i) for $\omega_0 > 4v_F\Delta k_F$:

$$D_1 = \frac{\omega_0}{\omega_0 - 2v_F\Delta k_F}, \tag{B.1}$$

$$D_2 = \frac{1}{2}\left[\frac{\omega_0(\omega_0 - 4v_F\Delta k_F)}{(\omega_0 - 2v_F\Delta k_F)^2} + \frac{\omega_0(\omega_0 - 4v_F\Delta k_F)}{(\omega_0 + 2v_F\Delta k_F)^2} + \right. \\ \left. + \frac{8v_F\Delta k_F\omega_0}{(\omega_0 - 2v_F\Delta k_F)(\omega_0 + 2v_F\Delta k_F)}\right]; \tag{B.2}$$

(*ii*) for $4v_F\Delta k_F > \omega_0 > 2v_F\Delta k_F$:

$$D_1 = -\frac{\omega_0}{2v_F\Delta k_F}, \tag{B.3}$$

$$D_2 = \frac{\omega_0(2\omega_0 - 4v_F\Delta k_F)}{2v_F\Delta k_F(2\omega_0 - 2v_F\Delta k_F)}; \tag{B.4}$$

while for smaller ω_0 they are both zero. The correct expression of the self energy correction of Eq. (2.8) is instead

$$\begin{aligned}\delta G^{(0)}_{R,0}(k,\omega) &= G^{(0)}_{R,0}(k,\omega)\left[-\frac{1}{2}\left(\frac{1}{2\pi v_F}\right)^2(\tilde{g_0}^2+\tilde{g_t}^2+\tilde{g_f}^2+\tilde{g_b}^2C_1)\frac{\delta K_0}{K_0}\right]+\\ &+ G^{(0)}_{R,0}(k,\omega)^2\left[C_2\left(\frac{\tilde{g_b}}{2\pi v_F}\right)^2 v_F\Delta k_F\frac{\delta K_0}{K_0}+\right.\\ &+ \left. C_3\left(\frac{\tilde{g_b}}{2\pi v_F}\right)^2 v_F(k-k^0_F)\frac{2\Delta k_F}{K_0}\frac{\delta K_0}{K_0}\right],\end{aligned} \tag{B.5}$$

where

(*i*) for $\omega_0 > 4v_F\Delta k_F$:

$$C_1 = \frac{1}{2}\left[\frac{\omega_0(\omega_0-4v_F\Delta k_F)}{(\omega_0-2v_F\Delta k_F)^2}+\frac{\omega_0(\omega_0-4v_F\Delta k_F)}{(\omega_0+2v_F\Delta k_F)^2}+\frac{8v_F\Delta k_F\omega_0}{\omega_0^2-4v_F^2\Delta k_F^2}\right], \tag{B.6}$$

$$C_2 = -\frac{1}{4}\left[\frac{4\omega_0(\omega_0-4v_F\Delta k_F)}{\omega_0^2-4v_F^2\Delta k_F^2}-\frac{2\omega_0}{v_F\Delta k_F}\log\frac{\omega_0+2v_F\Delta k_F}{\omega_0-2v_F\Delta k_F}\right], \tag{B.7}$$

$$C_3 = \frac{\omega_0^2}{4(\omega_0-2v_F\Delta k_F)^2}+\frac{3\omega_0^2}{4(\omega_0+2v_F\Delta k_F)^2}; \tag{B.8}$$

(*ii*) for $4v_F\Delta k_F > \omega_0 > 2v_F\Delta k_F$:

$$C_1 = \frac{\omega_0}{2v_F\Delta k_F}-\frac{\omega_0}{2\omega_0-2v_F\Delta k_F}, \tag{B.9}$$

$$C_2 = \frac{\omega_0}{2v_F\Delta k_F}\log\frac{\omega_0-v_F\Delta k_F}{v_F\Delta k_F}, \tag{B.10}$$

$$C_3 = -\frac{\omega_0^2}{8v_F^2\Delta k_F^2}; \tag{B.11}$$

and, similarly to D_1 and D_2, they vanish for smaller ω_0. Notice that C_1 is equal to D_2. This is an important result, whose consequence is that the pseudo–charge sector of the

model is correctly un–affected by the transverse hopping. The expressions of the wave function, fermi velocity and momentum renormalization factors are therefore:

$$\begin{aligned}
\delta z &= -\frac{1}{2}\left(\frac{1}{2\pi v_F}\right)^2 (\tilde{g}^2 + \tilde{g}_t{}^2 + \tilde{g}_f{}^2 + C_1 \tilde{g}_b{}^2)\frac{\delta\omega_0}{\omega_0} \\
\delta v_F &= v_F C_3 \left(\frac{\tilde{g}_b}{2\pi v_F}\right)^2 \frac{2\Delta k_F}{K_0}\frac{\delta\omega_0}{\omega_0} \\
\delta \Delta k_F &= -2\Delta k_F C_2 \left(\frac{\tilde{g}_b}{2\pi v_F}\right)^2 \frac{\delta\omega_0}{\omega_0}
\end{aligned} \tag{B.12}$$

On the other hand, the vertex corrections, which can be calculated using the diagrams in Fig. 3, and the expressions of D_1 and D_2, are:

$$\begin{aligned}
\tilde{g}\delta\Gamma &= -\frac{1}{2\pi v_F}\frac{\delta\omega_0}{\omega_0}(\tilde{g}_t^2 - I\tilde{g}_b^2) + \\
&\quad -\frac{1}{2}\left(\frac{1}{2\pi v_F}\right)^2 \frac{\delta\omega_0}{\omega_0}(-2\tilde{g}^3 - 2\tilde{g}\tilde{g}_f^2 - 2\tilde{g}_f\tilde{g}_t^2 - 2D_2\tilde{g}_f\tilde{g}_b^2) \\
\tilde{g}_f\delta\Gamma_f &= -\frac{1}{2\pi v_F}\frac{\delta\omega_0}{\omega_0}(I\tilde{g}_b^2 - \tilde{g}_t^2) + \\
&\quad -\frac{1}{2}\left(\frac{1}{2\pi v_F}\right)^2 \frac{\delta\omega_0}{\omega_0}(-2\tilde{g}_f^3 - 2\tilde{g}_f\tilde{g}^2 - 2\tilde{g}\tilde{g}_t^2 - 2D_2\tilde{g}\tilde{g}_b^2) \\
\tilde{g}_t\delta\Gamma_t &= -\frac{1}{2\pi v_F}\frac{\delta\omega_0}{\omega_0}2\tilde{g}_t(\tilde{g} - \tilde{g}_f) + \\
&\quad -\frac{1}{2}\left(\frac{1}{2\pi v_F}\right)^2 \frac{\delta\omega_0}{\omega_0}(-4\tilde{g}_t\tilde{g}\tilde{g}_f - 4D_1\tilde{g}_t\tilde{g}_b^2) \\
\tilde{g}_b\delta\Gamma_b &= -\frac{1}{2\pi v_F}\frac{\delta\omega_0}{\omega_0}2\tilde{g}_b(\tilde{g}_f - \tilde{g}) + \\
&\quad -\frac{1}{2}\left(\frac{1}{2\pi v_F}\right)^2 \frac{\delta\omega_0}{\omega_0}(-4D_1\tilde{g}_b\tilde{g}_t^2 - 4\tilde{g}\tilde{g}_b\tilde{g}_f)
\end{aligned} \tag{B.13}$$

We are now able to write down the RG equations at any order in Δk_F. First of all, let us

recall that, for a generic vertex, the correction to the invariant coupling is given by[18]

$$\delta g_i = g_i \delta\Gamma_i + 2 g_i \delta z,$$

where $g_i = g$, g_f, g_t, or g_b. This formula, together with the expressions of the vertex corrections, of the wave–function and fermi velocity renormalization factors and with the definition of the a–dimensional invariant couplings Eqs. (2.13–2.17) allows to write the RG equations:

$$\begin{aligned}
\frac{\mathrm{d}g_\rho}{\mathrm{d}\log\omega_0} &= 0 \\
\frac{\mathrm{d}g_\sigma}{\mathrm{d}\log\omega_0} &= 2g_t^2 - 2Ig_b^2 + 2g_\sigma\left[g_t^2 + D_2 g_b^2 + C_3 h g_b^2\right] \\
\frac{\mathrm{d}g_t}{\mathrm{d}\log\omega_0} &= 2g_t g_\sigma + g_t\left[g_\sigma^2 + g_t^2 - 2D_1 g_b^2 + C_1 g_b^2 + 2C_3 h g_b^2\right] \\
\frac{\mathrm{d}g_b}{\mathrm{d}\log\omega_0} &= -2g_b g_\sigma + g_b\left[g_\sigma^2 - 2D_1 g_t^2 + g_t^2 + C_1 g_b^2 + 2C_3 h g_b^2\right] \\
\frac{\mathrm{d}h}{\mathrm{d}\log\omega_0} &= h\left[2C_2 g_b^2 - 1\right] \\
\frac{\mathrm{d}z}{\mathrm{d}\log\omega_0} &= \frac{1}{4}(g_\rho^2 + g_\sigma^2 + 2g_t^2 + 2C_1 g_b^2) \\
\frac{\mathrm{d}v_F}{\mathrm{d}\log\omega_0} &= -2v_F h C_3 g_b^2
\end{aligned} \tag{B.14}$$

For small $h = 2v_F\Delta k_F/\omega_0$, it is easy to show that $I \simeq 1 + h$, $D_1 \simeq 1 + h$, $D_2 = C_1 \simeq 1$, $C_2 \simeq 1 + 2h$ and $C_3 \simeq 1$, and the Eqs. (B.14–B.14) reduce to Eqs. (2.18–2.24). The equivalence between D_2 and C_1 is crucial in giving Eq. (B.14).

Bibliography

[1] L. Landau, Sov. Phys.–JETP **3**, 920 (1956); **5**, 101 (1957); **8**, 70 (1959)

[2] P. Nozières and J. M. Luttinger, Phys. Rev. **127**, 1423 (1962); J. M. Luttinger and P. Nozières, Phys. Rev. **127**, 1431 (1962)

[3] J. M. Luttinger, J. Math. Phys. **4**, 1154 (1963)

[4] D. C. Mattis and E. H. Lieb, J. Math. Phys. **6**, 304 (1965)

[5] F. D. M. Haldane, Phys. Rev. Lett. **45**, 1358 (1980)

[6] H. J. Schulz, Int. J. Mod. Phys. B **5**, 57 (1991)

[7] P. W. Anderson, Science **235**, 1196 (1987)

[8] C. M. Varma, P. B. Littlewood, S. Schmitt–Rink, E. Abrahams, and A. E. Ruckenstein, Phys. Rev. Lett. **63**, 1996 (1989)

[9] R. B. Laughlin, in *Mechanism of High Temperature Superconductivity*, editors H. Kamimura and A. Oshiyama (Springer Verlag, Berlin, 1989)

[10] P.W. Anderson, Phys. Rev. Lett. **64**, 1839 (1990), Phys. Rev. Lett., **65**, 2306 (1990), Phys. Rev. Lett., **66**, 3226 (1991)

[11] M. Fabrizio, A. Parola, and E. Tosatti, Phys. Rev. B 44, 1033 (1991)

[12] V. M. Galitskii, Sov. Phys.–JETP **34**, 104 (1958)

[13] P. Bloom, Phys. Rev. **B 12**, 125 (1975)

[14] Jan R. Engelbrecht, M. Randeria, Phys. Rev. Lett. **65**, 1032 (1990)

[15] H. Fukuyama, O. Narikiyo, and Y. Hasegawa J. Phys. Soc. Jpn. **60**, 372 (1991)

[16] Jan R. Engelbrecht, M. Randeria and L. Zhang, Phys. Rev. B **45**, 10135 (1992)

[17] T. Hsu, J. Wheatley and P. W. Anderson, Nature **333**, 121 (1988)

[18] J. Sólyom, Adv. Phys. **28**, 201 (1979)

[19] C. Bourbonnais and L. G. Caron, Int. J. Mod. Phys. B **5**, 57 (1991) and reference therein

[20] D. Jérome and H. J. Schulz, Adv. Phys. **31**, 299 (1982), see also Ref. Bourbonnais

[21] P. W. Anderson, Phys. Rev. Lett. **67**, 3845 (1991)

[22] C. Castellani, C. Di Castro and W. Metzner, *Instabilities of anisotropic interacting Fermi systems*, preprint (1992)

[23] D. C. Mattis, Rev. Mod. Phys. **58**, 361 (1986), S. Rudin, Phys. Rev. **A 31**, 3441 (1985)

[24] A. Parola, S. Sorella, M. Parrinello, E. Tosatti, in *Dynamics of magnetic fluctuations in High Temperature Superconductors* edited by G. Reiter, P. Horsch and G. Psaltakis (Plenum, N.Y. 1990)

[25] V. A. Belyakov, Sov. Phys.–JETP **13**, 850 (1961)

[26] This singularity in the vertex part for zero total momentum, is a particular example of a very general result of the many-body theory (see for example A. A. Abrikosov, L. P. Gorkov, and I. E. Dzyaloshinski, *Methods of Quantum Field Theory in Statistical Mechanics* (Dover, New York, 1975), Sec. 20.)

[27] Cancellation of the backward channel is instead important when one calculates the imaginary part of the self energy in the T-matrix technique formalism. In fact, ignoring the vanishing of the backward scattering, would yield the wrong result even at leading order, as recently pointed out by H. Fukuyama *et al.*[15].

[28] The $1/\log^2 \rho a^2$ coefficient given here is the correct one, and differs from the numerical result given by Bloom [Ref.[13]], which is 4 instead of 4log2.

[29] V. N. Efimov, M. Ya. Amus'ya, Sov. Phys.–JETP **20**, 388 (1965)

[30] A. A. Abrikosov and I. M. Khalatnikov, Sov. Phys. JETP **6**, 888 (1958)

[31] Y. Ren and P. W. Anderson, *The one dimensional Hubbard model with repulsive interaction*, preprint

[32] P. W. Anderson, Phys. Rev. Lett. **18**, 1049 (1967); Phys. Rev. **164**, 352 (1967)

[33] A. Parola and M. Fabrizio, unpublished.

[34] P. C. E. Stamp, Phys. Rev. Lett. **68**, 2180 (1992)

[35] F. D. M. Haldane, lectures held at the E. Fermi school on *Perspectives in many–particle physics*, Varenna, july 1992.

[36] A. M. Luther, Phys. Rev. B **19**, 320 (1979)

[37] T. Giamarchi and H. J. Schulz, J. Phys. **49**, 819 (1988)

[38] K. A. Muttalib and V. J. Emery, Phys. Rev. Lett. **57**, 1370 (1986)

[39] A. A. Nersesyan, Phys. Lett. A **153**, 49 (1991)

[40] V. N. Prigodin and Yu. A. Firsov, Sov. Phys. JETP **49**, 369 (1979)

[41] P. A. Lee, T. M. Rice, R. A. Klemm, Phys. Rev. B **15**, 2984 (1977)

[42] A. Luther and I. Peschel, Phys. Rev. B **9**, 2911 (1974)

D. C. Mattis, J. Math. Phys. **15**, 609 (1974)

F. D. M. Haldane, J. Phys. C **14**, 2585 (1981)

[43] H. J. Schulz, Phys. Rev. B **22**, 5274 (1980)

[44] A. Luther and V. J. Emery, Phys. Rev. Lett. **33**, 589 (1974)

[45] V. J. Emery, in *Highly Conducting One-Dimensional Solids* (Plenum, New York, 1979), pag. 327

[46] M. Fabrizio, A. Parola, E. Tosatti, Phys. Rev. B **46**, 3159 (1992)

[47] K. Penc, J. Sólyom, Phys. Rev. B **41**, 704 (1990)

[48] Anticipating later results, our fixed point $LL2$ (see Fig. 2.9) corresponds to F_1 in Table I of Ref. [47]; I to the first fixed point of Table II in the same Reference, and II to the second fixed point on the same Table.

[49] We note that both Π^{I} in I and Π^{III} in III are such that $\langle c^{\dagger}_{i,\alpha,\uparrow} c_{i,\alpha,\downarrow} \rangle = 0$, consistent with strong coupling (see Ref. [7]). This is not the case in II, where all couplings are attractive (Table 2.1) and there is regular s–wave pairing.

[50] H. J. Schulz, Phys. Rev. Lett. **64**, 2831 (1990)

[51] Z. Y. Weng, D. N. Sheng and C. S. Ting, *Large–U Hubbard model: from one–dimension to two–dimensions*, preprint (1992)

[52] E. A. Jagla, K. Hallberg, and C. A. Balseiro, *A visualization of charge and spin separation in low dimensional systems*, preprint (1992)

[53] J. Voit, *Charge–Spin separation and the spectral properties of Luttinger liquids*, preprint (1992)

[54] M. Fabrizio, and A. Parola, *Spin–Charge separation in a model of two coupled chains*, preprint (1992)

[55] W. Kohn and J. M. Luttinger, Phys. Rev. **118**, 41 (1960)